Triple oxygen (^{16}O, ^{17}O, ^{18}O) and carbon (^{12}C, ^{13}C) isotope variations in bioapatite of small mammals – new insights concerning the reconstruction of palaeo-CO_2 concentrations and palaeotemperatures

Dissertation

zur Erlangung des mathemathisch-naturwissenschaftlichen Doktorgrades

Doctor rerum naturalium (Dr. rer. nat.)

an der Georg-August-Universität Göttingen

Geowissenschaftliches Zentrum der Georg-August-Universität Göttingen

Abteilung Isotopengeologie

vorgelegt von Diplom-Geowissenschaftler

Alexander Gehler aus Wolfsburg

Göttingen 2012

Gutachter:

1. Prof. Dr. Andreas Pack

2. Prof. Dr. Jochen Hoefs

Tag der mündlichen Prüfung: 18.01.2012

Acknowledgements

Most notably, I like to thank Andreas Pack, who had the initial idea for my doctoral thesis and attended for the financial support. He always was open for new ideas and critical discussions and was persistently prepared to support me with his extensive knowledge in isotope geochemistry and mathematics as well as in all technical aspects of stable isotope analysis.

Special thanks go to Jochen Hoefs for his willingness to act as the co-supervisor for the present work and to Thomas Tütken for the access to lab facilities in Bonn and fruitful discussions concerning stable isotopes in mammalian bioapatite.

I sincerely thank my doctoral student colleagues Magdalena Hofmann and Verena Bendel for manifold theoretical and practical support, the same prevails for the remaining scientific staff in our divison, Balázs Horváth, Tommaso di Rocco and Daniel Herwartz.

For their assistance during analytical work I like to thank Ingrid Reuber and Reinhold Przybilla, further thanks are due to Axel Dierschke and Heinrich Herborg who were a great help in case of technical problems.

For various help with the sample pre-treatment and stable isotope analysis I am grateful to all student assistants that worked during my employment in the isotope geology division, namely Nina Albrecht, Andres Höweling, Marja Kröger, Christian Seidler and Maximilian Troche.

For providing the sample material for the existing thesis I like to thank Bernd von Bülow, Philip D. Gingerich, Kurt Heissig, Wighard von Koenigswald, Thomas Lehmann, Lutz Maul, Frieder Mayer, Armin Pack, Mike Reich, Gertrud Rößner, Michael Rummel, Stephan Schaal, Gert Tröster and Beatrix Wuntke. For literature support and advice in the tooth growth mechanisms of rodents my gratitude goes to Lutz Maul and Wighard von Koenigwald.

Vanessa Roden and Tanja Stegemann are acknowledged for lingustic and typo corrections of most of the manuscripts and the remaining chapters of the present thesis.

I am deeply indebted to Wiebke Kallweit who provided continuous encouragement to me during the preparation of this thesis and also to my parents Doris and Heinz Gehler who in the first place enabled my scientific education.

The studies included in this thesis were founded by the German National Science Foundation, DFG grant PA909/5-1.

Preface

This doctoral thesis comprises the following articles that are either published, in press or in preparation, as indicated below:

Gehler, A., Tütken, T., Pack, A. (2011). Triple oxygen isotope analysis of bioapatite as tracer for diagenetic alteration of bones and teeth. *Palaeogeography, Palaeoclimatology, Palaeoecology* **310**, 84-91.

Pack, A., Gehler, A., Süssenberger, A. (in press). Exploring the usability of isotopically anomalous oxygen in bones and teeth as paleo-CO_2-barometer. *Geochimica et Cosmochimica Acta*, http://dx.doi.org/10.1016/j.gca.2012.10.017.

Gehler, A., Gingerich, P.D., Pack, A. (in preparation). Temperature and atmospheric CO_2-concentration changes across the Palaeocene-Eocene Thermal Maximum (PETM) – new insights from triple oxygen isotope analysis of mammalian bioapatite.

Gehler, A., Tütken, T., Pack, A. (2012). Oxygen and Carbon Isotope Variations in a Modern Rodent Community – Implications for Palaeoenvironmental Reconstructions. *PloS ONE* **7**, e49531.

Abstract

The ratios among the stable isotopes of oxygen (^{16}O, ^{17}O, ^{18}O) and carbon (^{12}C, ^{13}C) in biogenic apatite of mammal teeth and bones have the potential to provide insight into the isotopic composition of the respective oxygen and carbon sources. The isotope ratios of these sources (e.g. drinking water, air oxygen, diet) are connected to specific environmental and climatic conditions, such as temperature, relative humidity, CO_2 concentration, bioproductivity, palaeovegetation and vegetation density. Analysis of the oxygen and carbon isotope composition of diagenetically unaltered skeletal tissue of fossil mammals can provide evidence on these climatic and environmental parameters far back into Earth's history. Furthermore, it is possible to receive information regarding the mode of life and specific behaviour of the examined taxa, e.g. migrational behaviour, birth seasonality, drinking behaviour, food preferences, resource partitioning and habitat use.

From the early beginning of research in this specific field of biogeochemistry in the 1970s and 1980s until today, a large number of studies have been published which examine the oxygen and carbon isotope composition ($^{18}O/^{16}O$, $^{13}C/^{12}C$) in tooth and bone material of (in most cases large) modern and fossil mammals. Less than two decades ago, an anomalous triple oxygen isotope composition ($^{17}O/^{16}O$, $^{18}O/^{16}O$) has been observed in tropospheric oxygen, which is significantly different from nearly all other terrestrial materials. This anomaly in molecular oxygen is the result of non-mass-dependent fractionation due to photochemical processes in the stratosphere and is transferred to the troposphere by gas exchange. Its magnitude is a function of the atmospheric CO_2 concentration and global bioproductivity. If it is possible to reconstruct the triple isotope composition of tropospheric oxygen to certain times in Earth's history, conclusions can be drawn on the respective CO_2 level or bioproductivity. However, geological archives, which are capable of this, are extremely scarce.

As inhaled air oxygen is one of the most important oxygen sources in mammals, bioapatite of modern and fossil mammals is one of the few materials that have the potential to be such an archive.

The present thesis evaluates variations in the triple oxygen isotope composition of bioapatite from modern mammals as well as its application potential as a new proxy for palaeo-CO_2 reconstruction and as a tracer of diagenetically altered fossil skeletal tissue.

Furthermore, interspecific, intraspecific and intraindividual variations of the oxygen and carbon isotope composition of bioapatite of modern rodents are investigated to reach a better interpretative background for respective analytical result from fossil representatives of this largest mammalian order.

Chapter 2 evaluates the question, whether the anomalous isotope signature of tropospheric oxygen can be used as a tracer for diagenetic alteration of tooth and bone phosphate of fossil mammals. Therefore, the triple oxygen isotope composition of tooth enamel, dentine and to a minor extent also bone material of several individuals of Cenozoic small mammals (i.e. rodents) has been analysed separately. While all tooth enamel samples have a pronounced oxygen isotope anomaly within a range that is expected for diagenetically unaltered bioapatite of small mammals, all dentine samples have a considerably lower or no anomaly, which suggests isotopic exchange with diagenetic fluids.

In **chapter 3**, the variations of the anomalous isotope signature of tropospheric oxygen in the skeletal tissue of modern mammals are evaluated. This has been conducted using two independent approaches: (1) By triple oxygen isotope analysis of bioapatite of modern mammals and (2) by developing a detailed mass balance model. The fraction of inhaled air oxygen in proportion to the other principal oxygen input sources is primarily a function of the specific metabolic rate, which largely scales with body mass. Therefore, samples of species that comprise a wide range of body masses, from a few g to several 1000 kg, were analysed, leading to the observation of an increasing anomalous oxygen isotope signature with decreasing body mass. Based on the obtained findings, it has been attempted to determine the magnitude of the anomalous oxygen isotope signature of the troposphere at different times within the Cenozoic era from Eocene, Oligocene and Miocene rodent tooth enamel, which gives insight into the respective CO_2-levels. The theoretical mass balance model agrees well with the analytical data, and both indicate an increasing oxygen isotope anomaly in the bioapatite with decreasing body mass. The reconstructed CO_2 concentrations generally agree with previous data obtained with other methods, but the associated error precludes resolving CO_2 fluctuations in a range of a few 100 ppm.

At the Palaeocene-Eocene boundary, one of the most remarkable environmental and climatic changes within the Cenozoic took place, which had its summit within the “Palaeocene Eocene Thermal Maximum” (PETM). This event was associated with a global

negative carbon isotope excursion (CIE), whose source is still discussed controversially. **Chapter 4** targets temperature change and CO_2 fluctuations at the transition of both chronostratigraphic series. This is conducted with the help of a sample series of tooth enamel of the mammal genus *Ectocion* originating from the Clarks Fork Basin (Wyoming, USA), encompassing the respective time interval. The reconstructed temperature change is in good accordance with previous studies on the $^{18}O/^{16}O$ ratio from biogenic apatite within this period. The reconstructed CO_2 levels also indicate that during the peak PETM phase a value of 1550 ppm was not exceeded. Thus, it is suggested that dissociation of marine methane clathrates has been the main source of the CIE.

Chapter 5 investigates inter- and intraspecific as well as intraindividual variations of the carbonate oxygen, phosphate oxygen and the carbon isotope composition of seven different rodent species sampled from owl pellets of a single locality. The results are compared to similar studies on large mammals, and conclusions are drawn on the handling of sample material of small mammals when used for palaeoclimate reconstruction by means of stable isotope analysis. The variability in the oxygen and carbon isotope composition of the analysed tooth and bone material is not higher than that of many large mammals, supporting the relevance of rodents, which are considerably more abundant in the fossil record, for such studies. However, attention has to be paid to the fact that bioapatite-temperature calibrations derived from modern species need to be based exactly on the same skeletal tissue that is analysed from fossil material. This is important because of variations within the time intervals of the mineralisation of different teeth and bone material, in which significant differences of the isotope compositions could be observed, in particular regarding oxygen isotopes.

Kurzfassung

Die Verhältnisse der stabilen Isotope des Sauerstoffs (^{16}O, ^{17}O, ^{18}O) und des Kohlenstoffs (^{12}C, ^{13}C) im biogenen Apatit des Zahn- und Knochenmaterials von Säugetieren lassen Rückschlüsse auf die Isotopie der entsprechenden Sauerstoff- und Kohlenstoffquellen zu. Die Isotopenverhältnisse dieser Quellen (z.B. Trinkwasser, Luftsauerstoff, Nahrung) sind an bestimmte Umwelt- und Klimabedingungen wie Temperatur, Luftfeuchtigkeit, CO_2-Konzentration, Bioproduktivität, Art der Vegetation, Grad der Vegetationsdichte etc. geknüpft. Bestimmt man die Sauerstoff- und Kohlensoffisotopenverhältnisse in diagenetisch unalteriertem fossilem Säugetiermaterial können Aussagen über solche Klima- und Umweltparameter weit in die Erdgeschichte zurück getroffen werden. Darüber hinaus ist es möglich Informationen über Lebensweise und Verhalten der untersuchten Taxa, wie z.B. Wanderverhalten, Geburtensaisonalität, Trinkverhalten, Nahrungspräferenzen, Ressourcenteilung und Habitatnutzung zu erlangen.

Seit dem Beginn der Forschungen auf diesem Gebiet in der 70er und 80er Jahren des 20. Jahrhunderts ist eine große Zahl von Studien erschienen, welche sich der Untersuchung der Sauerstoff- und Kohlenstoffisotopie ($^{18}O/^{16}O$, $^{13}C/^{12}C$) des Zahn- und Knochenmaterials rezenter und fossiler (vorwiegend großer) Säugetiere zu diesen Zwecken widmen. Noch keine zwei Jahrzehnte ist es her, dass erkannt wurde, das troposphärischer Sauerstoff eine anomale 3-O-Isotopenzusammensetzung ($^{17}O/^{16}O$, $^{18}O/^{16}O$) besitzt, die signifikant von fast allen anderen terrestrischen Materialien abweicht. Diese wird in Folge von nicht massenabhängiger Fraktionierung durch photochemische Prozesse in der Stratosphäre hervorgerufen und durch Gasaustausch in die Troposphäre übertragen. Die Magnitude dieser Sauerstoffisotopenanomalie ist eine Funktion der atmosphärischen CO_2-Konzentration, sowie der globalen Bioproduktivität. Kann die 3-O-Isotopie des Luftsauerstoffs zu vergangenen Zeitpunkten in der Erdgeschichte rekonstruiert werden, lässt dies somit auch Rückschlüsse auf die entsprechende CO_2-Konzentration bzw. die globale Bioproduktivität zu. Geologische Archive die dies ermöglichen sind jedoch kaum vorhanden.

Da für Säugetiere der eingeatmete Luftsauerstoff neben Trinkwasser und freiem Wasser in der Nahrung zu den wichtigsten Sauerstoffquellen zählt, ist biogener Apatit rezenter und fossiler Säugetiere eines der wenigen möglichen Materialien die das Potential haben, ein solches Archiv darzustellen.

Die vorliegende Arbeit untersucht die Variation der 3-O-Isotopenzusammensetzung im Bioapatit rezenter Säugetiere, sowie deren Bedeutung als neuen Proxy zur paläo-CO_2-Rekonstruktion und als Indikator für diagenetisch alteriertes Skelettmaterial. Desweiteren werden zwischenartliche, innerartliche und intraindividuelle Variationen der Sauerstoff- und Kohlenstoffisotopie im Bioapatit rezenter Nagetiere untersucht um eine bessere Interpretationsgrundlage für entsprechende Analysedaten fossiler Vertreter dieser größten Ordnung der Säugetiere herzustellen.

Kapitel 2 beschäftigt sich mit der Frage, ob die anomale Isotopensignatur troposphärischen Sauerstoffs als Indikator für diagenetische Alteration des Zahn- und Knochenmaterial von fossilen Säugern genutzt werden kann. Hierzu wurde die 3-O-Isotopie von Zahnschmelz, Dentin und in geringem Umfang auch Knochenmaterial von einzelnen Individuen känozoischer Nagetiere separat analysiert. Während alle Zahnschmelzproben eine deutliche Sauerstoffisotopenanomalie aufweisen, welche in einer Größenordnung liegt die für diagenetisch unalterierten Bioapatit kleiner Säugetiere zu erwarten wäre, zeigen alle Dentinproben eine deutlich niedrigere bis gar keine Anomalie, was auf Isotopenaustausch mit diagenetischen Fluiden hindeutet.

In **Kapitel 3** werden die Variationen der anomalen Isotopensignatur troposphärischen Sauerstoffs im Skelettmaterial von rezenten Säugetieren evaluiert. Dies geschieht anhand zweier voneinander unabhängiger Ansätze: 1. durch 3-O-Isotopenanalyse von rezentem Bioapatit und 2. durch ein detailliertes Massenbilanzmodell. Da der Anteil des veratmeten Luftsauerstoffs im Verhältnis zu den weiteren Sauerstoffquellen in erster Linie von der spezifischen metabolischen Rate abhängt, die weitgehend mit dem Körpergewicht skalierbar ist, wurden Arten aus einem möglichst großen Körpergewichtsbereich von wenigen g bis zu einigen tausend kg untersucht. Es zeigte sich, dass das anomale Isotopensignal mit sinkender Körpermasse zunimmt. Auf Basis der daraus gewonnenen Erkenntnisse wurde versucht die Magnitude der anomalen Sauerstoffisotopensignatur in der Troposphäre zu verschiedenen Zeitpunkten im Känozoikum durch 3-O-Isotopenanalyse von eozänem, oligozänem und miozänem Zahnschmelzmaterial von Nagetieren zu bestimmen um daraus Erkenntnisse über die entsprechenden CO_2-Konzentrationen zu erhalten. Das theoretische Massenbilanzmodell stimmt gut mit den analytisch gewonnenen Daten überein, beide zeigen eine Vergrößerung der 3-O-Isotopenanomalie im Bioapatit mit sinkender Körpermasse. Die rekonstruierten CO_2-

Konzentrationen stimmen generell mit vorhandenen Daten diverser Proxies überein, jedoch erlaubt der assoziierte Fehler es nicht, CO_2-Schwankungen im Bereich von wenigen 100 ppm aufzulösen.

An der Grenze von Paläozän zu Eozän fand eine der einschneidendsten Umwelt- und Klimaveränderungen des Känozoikums statt, welche ihren Höhepunkt im sogenannten "Palaeocene Eocene Thermal Maximum" (PETM) hatte. Dieses war verbunden mit einer globalen negativen Kohlenstoffisotopenexkursion (CIE), deren Quelle bis heute kontrovers diskutiert wird. **Kapitel 4** beschäftigt sich mit den Temperaturschwankungen und Veränderungen der CO_2-Konzentration im Übergangsbereich dieser beiden Zeitalter. Dies geschieht anhand einer diesen Zeitabschnitt umspannenden Probenserie von Zahnschmelz der Säugetiergattung *Ectocion* aus dem Clarks Fork Basin (Wyoming, USA). Die rekonstruierten Temperaturschwankungen stimmen gut mit bereits vorhandenen Studien des $^{18}O/^{16}O$ Verhältnisses an biogenem Apatit aus diesem Zeitintervall überein. Die aus der 3-O-Isotopenzusammensetzung rekonstruierten CO_2-Konzentration deuten darauf hin, dass auch während des Temperaturmaximums an der Paläozän-Eozän Grenze ein Wert von 1550 ppm nicht überschritten wurde, was auf die Dissoziierung von marinem Methanhydrat als Hauptquelle der CIE hinweist.

Kapitel 5 untersucht die zwischenartlichen, innerartlichen und intraindividuellen Variationen der Karbonatsauerstoff-, Phosphatsauerstoff- und Kohlenstoffisotopie sieben verschiedener Nagetierarten anhand von Proben aus Eulengewöllen eines einzelnen Fundortes. Die Ergebnisse werden mit ähnlichen Studien an Großsäugern verglichen, und es werden Schlüsse zum Umgang mit Probenmaterial kleiner Säugetiere bei der Verwendung zur Paläoklimarekonstruktion mittels stabiler Isotope gezogen. Die Variabilität der Sauerstoff- und Kohlenstoffisotopie der untersuchten Zähne und Knochen ist nicht höher als die vieler Großsäuger, was die Relevanz der im Fossilbericht viel häufigeren Nagetiere für derartige Studien unterstützt. Jedoch sollte strikt darauf geachtet werden, dass auf Rezentmaterial basierende Bioapatit-Temperatur-Kalibrationen exakt auf dem gleichen Skelettelement beruhen welches auch als Fossilmaterial untersucht wird, da durch die unterschiedliche Mineralisierungsintervalle verschiedener Zähne und Knochen deutliche Unterschiede in den entsprechenden Isotopenzusammensetzungen, insbesondere in der des Sauerstoffs beobachtet werden konnten.

Table of contents

1. Introduction

The understanding of past climate fluctuations is crucial for an enhanced comprehension of future climate change and the adherent challenges for mankind. To gain insight (beyond theoretical model approaches) into past climatic conditions, certain archives throughout Earth's history are utilised. Those archives to a large extent recruit from the fossilised tissues of ancient life forms. Often, the stable isotope composition of light elements (e.g. oxygen and carbon) in these preserved fossil remains (if diagenetically unaltered) is used in this context. The stable isotope composition of animal and plant tissues is related to that of the substances involved in their formation (e.g. water, air, diet). Those are informative concerning numerous palaeoclimatic and palaeoenvironmental parameters, such as fluctuations in temperature and greenhouse gas levels and associated faunal and floral adaptions or change. One particular of these archives is biogenic apatite of mammals, which in a narrow sense are known to be present on Earth since the Middle Jurassic (Kemp, 2007). The present thesis evaluates new approaches for palaeoclimatic reconstructions utilising the triple oxygen isotope composition of mammalian bioapatite and contributes to an enhanced understanding of oxygen and carbon isotope variations in the skeletal tissues of modern and fossil mammals.

1.1 Basic Definitions

Due to the generally small variations of stable isotope ratios in nature, they are typically not reported as absolute values but as relative deviations from an international reference material to provide a higher precision (e.g. Sharp, 2007; Hoefs, 2009). These relative deviations are reported as δ-values according to the following recommended basic equation (Coplen, 2011):

$$\delta = \left[\left(R_{sample} / R_{standard} \right) - 1 \right], \qquad \text{Eq. 1.1}$$

where R_{sample} and $R_{standard}$ are the heavy to light isotopic ratios in sample and reference material, respectively.

Usually, the δ-values are reported as per mil (‰) variations as follows (e.g. Sharp, 2007; Hoefs, 2009):

$$\delta(‰) = \left[\left(R_{sample} / R_{standard} \right) - 1 \right] \times 1000 \qquad \text{Eq. 1.2}$$

This definition is used in all chapters of the present thesis.

1.2 Oxygen isotopes

1.2.1 General considerations

Oxygen has three stable isotopes (^{16}O, ^{17}O and ^{18}O) with natural abundances of 99.757%, 0.038% and 0.205%, respectively (Rosman and Taylor, 1998).

Despite of the occurrence of three stable isotopes, typically only the $^{18}O/^{16}O$ ratio is analysed when dealing with oxygen isotope ratios, which is motivated by the higher abundance of ^{18}O and the greater mass difference of ^{18}O to ^{16}O compared to ^{17}O to ^{16}O (e.g. Sharp, 2007; Hoefs, 2009). This is reasonable because almost all oxygen fractionation processes on Earth fractionate mass-dependently, i.e. variations in the $^{17}O/^{16}O$ ratio are about half the size than variations in the $^{18}O/^{16}O$ ratio.

However, the occurrence of non mass-dependent fractionation was first observed by Clayton et al. (1973) in meteorites and preliminarily explained by mixing of two distinct oxygen reservoirs in the outer space. In the early 1980s, first evidence of a chemically produced mass-independent oxygen isotope fractionation (^{17}O-excess or ^{17}O-anomaly) was provided by ozone generation via electrical discharge from molecular oxygen (Heidenreich and Thiemens, 1983; Thiemens and Heidenreich, 1983). A naturally produced ^{17}O-anomaly in stratospheric O_3 has first been documented by Mauersberger (1987). In the following years ^{17}O-anomalies have been observed in several other atmospheric gas species, atmospheric aerosols and terrestrial aerosol deposits (Thiemens, 2006 and refs. therein; Fig. 1.1).

A ^{17}O-anomaly in atmospheric O_2 has first been proposed by M. Thiemens (in Bender et al., 1994) and was later confirmed and quantified in detail by Luz et al. (1999) and Luz and Barkan (2005; 2011, Fig. 1.2). This anomaly is induced by photolysis of stratospheric O_3, which ultimately produces ^{17}O-enriched CO_2 and ^{17}O-depleted O_2 due to symmetry effects in the ozone molecule (Yung et al., 1991; Bender et al., 1994, Eq. 1.3-1.4).

$$O_3 + h\nu \rightarrow O_2 + O(^1D) \qquad \text{Eq. 1.3}$$

$$O(^1D) + CO_2 \rightarrow CO_3^* \rightarrow CO_2 + O(^3P) \qquad \text{Eq. 1.4}$$

Thus, a higher pCO_2 results in the production of more ^{17}O-enriched CO_2 related to a larger ^{17}O-depletion of the O_2 reservoir. The small negative ^{17}O-anomaly of tropospheric O_2 results from gas exchange between the troposphere and stratosphere and is counteracted by the production of isotopically "normal" O_2 by photosynthesis. Thus, the magnitude of the ^{17}O-anomaly in tropospheric O_2 is a function of the atmospheric CO_2 concentration (pCO_2) and the global gross primary productivity (GPP) (Luz et al., 1999). Consequently, the triple oxygen isotope composition hitherto has been used to estimate Pleistocene GPP from ice cores (Luz et al., 1999; Blunier et al., 2002; Landais et al., 2007) and Neoproterozoic pCO_2 from terrestrial sulphates formed by oxidative weathering (Bao et al., 2008).

1.2.2 Definitions

The $\delta^{17}O$ and $\delta^{18}O$ values can be defined as:

$$\delta^{17}O(‰) = \left(\frac{\left(\frac{^{17}O}{^{16}O}\right)_{sample}}{\left(\frac{^{17}O}{^{16}O}\right)_{VSMOW}} - 1 \right) \times 1000 \qquad \text{Eq. 1.5}$$

and

$$\delta^{18}O(‰) = \left(\frac{\left(\frac{^{18}O}{^{16}O}\right)_{sample}}{\left(\frac{^{18}O}{^{16}O}\right)_{VSMOW}} - 1 \right) \times 1000 \qquad \text{Eq. 1.6}$$

The abbreviation VSMOW stands for Vienna Standard Mean Ocean Water, which is the internationally accepted reference material for oxygen isotope studies in water and solid materials other than carbonates. Oxygen isotopes in carbonates are commonly reported relative to VPDB (Vienna Pee Dee Belemnite) but it is also possible to report them on the

VSMOW scale. Oxygen isotope values can easily be converted from the VSMOW to the VPDB scale and vice versa by the following equations presented by Coplen et al. (1983):

$$\delta^{18}\mathrm{O(VSMOW)} = 1.03091\,\delta^{18}\mathrm{O(VPDB)} + 30.91 \qquad \text{Eq. 1.7}$$

$$\delta^{18}\mathrm{O(VPDB)} = 0.97002\,\delta^{18}\mathrm{O(VSMOW)} - 29.98 \qquad \text{Eq. 1.8}$$

In equilibrium or kinetic fractionation processes of elements with more than two stable isotopes, the abundance of the stable isotopes is mass-dependently correlated. Thus, $\delta^{18}O$ is related to $\delta^{17}O$ by a power law function:

$$\left(\frac{\left(\frac{^{17}\mathrm{O}}{^{16}\mathrm{O}}\right)_{\mathrm{sample}}}{\left(\frac{^{17}\mathrm{O}}{^{16}\mathrm{O}}\right)_{\mathrm{VSMOW}}}\right) = \left(\frac{\left(\frac{^{18}\mathrm{O}}{^{16}\mathrm{O}}\right)_{\mathrm{sample}}}{\left(\frac{^{18}\mathrm{O}}{^{16}\mathrm{O}}\right)_{\mathrm{VSMOW}}}\right)^{\lambda} \qquad \text{Eq. 1.9}$$

where the exponent λ can have a value between 0.50 and 0.53 (Matsuhisa et al., 1978; Young et al., 2002). In the present study, the triple isotope exponent is denoted as λ if isotope variations of a total reservoir, associated to more than a single physical process, were reported (e.g. rocks and minerals, meteoric water, leaf water). In contrast, it is characterised as θ, if a single equilibrium fractionation process between two specific phases (e.g. bioapatite-water, water-water vapour) is involved.

For an accurate quantification of triple oxygen isotope ratios, the linearised form of the δ-notation ($\delta'^{17}O$, $\delta'^{18}O$) must be used (Hulston and Thode, 1965; Miller, 2002), which is defined as:

$$\delta'^{17}\mathrm{O} = 1000 \times \ln\left(\frac{\delta^{17}\mathrm{O}}{1000} + 1\right) \qquad \text{Eq. 1.10}$$

and

$$\delta'^{18}\mathrm{O} = 1000 \times \ln\left(\frac{\delta^{18}\mathrm{O}}{1000} + 1\right) \qquad \text{Eq. 1.11}$$

Typically, triple oxygen isotope ratios are expressed as $\Delta^{17}O$ values. In a $\delta'^{17}O$ vs. $\delta'^{18}O$ diagram, $\Delta^{17}O$ is defined by the deviation from a given reference line (RL) with:

$$\Delta^{17}O_{RL}^{sample} = \delta'^{17}O_{VSMOW}^{sample} - \lambda_{RL} \times \delta'^{18}O_{VSMOW}^{sample} - \gamma_{RL} \quad \text{Eq. 1.12}$$

where λ denotes the slope of the RL and γ the intercept of the RL.

1.2.3 Reference line, slope and intercept

Reference line

In the studies of the present thesis, a terrestrial rocks and minerals based reference line (Terrestrial Fractionation Line, TFL) is used, which is commonly utilised as a reference line to report $\Delta^{17}O$ values (e.g. Clayton and Mayeda, 1983; Wiechert et al., 2004; Dominguez et al., 2008; Hofmann et al., 2012). The reported $\Delta^{17}O$ data can also be easily converted to the Global Meteoric Water Line (GMWL, Luz and Barkan, 2010), which represents another large terrestrial oxygen reservoir, or to other reference lines that are specifically chosen for the purpose of the respective study.

Slope of the reference line (λ)

In **chapter 2**, a TFL with a slope β (which sometimes is used instead of λ) of 0.5250 ± 0.0007 (1σ) is used, based on 290 single analyses of terrestrial rocks and minerals. **Chapter 3** and **4** use an improved, slightly different slope λ of 0.5251 ± 0.0007 (1σ), based on a considerably higher number (n=1071) of terrestrial rock and mineral samples. Both slopes agree within error with previously reported TFL slopes (Miller, 2002; Pack et al., 2007; Rumble et al., 2007; Hofmann and Pack, 2010).

Intercept of the reference line (γ)

Whereas in **chapter 2** a zero intercept γ is used for simplicity, **chapter 3** and **4** use an intercept γ of -0.048 ± 0.005‰, which represents a weighted mean between the results of two recently conducted studies (M. Hofmann, pers. comm., γ = -0.036 ± 0.018‰; Tanaka and Nakamura, 2012, γ = -0.051 ± 0.005‰, both given relative to a TFL of 0.5251).

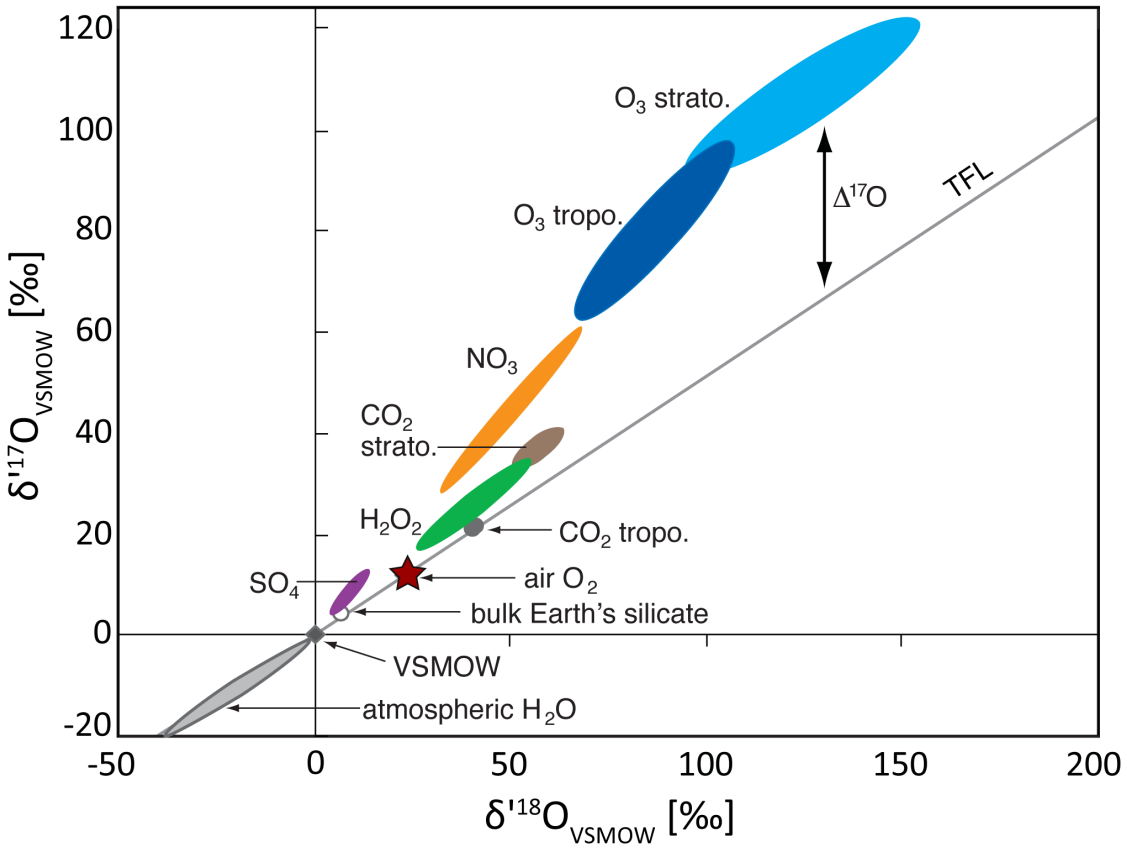

Fig. 1.1: Triple oxygen isotope composition of atmospheric and terrestrial substances, illustrating their deviations from a Terrestrial Reference Line (from Thiemens, 2006, modified). The largest ^{17}O-anomalies can be observed in O_3 and NO_3, whereas the small ^{17}O-excess of air O_2 (red star) is not identifiable within the chosen scale.

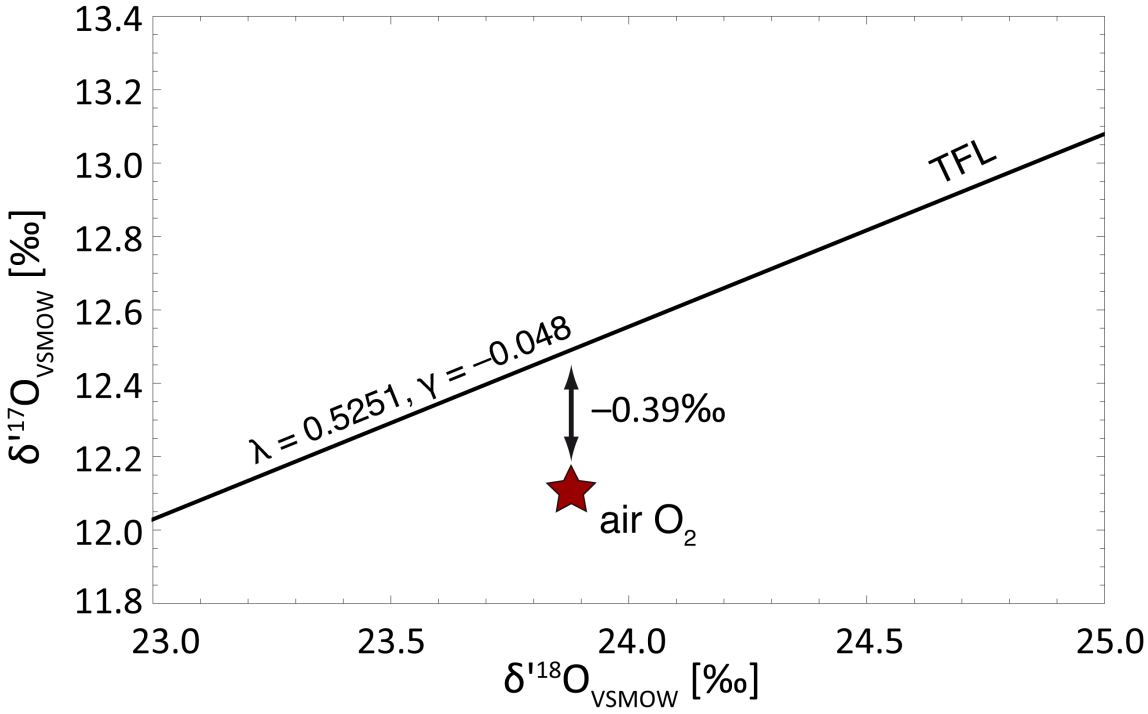

Fig. 1.2: Detail of Fig. 1.1, illustrating the small ^{17}O-anomaly of air O_2 (red star) in relation to the TFL with slope λ = 0.5251 and intercept γ = –0.048, used within chapters 3 and 4 of the present thesis.

1.2.4 Stable oxygen isotopes in mammalian bioapatite

The calcium hydroxyl apatite of teeth and bones of mammals can be characterised by the chemical formula $Ca_{4.5}[(PO_4)_{2.7}(HPO_4)_{0.2}(CO_3)_{0.3}](OH)_{0.5}$ (Driessens and Verbeeck, 1990). The major portion of oxygen in mammalian bioapatite is present in the phosphate, minor fractions are held in the carbonate and in the hydroxyl group, e.g. 91.5% phosphate oxygen vs. 6.5% and 2.9% as carbonate and hydroxyl, respectively, in the case of tooth enamel (Elliot, 1997).

Mammalian bioapatite precipitates in equilibrium from mammalian body water at a constant body temperature which typically ranges between 30 and 40°C (e.g. Clarke and Rothery, 2008), dependent from the respective taxa. The oxygen isotope composition of mammalian body water is related to its different oxygen isotope sources and controlled by a total of all oxygen input and output fluxes through the body water pool. Oxygen input sources for mammals are drinking water, food water, air oxygen, organic food compounds and water vapour in air, which all are linked to either local surface water or air oxygen, in which the latter has a constant value of ~24‰ (Barkan and Luz, 2005). Output fluxes are exhaled CO_2, liquid water in sweat, urine and feces as well as orally, nasally and transcutaneously released water vapour (Luz and Kolodny, 1985; Bryant and Froelich, 1995; Kohn, 1996; Fig. 1.3).

The applicability of the oxygen isotope composition ($\delta^{18}O$) of mammalian bioapatite for palaeoclimatic research has been first suggested by Longinelli (1974) and was fundamentally evaluated by a number of pioneering studies in the mid 1980s (Longinelli, 1984; Luz et al., 1984; Luz and Kolodny, 1985), that demonstrated a linear relationship between $\delta^{18}O$ of mammalian bioapatite and ingested drinking water. Combined with the knowledge of a strong correlation between the oxygen isotope composition of precipitation (i.e. surface water) and air temperature (Dansgaard, 1964), the potential to infer palaeotemperatures from fossil mammalian bioapatite had been offered.

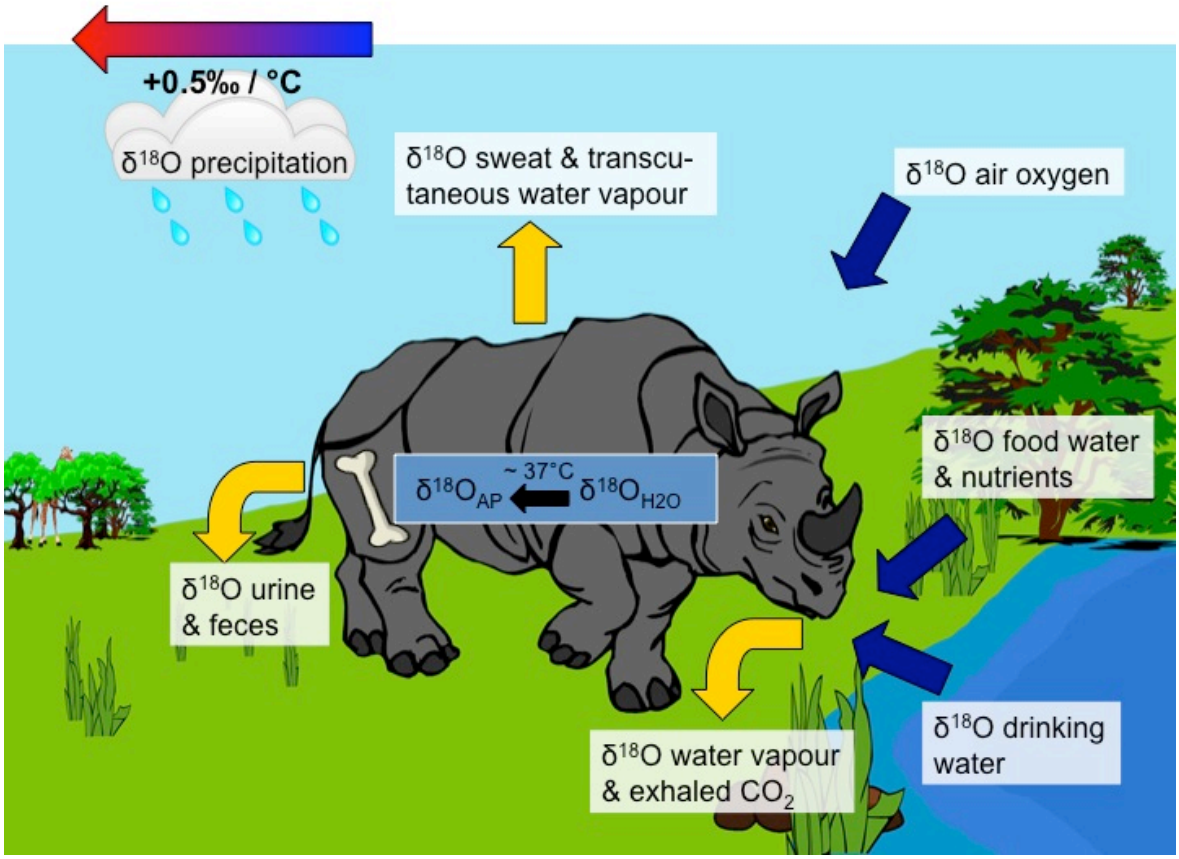

Fig. 1.3: Sketch, illustrating the different input and output fluxes of oxygen in a mammalian body. The principal oxygen sources are drinking water, free water in food and air O_2. The fractionation between body water and bioapatite phosphate and carbonate is constant due to a constant body temperature.

With some delay after the initial studies, the link between mammalian bioapatite, drinking water and other environmental factors such as humidity has been explored further (e.g. Ayliffe and Chivas, 1990; D'Angela and Longinelli, 1990; Luz et al., 1990). The first oxygen isotope studies on bioapatite of fossil mammals have been published in the late 1980s and early 1990s (e.g. Koch et al., 1989; Ayliffe et al., 1992; Quade et al., 1992; D'Angela and Longinelli, 1993; Bryant et al., 1994; Sánchez Chillón et al., 1994). Beyond palaeotemperature reconstruction, $\delta^{18}O$ of bioapatite can provide insight into climate seasonality, relative humidity or aridity of palaeoenvironments as well as mobility, birth seasonality and drinking behaviour of specific mammalian taxa (e.g. Balasse et al., 2002; 2003; Kohn and Cerling, 2002; Levin et al., 2006; Tütken et al., 2006; Tütken and Vennemann, 2009).

Both, the phosphate ($\delta^{18}O_{PO4}$) as well as the carbonate component ($\delta^{18}O_{CO3}$) of mammalian bioapatite are commonly analysed for palaeoclimatic, (palaeo)ecological and (palaeo)environmental studies. In general, analysis of $\delta^{18}O_{PO4}$ is much more laborious than that of $\delta^{18}O_{CO3}$. However, $\delta^{18}O_{PO4}$ is less prone to diagenetic alteration than $\delta^{18}O_{CO3}$

and thus it is often preferred when dealing with fossil material (e.g. Kohn and Cerling, 2002). A nearly constant offset ($\Delta^{18}O_{CO3\text{-}PO4}$) exists between both oxygen-bearing components that can vary by a few ‰ within and between taxa. In a wider sense it is related to physiological reasons but this is not completely deciphered until now (e.g. Martin et al., 2008). Previously reported values for $\Delta^{18}O_{CO3\text{-}PO4}$ range from 7.5 to 11.4‰ (Chenery et al., 2012; Gehler et al., 2012 and refs. therein).

A completely new approach, based on the triple oxygen isotope composition, has been supposed by A. Pack (pers. comm.) and is basically evaluated within three of the four studies included in the thesis presented here (Gehler et al., 2011; Gehler et al., in preparation; Pack et al., in press).

The approach is based on the fact that tropospheric O_2, along with drinking water and free water in food, is one of the main oxygen sources for mammals (e.g. Kohn, 1996). Thus, it seemed to be likely that a fraction of its ^{17}O-anomaly (proportionate to the other oxygen sources) should also be detectable in mammalian bioapatite by triple oxygen isotope analysis. If it is then possible to relate $\Delta^{17}O$ of mammalian bioapatite to that of tropospheric O_2 by empirical studies on modern mammals and/or by mass balance modelling, independent information could be obtained on the parameters that determine the magnitude of $\Delta^{17}O$ of air O_2 such as pCO_2 and GPP.

1.3 Carbon isotopes

1.3.1 General considerations and definitions

Carbon has two stable isotopes (^{12}C and ^{13}C) with natural abundances of 98.93% and 1.07%, respectively (Rosman and Taylor, 1998).

The $\delta^{13}C$ value can be defined as:

$$\delta^{13}\mathrm{C}(‰) = \left(\frac{\left(\frac{^{13}\mathrm{C}}{^{12}\mathrm{C}} \right)_{\mathrm{sample}}}{\left(\frac{^{13}\mathrm{C}}{^{12}\mathrm{C}} \right)_{\mathrm{VPDB}}} - 1 \right) \times 1000 \qquad \text{Eq. 1.13}$$

The abbreviation VPDB stands for Vienna Pee Dee Belemnite, which is the internationally accepted reference material for carbon isotope studies.

1.3.2 Stable carbon isotopes in mammalian bioapatite

The carbon isotope composition of mammalian bioapatite can be analysed from the carbonate fraction in teeth and bones. In the bioapatite of terrestrial mammals, $\delta^{13}C$ is controlled by the carbon isotope composition of the ingested diet. A ^{13}C-enrichment by 9 to 15‰ relative to the respective diet occurs due to specific fractionation processes within the mammalian body. Differences in this enrichment factor among mammalian taxa are suggested to be mainly related to differences in the digestive physiology (e.g. Kohn and Cerling, 2002; Passey et al., 2005; Koch, 2007).

The first studies that determined the $\delta^{13}C$ of mammalian bioapatite on modern mammals have been conducted in the late 1970s by DeNiro and Epstein (1978a; 1978b) and Land et al. (1980). Soon after these initial studies, also the first fossil mammals have been analysed for $\delta^{13}C$ with the intent of dietary reconstructions (Ericson et al., 1981; Sullivan and Krueger, 1981). In the following more than three decades, a very large number of studies has been published that aim to track the $\delta^{13}C$ of ingested food of modern and fossil mammals. In particular, herbivorous mammals have been investigated. The reconstructed $\delta^{13}C$ of ingested plant material can be informative on specific habitats, type of vegetation cover (i.e., C_3 versus C_4 plants) and vegetation density, as well as on habitat use, resource partitioning, feeding behaviour and seasonal changes of diet (e.g. Quade et

al., 1992; MacFadden et al., 1994; Quade et al., 1995; MacFadden and Cerling, 1996; Cerling et al., 1997; Cerling et al., 1999; MacFadden et al., 1999; Harris and Cerling, 2002; Drucker et al., 2003; Cerling et al., 2004; MacFadden and Higgins, 2004; Feranec and MacFadden, 2006; Feranec, 2007; Nelson, 2007; Zanazzi and Kohn, 2008; Tütken and Vennemann, 2009).

1.4 Focus of the present thesis

The main goal of the present thesis (**chapters 2**, **3** and **4**) is to provide insight into the triple oxygen isotope composition of bioapatite of modern mammals and to explore the respective potential for palaeoclimate reconstructions, particularly as a new proxy for pCO_2 throughout the Cenozoic, when mammals became common on Earth.

A second goal was to supply a basic contribution to the oxygen and carbon isotope variability in rodents, which are utilised by an increasing number of studies for palaeoclimatic and palaeoenvironmental reconstructions within the last decade (**chapter 5**).

A detailed focus of the studies included in the present thesis is given below:

Chapter 2: *Triple oxygen isotope analysis of bioapatite as tracer for diagenetic alteration of bones and teeth*

Tropospheric oxygen has a small but distinct ^{17}O-anomaly. As inhaled air oxygen is an important oxygen input flux for mammals, a fraction of this anomaly is transferred to mammalian body water and subsequently to the bioapatite that forms the teeth and bones of mammals. Thus, diagenetically unaltered fossil mammal remains should record an anomalous oxygen isotope signal, whereas skeletal tissues that underwent oxygen isotope exchange with an isotopically "normal" diagenetic fluid may have lost it. The intent of this study is to evaluate this on different skeletal materials (i.e. tooth enamel, dentine, bone) that are thought to be unequally prone to diagenetic alteration. Small mammals, i.e. rodents, have been chosen for this purpose, as their physiology suggests the largest portion of inhaled air oxygen in relation to the other principal oxygen sources.

Chapter 3: *Exploring the usability of isotopically anomalous oxygen in bones and teeth as palaeo-CO_2-barometer*

The fraction of inhaled anomalous tropospheric oxygen in proportion to the other isotopically "normal" oxygen input fluxes of mammals (i.e. drinking water and free water in food) is primarily a function of the specific metabolic rate, which largely scales with body mass. **Chapter 3** focuses on the exploration of the variations of $\Delta^{17}O$ in mammalian bioapatite using species over a large range of body masses (~2 g to ~5000 kg) and with different nutritional behaviours (herbivores, omnivores, carnivores). In addition to the analytical approach on bioapatite of modern mammals, a detailed mass balance model is developed. In a further step, tooth enamel of Eocene, Oligocene and Miocene rodents is

analysed for its triple oxygen isotope composition. Based on the findings of the first part of the study, it is aimed to determine the $\Delta^{17}O$ of tropospheric oxygen within the respective era, which is informative on pCO_2.

Chapter 4: *Temperature and atmospheric CO_2-concentration changes across the Palaeocene-Eocene Thermal Maximum (PETM) – new insights from triple oxygen isotope analysis of mammalian bioapatite*

The Palaeocene-Eocene transition is associated with an abrupt environmental change, characterised by increased temperatures of several °C and a globally abundant large negative carbon isotope excursion (CIE) within a period of less than 200,000 years. This time interval is termed the "Palaeocene-Eocene Thermal Maximum" (PETM). In **chapter 4** for the first time $\delta^{18}O$ of bioapatite is used to track the temperature change across the PETM (as done successfully also in previous studies) is used together with the newly developed triple oxygen isotope approach of **chapter 3**, attempting to track both, temperature and pCO_2 simultaneously by a single proxy. This is conducted on a sample series of tooth enamel of the condylarth mammal *Ectocion* from pre-, peak- and post-PETM/CIE strata located in the Clark Forks Basin (Wyoming, USA).

Chapter 5: *Oxygen and Carbon Isotope Variations in a Modern Rodent Community – Implications for Palaeoenvironmental Reconstructions*

Today, new and improved mass spectrometric techniques allow oxygen and carbon isotope analysis of only mg-sized sample amounts of bioapatite, bringing also rodents into the focus of interest. A considerable number of studies have been published within the last decade that infer palaeoclimatic and palaeoenvironmental conditions on the basis of $\delta^{18}O$ and $\delta^{13}C$ of bioapatite from fossil rodents. However, an important prerequisite for this is a thorough understanding of the inter-specific, intra-specific and intra-individual oxygen and carbon isotope variabilities of the examined taxa. Whereas this is well investigated for a number of large mammals, respective studies are almost completely lacking for rodents. To address this deficiency, **chapter 5** investigates incisors, different molars and bone material of multiple individuals of seven sympatric modern rodent species derived from owl pellets of a single locality.

References

Ayliffe, L.K., Chivas, A.R. (1990). Oxygen isotope composition of bone phosphate of Australian kangaroos: potential as a palaeoenvironmental recorder. *Geochimica et Cosmochimica Acta* **54**, 2603-2609.

Ayliffe, L.K., Lister, A.M., Chivas, A.R. (1992). The preservation of glacial-interglacial climatic signatures in the oxygen isotopes of elephant skeletal phosphate. *Palaeogeography, Palaeoclimatology, Palaeoecology* **99**, 179-191.

Balasse, M., Ambrose, S.H., Smith, A.B., Price, T.D. (2002). The seasonal Mobility Model for Prehistoric Herders in the South-western Cape of South Africa Assessed by Isotopic Analysis of Sheep Tooth Enamel. *Journal of Archaeological Science* **29**, 917-932.

Balasse, M., Smith, A.B., Ambrose, S.H., Leigh, S.R. (2003). Determining Sheep Birth Seasonality by Analysis of Tooth Enamel Oxygen Isotope Ratios: The Late Stone Age Site of Kasteelberg (South Africa). *Journal of Archaeological Science* **30**, 205-215.

Bao, H., Lyons, J., Zhou, C. (2008). Triple oxygen isotope evidence for elevated CO_2 levels after a Neoproterozoic glaciation. *Nature* **453**, 504-506.

Barkan, E., Luz, B. (2005). High precision measurements of $^{17}O/^{16}O$ and $^{18}O/^{16}O$ ratios in H_2O. *Rapid Communications in Mass Spectrometry* **19**, 3737-3742.

Bender, M., Sowers, T., Labeyrie, L. (1994). The Dole effect and its variations during the last 130,000 years as measured in the Vostok ice core. *Global Biogeochemical Cycles* **8**, 363-376.

Blunier, T., Barnett, B., Bender, M.L., Hendricks, M.B. (2002). Biological oxygen productivity during the last 60,000 years from triple oxygen isotope measurements. *Global Biogeochemical Cycles* **16**, 1-15.

Bryant, J.D., Froelich, P.N. (1995). A model of oxygen isotope fractionation in body water of large mammals. *Geochimica et Cosmochimica Acta* **59**, 4523-4537.

Bryant, J.D., Luz, B., Froelich, P.N. (1994). Oxygen isotopic composition of fossil horse tooth phosphate as a record of continental paleoclimate. *Palaeogeography, Palaeoclimatology, Palaeoecology* **107**, 303-316.

Cerling, T.E., Harris, J.M., Ambrose, S.H., Leakey, M.G., Solounias, N. (1997). Dietary and environmental reconstruction with stable isotope analysis of herbivore tooth enamel from the Miocene locality of Fort Ternan, Kenya. *Journal of Human Evolution* **33**, 635-650.

Cerling, T.E., Harris, J.M., Leakey, M.G. (1999). Browsing and grazing in elephants: the isotope record of modern and fossil proboscideans. *Oecologica* **120**, 364-374.

Cerling, T.E., Hart, J.A., Hart, T.B. (2004). Stable isotope ecology in the Ituri Forest. *Oecologica* **138**, 5-12.

Chenery, C.A., Pashley, V., Lamb, A.L., Sloane, H.J., Evans, J.A. (2012). The oxygen isotope relationship between the phosphate and structural carbonate fractions of human bioapatite. *Rapid Communications in Mass Spectrometry* **26**, 309-319.

Clarke, A., Rothery, P. (2008). Scaling of body temperature in mammals and birds. *Functional Ecology* **22**, 58-67.

Clayton, R.N., Grossman, L., Mayeda, T.K. (1973). A component of primitive nuclear composition in carbonaceous meteorites. *Science* **182**, 485-488.

Clayton, R.N., Mayeda, T.K. (1983). Oxygen Isotopes in Eucrites, Shergottites, Nakhlites, and Chassignites. *Earth and Planetary Science Letters* **62**, 1-6.

Coplen, T.B. (2011). Guidelines and recommended terms for expression of stable-isotope-ratio and gas-ratio measurement results. *Rapid Communications in Mass Spectrometry* **25**, 2538-2560.

Coplen, T.B., Kendall, C., Hopple, J. (1983). Comparison of stable isotope reference samples. *Nature* **302**, 236-238.

D'Angela, D., Longinelli, A. (1990). Oxygen isotopes in living mammal's bone phosphate: further results. *Chemical Geology* **86**, 75-82.

D'Angela, D., Longinelli, A. (1993). Oxygen isotopic composition of fossil mammal bones of Holocene age: Palaeoclimatological considerations. *Chemical Geology* **103**, 171-179.

Dansgaard, W. (1964). Stable isotopes in precipitation. *Tellus* **16**, 436-468.

DeNiro, M.J., Epstein, S. (1978a). Carbon isotopic evidence for different feeding patterns in two hyrax species occupying the same habitat. *Science* **201**, 906-908.

DeNiro, M.J., Epstein, S. (1978b). Influence of diet on the distribution of carbon isotopes in animals. *Geochimica et Cosmochimica Acta* **42**, 495-506.

Dominguez, G., Jackson, T., Brothers, L., Barnett, B., Nguyen, B., Thiemens, M.H. (2008). Discovery and measurement of an isotopically distinct source of sulfate in Earth's atmosphere. *Proceedings of the National Academy of Sciences* **105**, 12769-12773.

Driessens, F.M.C., Verbeeck, R.M.H. (1990). *Biominerals*. CRC Press (Boca Raton), 428 pp.

Drucker, D., Bocherens, H., Bridault, A., Billiou, D. (2003). Carbon and nitrogen isotopic composition of red deer (*Cervus elaphus*) collagen as a tool for tracking palaeoenvironmental change during the Late-Glacial and Early Holocene in the northern Jura (France). *Palaeogeography, Palaeoclimatology, Palaeoecology* **195**, 375-388.

Elliot, J.C. (1997). Structure, crystal chemistry and density of enamel apatites. In: Chadwick, D.J., Cardew, G. (Eds.), *Dental Enamel*. Wiley & Sons (Chichester), pp. 54-67.

Ericson, J.E., Sullivan, C.H., Boaz, N.T. (1981). Diets of Pliocene mammals from Omo, Ethiopia, deduced from carbon isotopic ratios in tooth apatite. *Palaeogeography, Palaeoclimatology, Palaeoecology* **36**, 69-73.

Feranec, R.S. (2007). Stable carbon isotope values reveal evidence of resource partitioning among ungulates from modern C_3-dominated ecosystems in North America. *Palaeogeography, Palaeoclimatology, Palaeoecology* **252**, 575-585.

Feranec, R.S., MacFadden, B.J. (2006). Isotopic discrimination of resource partitioning among ungulates in C_3-dominated communities from the Miocene of Florida and California. *Paleobiology* **32**, 191-205.

Gehler, A., Gingerich, P.D., Pack, A. (in preparation). Temperature and atmospheric CO_2-concentration changes across the Palaeocene-Eocene Thermal Maximum (PETM) – new insights from triple oxygen isotope analysis of mammalian bioapatite.

Gehler, A., Tütken, T., Pack, A. (2011). Triple oxygen isotope analysis of bioapatite as tracer for diagenetic alteration of bones and teeth. *Palaeogeography, Palaeoclimatology, Palaeoecology* **310**, 84-91.

Gehler, A., Tütken, T., Pack, A. (2012). Oxygen and Carbon Isotope Variations in a Modern Rodent Community – Implications for Palaeoenvironmental Reconstructions. *PloS ONE* **7**, e49531.

Harris, J.M., Cerling, T.E. (2002). Dietary adaptions of extant and Neogene African suids. *Journal of the Zoological Society of London* **256**, 45-54.

Heidenreich, J.E., Thiemens, M. (1983). A non-mass-dependent isotope effect in the production of ozone from molecular oxygen. *Journal of Chemical Physics* **78**, 892-895.

Hoefs, J. (2009). *Stable Isotope Geochemistry*. Springer (Berlin, Heidelberg), 285 pp.

Hofmann, M.E.G., Horváth, B., Pack, A. (2012). Triple oxygen isotope equilibrium fractionation between carbon dioxide and water. *Earth and Planetary Science Letters* **319-320**, 159-164.

Hofmann, M.E.G., Pack, A. (2010). Technique for High-Precision Analysis of Triple Oxygen Isotope Ratios in Carbon Dioxide. *Analytical Chemistry* **82**, 4357-4361.

Hulston, J.R., Thode, H.G. (1965). Variations in the S^{33}, S^{34} and S^{36} contents of meteorites and their relation to chemical and nuclear effects. *Journal of Geophysical Research* **70**, 3475-3484.

Kemp, T.S. (2007). *The Origin and Evolution of Mammals*. Oxford University Press (New York), 331 pp.

Koch, P. (2007). Isotopic study of the biology of modern and fossil vertebrates. In: Michener, R., Lajtha, L. (Eds.), *Stable Isotopes in Ecology and Environmental Science*. Blackwell Publishing (Boston), pp. 99-154.

Koch, P.L., Fisher, D.C., Dettman, D. (1989). Oxygen Isotope variation in the tusks of extinct proboscideans: A Measure of season of death and seasonality. *Geology* **17**, 515-519.

Kohn, M.J. (1996). Predicting animal $\delta^{18}O$: accounting for diet and physiological adaption. *Geochimica et Cosmochimica Acta* **60**, 4811-4829.

Kohn, M.J., Cerling, T.E. (2002). Stable Isotope Compositions of Biological Apatite. *Reviews in Mineralogy and Geochemistry* **48**, 455-488.

Land, L.S., Lundelius, E.L., Valastro, S. (1980). Isotopic ecology of deer bones. *Palaeogeography, Palaeoclimatology, Palaeoecology* **32**, 143-151.

Landais, A., Lathiere, J., Barkan, E., Luz, B. (2007). Reconsidering the change in global biosphere productivity between the Last Glacial Maximum and present day from the triple oxygen isotopic composition of air trapped in ice cores. *Global Biogeochemical Cycles* **21**, GB1025.

Levin, N.E., Cerling, T.E., Passey, B.H., Harris, J.M., Ehleringer, J.R. (2006). A stable isotope aridity index for terrestrial environments. *Proceedings of the National Academy of Sciences* **103**, 11201-11205.

Longinelli, A. (1974). Preliminary oxygen isotope measurements of phosphate from mammal teeth and bones. In: Labeyri, J. (Ed.), *Les méthodes quantitatives d'étude des variations du climat au cours du pléistocène, Gif-sur-Yvette, 5 9 juin 1973* (= Colloques internationaux du Centre National de la Recherche Scientifique **219**), pp. 267-271.

Longinelli, A. (1984). Oxygen isotopes in mammal bone phosphate: a new tool for paleohydrological and paleoclimatological research? *Geochimica et Cosmochimica Acta* **48**, 385-390.

Luz, B., Barkan, E. (2005). The isotopic ratios $^{17}O/^{16}O$ and $^{18}O/^{16}O$ in molecular oxygen and their significance in biogeochemistry. *Geochimica et Cosmochimica Acta* **69**, 1099-1110.

Luz, B., Barkan, E. (2010). Variations of $^{17}O/^{16}O$ and $^{18}O/^{16}O$ in meteoric waters. *Geochimica et Cosmochimica Acta* **74**, 6276-6286.

Luz, B., Barkan, E. (2011). The isotopic composition of atmospheric oxygen. *Global Biogeochemical Cycles* **25**, GB3001.

Luz, B., Barkan, E., Bender, M.L., Thiemens, M.H., Boering, K.A. (1999). Triple-isotope composition of atmospheric oxygen as a tracer of biosphere productivity. *Nature* **400**, 547-550.

Luz, B., Cormie, A.B., Schwarcz, H.P. (1990). Oxygen isotope variations in phosphate of deer bones. *Geochimica et Cosmochimica Acta* **54**, 1723-1728.

Luz, B., Kolodny, Y. (1985). Oxygen isotope variations in phosphate of biogenic apatites, IV. Mammal teeth and bones. *Earth and Planetary Science Letters* **75**, 29-36.

Luz, B., Kolodny, Y., Horowitz, M. (1984). Fractionation of oxygen isotopes between mammalian bone phosphate and environmental drinking water. *Geochimica et Cosmochimica Acta* **48**, 1689-1693.

MacFadden, B.J., Cerling, T.E. (1996). Mammalian herbivore communities, ancient feeding ecology and carbon isotopes: a 10-million-year sequence from the Neogene of Florida. *Journal of Vertebrate Paleontology* **16**, 103-115.

MacFadden, B.J., Higgins, P. (2004). Ancient ecology of 15-million-year-old browsing mammals within C3 plant communities from Panama. *Oecologica* **140**, 169-182.

MacFadden, B.J., Solounias, N., Cerling, T.E. (1999). Ancient Diets, Ecology, and Extinction of 5-Million-Year-Old Horses from Florida. *Science* **283**, 824-827.

MacFadden, B.J., Wang, Y., Cerling, T.E., Anaya, F. (1994). South American fossil mammals and carbon isotopes: a 25 million-year sequence from the Bolivian Andes. *Palaeogeography, Palaeoclimatology, Palaeoecology* **107**, 257-268.

Martin, C., Bentaleb, I., Kaandorp, R., Iacumin, P., Chatri, K. (2008). Intra-tooth study of modern rhinoceros enamel $\delta^{18}O$: Is the difference between phosphate and carbonate $\delta^{18}O$ a sound diagenetic test? *Palaeogeography, Palaeoclimatology, Palaeoecology* **266**, 183-187.

Matsuhisa, Y., Goldsmith, J.R., Clayton, R.N. (1978). Mechanisms of hydrothermal crystallization of quartz at 250°C and 15 kbar. *Geochimica et Cosmochimica Acta* **42**, 173-182.

Mauersberger, K. (1987). Ozone isotope measurements in the stratosphere. *Geophysical Research Letters* **8**, 935-937.

Miller, M.F. (2002). Isotopic fractionation and the quantification of ^{17}O anomalies in the oxygen three-isotope system: an appraisal and geochemical significance. *Geochimica et Cosmochimica Acta* **66**, 1881-2055.

Nelson, S.V. (2007). Isotopic reconstructions of habitat change surrounding the extinction of *Sivapithecus*, a Miocene hominoid, in the Siwalik Group of Pakistan. *Palaeogeography, Palaeoclimatology, Palaeoecology* **243**, 204-222.

Pack, A., Gehler, A., Süssenberger, A. (in press). Exploring the usability of isotopically anomalous oxygen in bones and teeth as paleo-CO_2-barometer. *Geochimica et Cosmochimica Acta*, http://dx.doi.org/10.1016/j.gca.2012.10.017.

Pack, A., Toulouse, C., Przybilla, R. (2007). Determination of oxygen triple isotope ratios of silicates without cryogenic separation of NF_3 — technique with application to analyses of technical O_2 gas and meteorite classification. *Rapid Communications in Mass Spectrometry* **21**, 3721-3728.

Passey, B.H., Robinson, T.F., Ayliffe, L.K., Cerling, T.E., Sponheimer, M., Dearing, M.D., Roeder, B.L., Ehleringer, J.R. (2005). Carbon isotope fractionation between diet, breath CO_2, and bioapatite in different mammals. *Journal of Archaeological Science* **32**, 1459-1470.

Quade, J., Cerling, T.E., Andrews, P., Alpagut, B. (1995). Paleodietary reconstruction of Miocene faunas from Pasalar, Turkey using stable carbon and oxygen isotopes of fossil tooth enamel. *Journal of Human Evolution* **28**, 373-384.

Quade, J., Cerling, T.E., Barry, J.C., Morgan, M.E., Pilbeam, D.R., Chivas, A.R., Lee-Thorp, J.A., Van Der Merwe, N.J. (1992). A 16-Ma record of paleodiet using carbon and oxygen isotopes in fossil teeth from Pakistan. *Chemical Geology* **94**, 183-192.

Rosman, K.J.R., Taylor, P.D.P. (1998). Isotopic composition of the elements 1997 (Technical Report). *Pure and Applied Chemistry* **70**, 217-235.

Rumble, D., Miller, M.F., Franchi, I.A., Greenwood, J.P. (2007). Oxygen three-isotope fractionation lines in terrestrial silicate minerals: an inter-laboratory comparison for hydrothermal quartz and eclogite garnet. *Geochimica et Cosmochimica Acta* **71**, 3592-3600.

Sánchez Chillón, B., Alberdi, M.T., Leone, G., Bonadonna, F.P., Stenni, B., Longinelli, A. (1994). Oxygen isotopic composition of fossil equid tooth and bone phosphate: an archive of difficult interpretation. *Palaeogeography, Palaeoclimatology, Palaeoecology* **107**, 317-328.

Sharp, Z. (2007). *Principles of Stable Isotope Geochemistry*. Pearson / Prentice Hall (Upper Saddle River), 344 pp.

Sullivan, C.H., Krueger, H.W. (1981). Carbon isotope analysis of separate chemical phases in modern and fossil bone. *Nature* **292**, 333-335.

Tanaka, R., Nakamura, E. (2012). Kinetic isotope fractionation effect observed in oxygen triple isotope ratios in terrestrial silicate minerals, Sixth International Symposium on Isotopomers. Washington DC, p. 88.

Thiemens, M.H. (2006). History and Applications of Mass-Independent Isotope Effects. *Annual Review of Earth and Planetary Sciences* **34**, 217-262.

Thiemens, M.H., Heidenreich, J.E. (1983). The Mass-Independent Fractionation of Oxygen: A Novel Isotope Effect and Its Possible Cosmochemical Implications. *Science* **219**, 1073-1075.

Tütken, T., Vennemann, T. (2009). Stable isotope ecology of Miocene large mammals from Sandelzhausen, southern Germany. *Paläontologische Zeitschrift* **83**, 207-226.

Tütken, T., Vennemann, T.W., Janz, H., Heizmann, E.P.J. (2006). Palaeoenvironment and palaeoclimate of the Middle Miocene lake in the Steinheim Basin, SW Germany: A reconstruction from C, O, and Sr isotopes of fossil remains. *Palaeogeography, Palaeoclimatology, Palaeoecology* **241**, 457-491.

Wiechert, U.H., Halliday, A.N., Palme, H., Rumble, D. (2004). Oxygen isotope evidence for rapid mixing of the HED meteorite parent body. *Earth and Planetary Science Letters* **221**, 373-382.

Young, E.D., Galy, A., Nagahara, H. (2002). Kinetic and equilibrium mass-dependent isotope fractionation laws in nature and their geochemical and cosmochemical significance. *Geochimica et Cosmochimica Acta* **66**, 1095-1104.

Yung, Y.L., DeMore, W.B., Pinto, J.P. (1991). Isotopic exchange between carbon dioxide and ozone via $O(^1D)$ in the stratosphere. *Geophysical Research Letters* **18**, 13-16.

Zanazzi, A., Kohn, M.J. (2008). Ecology and physiology of White River mammals based on stable isotope ratios of teeth. *Palaeogeography, Palaeoclimatology, Palaeoecology* **257**, 22-37.

2. Manuscript I

Triple oxygen isotope analysis of bioapatite as tracer for diagenetic alteration of bones and teeth

Alexander Gehler[a,*], Thomas Tütken[b], Andreas Pack[a]

[a] Georg-August-Universität, Geowissenschaftliches Zentrum, Abteilung Isotopengeologie, Goldschmidtstraße 1, D-37077 Göttingen, Germany

[b] Rheinische Friedrich-Wilhelms-Universität, Steinmann-Institut für Geologie, Mineralogie und Paläontologie, Emmy Noether-Gruppe „Knochen-Geochemie“, Poppelsdorfer Schloss, D-53115 Bonn, Germany

Published in *Palaeogeography, Palaeoclimatology, Palaeoecology* ***310*** *(2011) 84–91*

Abstract

The detection of diagenetic alteration is critical for palaeoclimate reconstruction that is based on the oxygen isotope composition of fossil bones and teeth. So far, no direct chemical proxy has been found to track diagenetic modification of the oxygen isotope ratios. Here, a new approach to identify diagenetic changes of $\delta^{18}O_{PO4}$ values in skeletal apatite of small mammals by means of triple oxygen isotope analysis (^{16}O, ^{17}O and ^{18}O) is presented.

Our method is based on the fact that inhaled air oxygen (O_2) has an isotope anomaly on its rare isotope ^{17}O. Inhaled air O_2 is a major source of oxygen in small land-living mammals. A fraction of the anomaly is transferred via body water to skeletal apatite, where it can be detected by means of $\delta^{17}O$ and $\delta^{18}O$ analyses. The approach, considering the current analytical uncertainty, is restricted to small mammals with body masses ≤1 kg. This is due to the low specific metabolic rates of large mammals, resulting in a lower fraction of oxygen inhaled via breathing relative to oxygen from other sources in their body water.

Remnant negative ^{17}O anomalies derived from in vivo inhaled O_2 have been detected in enamel bioapatite of Eocene to Miocene rodent teeth while dentine of the same teeth lacks significant ^{17}O anomalies. This suggests preservation of the original phosphate oxygen isotope composition in enamel of these small mammal teeth. In contrast, ^{17}O anomalies in dentine have been erased due to diagenetic alteration with isotopically

normal diagenetic fluids. Triple oxygen isotope analysis of bioapatite thus seems to be a useful new proxy to directly detect diagenetic alterations of the $\delta^{18}O_{PO4}$ values of small mammal teeth.

2.1 Introduction

2.1.1 General considerations

Since the pioneering works of Longinelli (1984), Luz et al. (1984) and Luz and Kolodny (1985), palaeotemperature reconstructions based on the $^{18}O/^{16}O$ (expressed as $\delta^{18}O$, see section 1.2 for definitions) of bioapatite from fossil mammals rapidly became an established method and the number of studies on this topic is increasing continuously (e.g., Fricke, 2003; Grimes et al., 2003; 2004; 2005; Tütken et al., 2006; 2007; Zanazzi and Kohn, 2008; Chritz et al., 2009; Tütken and Vennemann, 2009).

The $\delta^{18}O$ of bioapatite can be used as a proxy for the $\delta^{18}O$ of ingested meteoric water, which is the main source of oxygen in large land-living animals. The oxygen isotope composition of meteoric water provides information about mean annual air temperature, relative humidity and local precipitation (Dansgaard, 1964; Rozanski et al., 1997; Fricke and O'Neil, 1999 and references therein). Skeletal apatite precipitates in equilibrium with body water. For most mammals, skeletal apatite precipitates at a body temperature of 37°C and has a $\delta^{18}O$, which is ~17.3‰ higher than the $\delta^{18}O$ of the water from which it has precipitated (Longinelli and Nuti, 1973). Therefore, the $\delta^{18}O$ of mammalian bioapatite relates to the $\delta^{18}O$ of ingested meteoric water and can thus be used as a climate proxy for air temperature, aridity and/or drinking behaviour (Longinelli, 1984; Ayliffe and Chivas, 1990; Delgado Huertas et al., 1995; Kohn et al., 1998; Levin et al., 2006; Tütken et al., 2006).

Most studies using $\delta^{18}O_{PO4}$ of mammalian bioapatite for continental palaeoclimate reconstructions have been conducted on teeth of large mammals (Koch et al., 1989; Ayliffe et al., 1992; Bryant et al., 1994; Gaboardi et al., 2005; Tütken et al., 2006, 2007; Chritz et al., 2009; Tütken and Vennemann, 2009). However, the number of studies using small mammals (mainly rodents) has increased over the last few years (Grimes et al., 2003, 2004, 2005; Navarro et al., 2004; Tütken et al., 2006; Ruddy, 2008; Héran et al., 2010). The advantages and disadvantages of using small mammal teeth for continental palaeoclimate reconstructions are reviewed in detail in Grimes et al. (2008).

An important precondition for the palaeoclimate reconstruction using $\delta^{18}O_{PO4}$ of bioapatite is that the original isotopic composition is preserved in the analysed skeletal remains and that it is not modified due to diagenetic alteration. Tooth enamel is the skeletal tissue of choice for oxygen isotope analysis. Its high mineral content (>99%), larger apatite crystal size and lower porosity makes it less prone to diagenetic alteration than dentine or bone (Kohn and Cerling, 2002).

Due to the small body and thus small tooth sizes of rodents, often bulk teeth are used for oxygen isotope analyses (Navarro et al., 2004; Tütken et al., 2006; Héran et al., 2010). However, dentine is prone to diagenetic alteration. Thus $\delta^{18}O_{PO4}$ analysis of enamel-dentine-mixtures may be biased by alteration. To examine possible diagenetic changes of the primary oxygen isotope composition in bulk small mammal teeth, previous studies used indirect indicators. Navarro (2004) and Héran (2010) assumed that phosphate yields during silver phosphate precipitation in accordance with the original bioapatite stoichiometry may indicate preservation of pristine $\delta^{18}O$ values in their tooth samples. Tütken et al. (2006) compared the oxygen isotope composition of structural carbonate ($\delta^{18}O_{CO3}$) in the apatite with that of phosphate ($\delta^{18}O_{PO4}$) of bulk teeth and found similar $\delta^{18}O_{CO3}$-$\delta^{18}O_{PO4}$ differences as for pure fossil enamel samples. They suggest that fossil bones and teeth have been affected by diagenesis if the difference between $\delta^{18}O_{CO3}$ and $\delta^{18}O_{PO4}$ deviates from the difference in modern analogues of the investigated fossil mammals because $\delta^{18}O_{CO3}$ is more prone to diagenetic alteration than $\delta^{18}O_{PO4}$ (Iacumin et al., 1996; Martin et al., 2008; Pellegrini et al., 2011-in this issue). However, if the $\delta^{18}O$ of the carbonate has been altered, there is no control whether the phosphate component is also biased diagenetically, except for serial intra-tooth analysis of $\delta^{18}O_{CO3}$ and $\delta^{18}O_{PO4}$ (Zazzo et al., 2004). Furthermore, the $\delta^{18}O_{CO3\text{-}PO4}$ value (i.e. isotopic fractionation between coexisting structural carbonate and phosphate) may vary from species to species (Martin et al., 2008, Pellegrini et al., 2011-in this issue). Therefore, a large dataset of comparable extant species is required to improve the reliability of this diagenetic test.

Here a new approach to detect diagenetic alteration of the oxygen bound in the PO_4-group of bioapatite of small mammals by means of triple oxygen isotope analysis is presented.

2.1.2 Triple oxygen isotope systematics

The oxygen isotope composition is reported relative to the international isotope reference standard VSMOW (Vienna Standard Mean Ocean Water) following the equation $\delta^{18}O$ or $\delta^{17}O$ (‰) = $[(R_{sample}/R_{SMOW}) - 1] \times 1000$. R_{sample} and R_{SMOW} indicate the $^{18}O/^{16}O$ or $^{17}O/^{16}O$ ratios of the samples and the standard.

Except for exotic photoreactions in the atmosphere (Thiemens, 2006), variations in the $^{17}O/^{16}O$ ratios are closely coupled with variations in the $^{18}O/^{16}O$ ratios (Young et al., 2002). This behaviour is called mass-dependent fractionation. Fractionation in $^{17}O/^{16}O$ ($\delta^{17}O$) and $^{18}O/^{16}O$ ($\delta^{18}O$) of a sample (e.g. apatite) relative to VSMOW can be expressed by the relation displayed in Eq. 2.1, in this case: a = sample and b = VSMOW.

$$\left(\frac{\left(\frac{^{17}O}{^{16}O}\right)_a}{\left(\frac{^{17}O}{^{16}O}\right)_b}\right) = \left(\frac{\left(\frac{^{18}O}{^{16}O}\right)_a}{\left(\frac{^{18}O}{^{16}O}\right)_b}\right)^{\beta} \qquad \text{Eq. 2.1}$$

Terrestrial rocks and minerals fall on a single line in a $\delta'^{17}O$ vs. $\delta'^{18}O$ diagram, the Terrestrial Rock Fractionation Line (TFL) (Clayton and Mayeda, 1983; Robert et al., 1992; Miller, 2002; Pack et al., 2007; Rumble et al., 2007). The β value used in the present study is 0.5250 ± 0.0007 and is based on a large number of analyses of terrestrial rocks and minerals (n=290) including silicates, oxides, and phosphates. The slope is, within analytical uncertainty, identical to slopes reported for rocks and minerals in other studies (Miller, 2002; Pack et al., 2007; Rumble et al., 2007; Hofmann and Pack, 2010).

Vertical deviations from the TFL are expressed as $\Delta^{17}O$ values or ^{17}O anomalies (Eq. 2.2), using the linearised δ-notation (δ') defined as

$$\delta'^{18}O = 1000 \times \ln\left(\frac{\delta^{18}O}{1000} + 1\right) \quad \text{and} \quad \delta'^{17}O = 1000 \times \ln\left(\frac{\delta^{17}O}{1000} + 1\right), \qquad \text{Eq. 2.2}$$

respectively.

Meteoric waters fall on a line with β = 0.528 (Meijer and Li, 1998; Landais et al., 2008) and an intercept of +0.047‰ (Landais et al., 2008). The relationship between $\delta'^{17}O$ and $\delta'^{18}O$ in meteoric waters can be expressed as $\delta'^{17}O_{MW} = 0.528(\delta'^{18}O) + 0.047‰$. Therefore, $\Delta^{17}O_{MW}$ of meteoric waters with $\delta^{18}O$ values ranging from –20 to +1‰ (Fricke and O'Neil, 1999) range between 0.00 and +0.05‰ with respect to the TFL.

Because of mass-independent fractionation mechanisms, the relation that is expressed in Eq. 2.1 is not valid for most oxygen bearing molecules from the tropo- and stratosphere (Thiemens, 2006). Tropospheric O_2 deviates from a line with β = 0.5250 and has a $\Delta^{17}O$ = –0.38‰ (Bender et al., 1994; Luz et al., 1999; Barkan and Luz, 2005).

This ^{17}O anomaly is caused by mass-independent photochemical reactions in the stratosphere, where ^{17}O-enriched CO_2 and ^{17}O-depleted O_2 are produced by exchange with isotopically anomalous O_3 (Yung et al., 1991; Bender et al., 1994). The magnitude of the ^{17}O anomaly in tropospheric O_2 is related to atmospheric CO_2 concentrations and global biosphere productivity (Luz et al., 1999; Blunier et al., 2002; Bao et al., 2008). Applying the data from Bao et al. (2008) for CO_2 concentrations between 200 and 1000 ppmv (Royer, 2006), $\Delta^{17}O_{air}$ should have varied between –0.28 and –0.75‰ in Cenozoic times.

Inhaled air oxygen is an important oxygen source for body water of small terrestrial vertebrates (e.g., Kohn, 1996). The ^{17}O anomaly of air O_2 is transferred through blood to skeletal apatite that precipitates in isotope equilibrium with body water. Analyses of bioapatite of extant small terrestrial mammals showed a $\Delta^{17}O_{PO4}$ down to –0.17‰ (Pack et al., 2009). The lowest $\Delta^{17}O_{PO4}$ values were observed in mammals of small body masses (≤1 kg) with an herbivorous diet. This is due to their high specific metabolic rate (Kleiber, 1947; Schmidt-Nielsen, 1984) inducing a relatively high input of air O_2 compared to the other oxygen sources. Large mammals do not have isotopically anomalous oxygen in their bioapatite because the oxygen isotope composition of their bone and tooth phosphate is largely controlled by that of non-anomalous drinking water.

Diagenesis is a process, during which skeletal bioapatite recrystallises and reacts with ambient diagenetic fluid. Oxygen isotope exchange with the surrounding fluids during diagenesis should result in a change of the in vivo obtained ^{17}O anomaly via air O_2 intake to an equilibrium $\Delta^{17}O$ value between the diagenetic fluid and the bioapatite, respectively. Because nearly all terrestrial fluids and rocks do not have a negative ^{17}O anomaly, diagenesis should erase the in vivo obtained anomalous triple oxygen isotope

composition. Therefore, a reset of bioapatite $\Delta^{17}O$ values of small herbivorous mammals towards a normal, "terrestrial" triple oxygen isotope composition should be a clear sign for diagenetic alteration (Figs. 2.1 and 2.2). The $\Delta^{17}O$ value of diagenetic apatite with respect to the TFL should range between 0 and 0.06‰ assuming a $\delta^{18}O_{H2O}$ of –20 to +5‰ for the diagenetic fluid, a $\delta^{18}O_{PO4}$ of 5 to 30‰ for the original bioapatite and $\beta_{H2O\text{-}AP} = \beta_{TFL}$ determined from shark tooth enameloid (see section 2 and 3).

We, therefore, suggest that triple oxygen isotope analysis of fossil bioapatite of small mammals (≤ 1 kg) may represent a new tool to directly detect diagenetic alteration of the $\delta^{18}O_{PO4}$ values in fossil bones and teeth. Future improvements of the analytical precision may also allow the application of this approach to larger mammals. The present study aims to explore the applicability and potential of this new method.

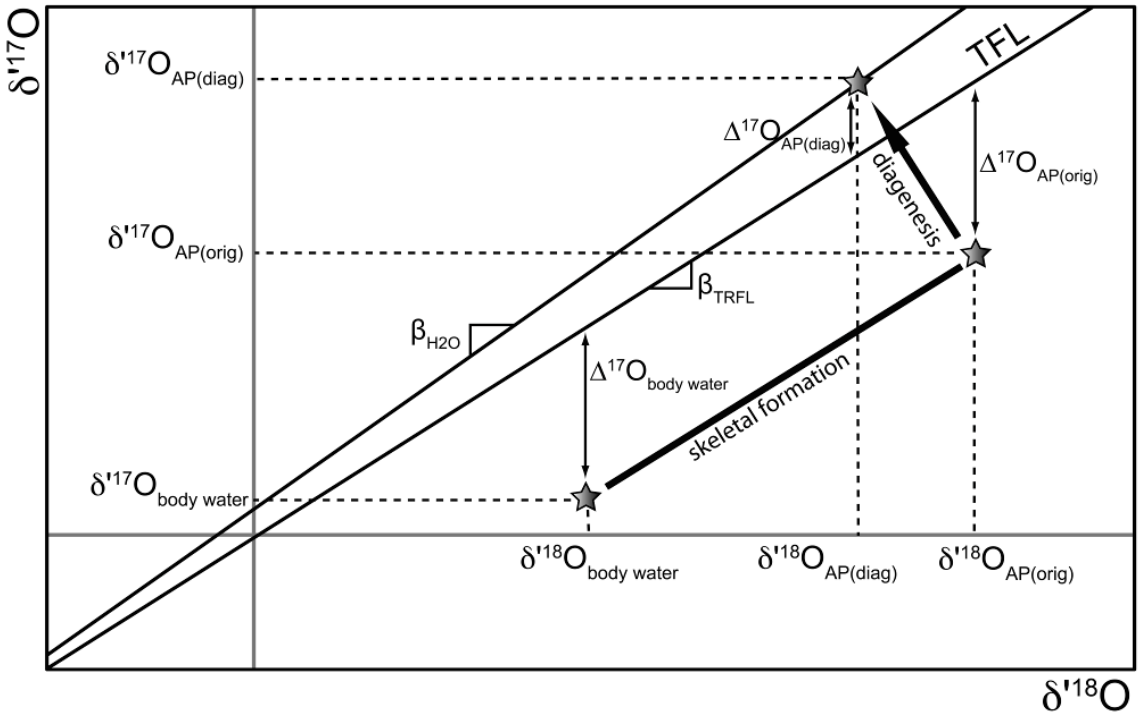

Fig. 2.1: Schematic illustration of the effect of tissue formation and diagenesis on the triple oxygen isotope composition of bioapatite samples in a $\delta'^{17}O$ vs. $\delta'^{18}O$ diagram. The $\Delta^{17}O$ of bioapatite ($\Delta^{17}O_{AP(orig)}$) formed in isotope equilibrium from the body water and of diagenetically bioapatite ($\Delta^{17}O_{AP(diag)}$) precipitated from the surrounding fluid are given. The negative $\Delta^{17}O$ value of the body fluid reflects inhalation of isotopically anomalous air O_2 and is incorporated into the bioapatite. During diagenetic recrystallisation of the apatite this negative anomaly will be progressively erased due to isotope exchange with a non-anomalous diagenetic fluid.

Fig. 2.2: Schematic illustration of the source of the ^{17}O anomaly in tropospheric oxygen, its incorporation in mammalian skeletal tissue and its possible obliteration by isotope exchange with the surrounding fluid.

2.2 Materials and Methods

2.2.1 Sample material

Five fossil teeth (four incisors and one molar) as well as one bone of rodents were analysed in this study. The fossil skeletal remains originate from five different localities in Germany ranging in age from Eocene (Lutetian) to Miocene (Langhian). The specimens are from different taphonomic and sedimentary settings, including limnic oil shale (Messel pit, Hesse, ~47 Ma), carstic fissure fillings (Möhren 13 and Herrlingen quarries, Baden-Wuerttemberg, ~26 Ma and ~32 Ma, respectively), limnic-fluviatile siliciclastic sediment (Sandelzhausen fossil site, Bavaria, ~16.5 Ma), and freshwater calcareous tufa (Steinberg/Ries, Bavaria, ~14.7 Ma) (Fig. 2.3).

Fig. 2.3: Map of Tertiary fossil localities in Germany from which fossil skeletal remains of rodents have been analysed for the triple oxygen isotope composition of the bioapatite. The map was generated with help of an online vector map creator, available at www.planiglobe.com.

Enamel and dentine of each tooth as well as one bone specimen were analysed for their triple oxygen isotope composition. Samples analysed comprise a right M2 and bone from the lower right jaw of an *Archaeomys* sp. (Herrlingen), an upper left I1 of a *Masillamys* sp. (Messel) as well as lower incisor teeth of three Rodentia indet. (Möhren 13, Sandelzhausen and Steinberg/Ries). Each sample was analysed between one and eight times.

For the determination of the $\beta_{H2O\text{-}AP}$ we have analysed shark tooth enameloid from an extant *Isurus oxyrinchus* from the coast off Bohol, Philippines.

2.2.2 Sample pretreatment

All samples were heated in an Argon-flushed horizontal tube furnace at 1000°C for 10 to 15 minutes to remove sorbed water, organic matter, structural carbonate and OH^- groups. It has been shown by Lindars et al. (2001) that at temperatures of between 850 and 1000°C all of these compounds are safely removed to ensure an isotopic analysis of only the phosphate oxygen isotope composition. To avoid exchange with atmospheric

water, samples were cooled down to below 100°C in an Ar atmosphere and then immediately stored in a desiccator.

2.2.3 Oxygen isotope analyses

Isotope analyses were conducted in the stable isotope laboratory at the University of Göttingen, Germany, by means of infrared (IR) laser fluorination in combination with gas chromatography and continuous flow isotope ratio monitoring gas mass spectrometry (GC-CF-IRMMS). Approximately 1.5 mg of pretreated bioapatite was loaded along with 1.05 to 1.1 mg NBS 28 quartz, NBS 120c Florida phosphate rock and other terrestrial rocks and minerals (including MORB, chromite, garnet, quartz, ruby and sapphire) into an 18-pit Ni sample holder. After evacuation and heating of the sample chamber to 70°C for a minimum of 12 h, materials were reacted in a ~25 to ~30 mbar atmosphere of purified F_2 gas by means of heating with a 50 W CO_2-laser. Liberated sample oxygen was cleaned from excess F_2 by reacting with NaCl (at 110°C). Released sample gas was cryofocused on a molecular sieve at –196°C, afterwards expanded into a stainless steel capillary and transported with He as carrier gas through a second cold trap, where a fraction of the sample gas was again cryofocused at –196°C on a molecular sieve. The O_2 was then released back into the He carrier gas stream at 92°C and transported through a 5 Å molecular sieve GC-column of a Thermo Scientific GasBench II. The column separated interfering NF_3 from O_2, which is important when analysing $\delta^{17}O$ (Pack et al., 2007). Purified sample O_2 was injected via an open split valve of the GasBench II into the source of a Thermo MAT 253 gas mass spectrometer. The signals of $^{16}O^{16}O$, $^{17}O^{16}O$ and $^{18}O^{16}O$ were simultaneously monitored on 3 Faraday cups. Sample peaks (m/z = 32) had an intensity of 20 to 30 V. Reference O_2 was injected before each sample through a second open split valve of the GasBench II. The standard deviation for replicates of the same bioapatite samples from different runs is typically better than ±0.05‰ in $\Delta^{17}O$. The long term standard deviation in $\Delta^{17}O$ derived from 290 single analyses of terrestrial rocks and minerals carried out in >30 analytical sessions in a period of one year is ±0.06‰. In the results section, this value is adopted as error for $\Delta^{17}O$ if only a single analysis has been conducted, otherwise errors are reported as standard error of the mean multiplied by Student's t-factor with 68% confidence limits (SEM•t).

2.3 Results

Multiple analyses (n=16, within 10 different analytical sessions) of the NBS 120c Florida phosphate rock standard, pretreated as described in section 2.2, gave a mean $\delta^{18}O_{PO4}$ value of 20.9 ± 0.1‰ and a mean $\Delta^{17}O$ of 0.00 ± 0.02‰.

Laser fluorination analyses of Ag_3PO_4 precipitated using a rapid precipitation method (Tütken et al., 2006) from NBS 120c (n=2) gave a mean $\delta^{18}O_{PO4}$ value of 21.7 ± 0.5‰ and a mean $\Delta^{17}O$ of 0.00 ± 0.05‰. TC/EA analysis of an aliquot of the same silver phosphate, conducted at the University of Tübingen using a Thermo Scientific TC/EA (n=3), gave a mean $\delta^{18}O_{PO4}$ value of 21.6 ± 0.4‰. This value is, within error, identical with the mean $\delta^{18}O$ of NBS 120c of 21.7±0.1‰, derived from 19 independent studies summarised in (Chenery et al., 2010). The $\Delta^{17}O$ value cannot be determined by TC/EA analysis. No significant discrepancy has been observed between direct laser fluorination of pretreated bioapatite and laser fluorination of Ag_3PO_4 precipitated from the same samples. The ~0.8‰ offset between direct Laser fluorination of pretreated NBS 120c and TC/EA analysis of NBS 120c precipitated as silver phosphate (Ag_3PO_4) may be due to the content of SiO_2 and other oxides in the NBS 120c powder that cannot be removed during our pretreatment procedure (see section 2.2.2) but will react during laser heating under fluorine atmosphere.

The triple oxygen isotope data from fossil tooth enamel from all 5 analysed rodent specimen have $\Delta^{17}O$ between –0.18 and –0.07‰ with respect to the TFL of 0.5250 (see section 2.1), The corresponding dentine samples have $\Delta^{17}O$ between –0.03 and +0.09‰ (Fig. 2.4 and Table 2.1).

Enamel $\delta^{18}O_{PO4}$ values of most rodent teeth are similar and range from 18.0 to 18.8‰ (n=4). Only one Rodentia indet. from Möhren 13 has a significantly higher $\delta^{18}O_{PO4}$ value of 20.1‰. In contrast, dentine $\delta^{18}O_{PO4}$ values of the teeth are much more variable ranging from 15.8 to 20.2‰. Dentine $\delta^{18}O_{PO4}$ are either lower than or similar to enamel $\delta^{18}O_{PO4}$ values. The intra-tooth difference between both dental tissues varies between 0.1 and 2.3‰ (Table 2.1).

Triple oxygen isotope analyses of the recent shark tooth enameloid for determination of the $\beta_{H2O\text{-}AP}$ gave a $\delta^{18}O_{PO4}$ = 20.7 ± 0.2‰ (n=9). The corresponding mean $\Delta^{17}O$ value is 0.00 ± 0.03‰.

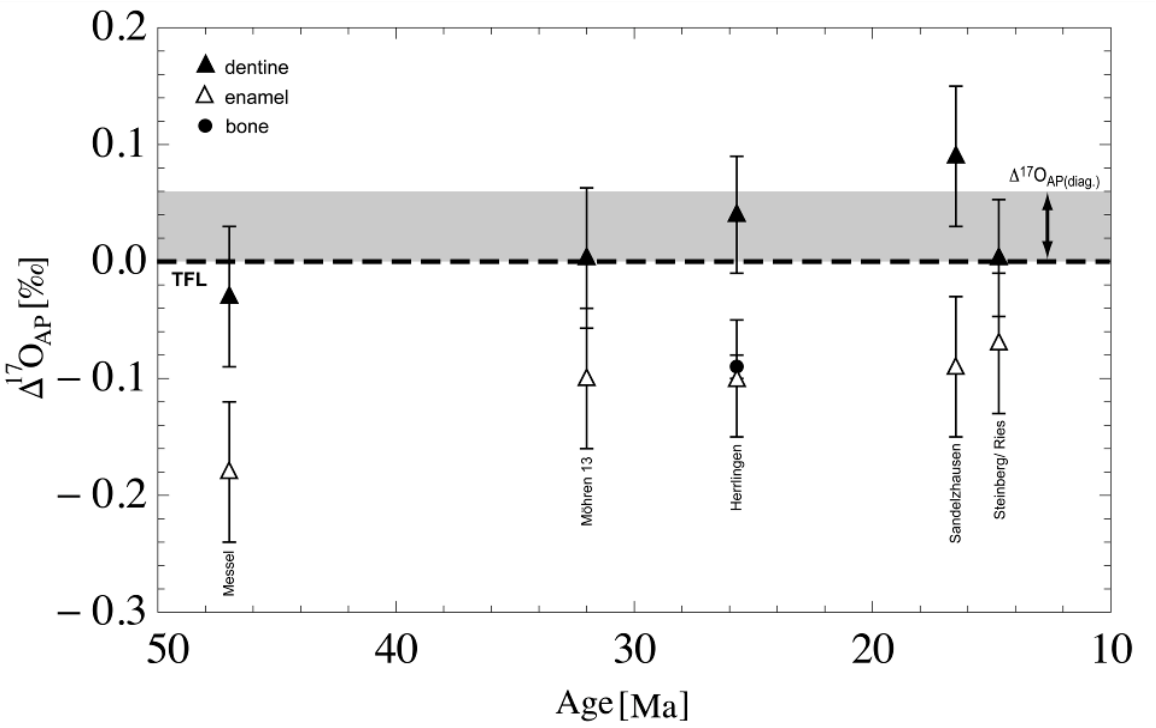

Fig. 2.4: Diagram comparing $\Delta^{17}O$ of tooth enamel (white triangles), dentine (black triangles) and bone (black dot) of the analysed samples. The dashed line is the TFL, the grey shaded area represents the theoretical range of $\Delta^{17}O$ values of diagenetically altered bioapatite due to exchange with the surrounding fluid as explained in the text and illustrated in Fig. 2.1.

Table 2.1: Tertiary rodent skeletal remains analysed for the triple oxygen isotope composition ($\delta^{18}O_{PO4}$, $\Delta^{17}O_{AP}$).

Taxon	Locality	Age	Tooth enamel		n	Dentine		n	Bone		n
			$\delta^{18}O$ (‰)	$\Delta^{17}O$ (‰)		$\delta^{18}O$ (‰)	$\Delta^{17}O$ (‰)		$\delta^{18}O$ (‰)	$\Delta^{17}O$ (‰)	
Rodentia indet.	Steinberg/Ries	Miocene, Langhian	18.1±0.5	-0.07±0.06	1	18.4±0.4	0.00±0.05	3	-	-	-
Rodentia indet.	Sandelzhausen	Miocene, Burdigalian	18.0±0.5	-0.09±0.06	1	18.1±0.5	0.09±0.06	1	-	-	-
Archaeomys sp.	Herrlingen	Oligocene, Chattian	18.8±0.5	-0.10±0.05	2	17.4±0.4	0.04±0.05	3	19.7±0.5	-0.09±0.01	8
Rodentia indet.	Möhren 13	Oligocene, Rupelian	20.1±0.5	-0.10±0.06	1	20.2±0.5	0.00±0.06	1	-	-	-
Masillamys sp.	Messel	Eocene, Lutetian	18.1±0.5	-0.18±0.06	1	15.8±0.5	-0.03±0.06	1	-	-	-

2.4 Discussion

The intra-tooth differences between the $\Delta^{17}O_{enamel}$ and $\Delta^{17}O_{dentine}$ values of –0.18 to +0.09‰ exceed the analytical uncertainty. The $\Delta^{17}O$ values of fossil enamel of the 5 analysed rodent specimens have pronounced negative ^{17}O anomalies that can only be explained by the in vivo incorporation of isotopically anomalous air O_2 (Fig. 2.3) (Pack et al., 2009). The low $\Delta^{17}O$ supports that the analysed tooth enamel has preserved the original oxygen isotope composition. In contrast, the $\Delta^{17}O$ values of the corresponding dentine have no negative ^{17}O anomalies. The dentine data overlap within error with the $\Delta^{17}O$ range that is expected by exchange with isotopically normal diagenetic fluids (Fig. 2.3). That implies at least a partial obliteration of the in vivo recorded oxygen isotope

composition of the dentine by oxygen exchange with diagenetic fluids and demonstrates the different diagenetic liability of enamel and dentine.

From a single *Archaeomys* jaw specimen enamel and bone of the same individual have a similar $\Delta^{17}O$ value of –0.1‰ and –0.09‰, respectively. This suggests the preservation of pristine oxygen isotope compositions in both enamel and bone, whereas dentine has a different $\Delta^{17}O$ of +0.04‰. However, more data are necessary to better constrain the diagenetic liability of bone compared to dentine.

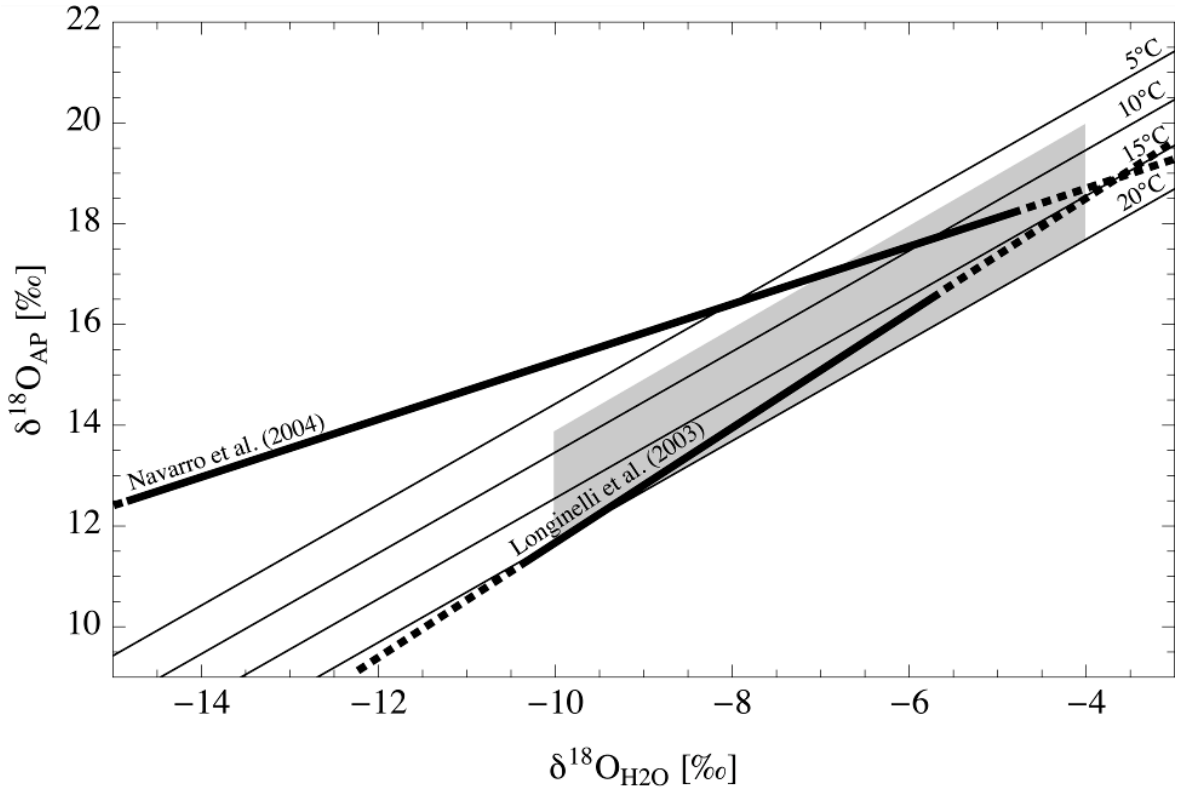

Fig. 2.5: Calculated phosphate oxygen isotope compositions ($\delta^{18}O_{PO4}$) of rodent bioapatite ($\delta^{18}O_{AP}$) using: a) the equation of Longinelli et al. (2003) and b) the equation of Navarro et al. (2004), correlated to a typical range of oxygen isotope compositions of meteoric waters ($\delta^{18}O_{MW}$). In comparison $\delta^{18}O$ values for diagenetically overprinted apatite ($\delta^{18}O_{AP(diag)}$), using the apatite-water fractionation equation of Shemesh et al. (1988) are shown, assuming 5°C, 10°C, 15°C and 20°C respectively, as temperatures of the diagenetic fluid. The shaded area illustrates a range of $\delta^{18}O_{MW}$ from –10 to –4‰, corresponding to typical Cenozoic mean annual air temperatures of Central Europe (Mosbrugger et al., 2005) and the range of $\delta^{18}O$ of inorganic phosphate formed at temperatures between 7.5 and 20°C.

For some modern wild rodents the relationship between the $\delta^{18}O_{PO4}$ of biogenic apatite and the $\delta^{18}O_{H2O}$ of meteoric water gives different calibration equations (D'Angela and Longinelli, 1990; Longinelli et al., 2003; Navarro et al., 2004). Figure 2.5 shows the calibration equations of Longinelli et al. (2003) and Navarro et al. (2004) for rodent $\delta^{18}O_{PO4}$ of the skeletal apatite ($\delta^{18}O_{AP}$). To evaluate the effect of diagenetic alteration on the $\delta^{18}O_{AP}$, the $\delta^{18}O_{PO4}$ of the diagenetic apatite ($\delta^{18}O_{AP(diag)}$) have been calculated for

various meteoric water $\delta^{18}O_{H2O}$ from about –10 to –4‰. This range corresponds to typical Cenozoic mean annual temperatures (Mosbrugger et al., 2005) and different taphonomic temperatures using the phosphate-water oxygen isotope thermometer equation of Shemesh et al. (1988). If the diagenetic fluid and rodent drinking water have similar $\delta^{18}O_{H2O}$, the diagenetic bioapatite may have $\delta^{18}O$ values close to those of the pristine apatite.

This can explain why the $\delta^{18}O_{PO4}$ of enamel and dentine analysed in this study are often similar (Table 2.1) despite a diagenetic alteration of the oxygen isotope composition as indicated by the intra-tooth $\Delta^{17}O$ difference between both dental tissues. The Upper Oligocene *Archaeomys* individual has similar $\Delta^{17}O$ in the enamel and bone, suggesting the preservation of original oxygen isotope ratios, but a $\delta^{18}O_{PO4}$ difference of 0.9‰ between both tissues. This may result from different ontogenetic periods during which both skeletal tissues have mineralised and during which the animal ingested water with different $\delta^{18}O_{H2O}$. Hence $\Delta^{17}O$ can indicate a diagenetic alteration of the phosphate oxygen isotope composition even when $\delta^{18}O_{PO4}$ values seem not affected by diagenetic alteration.

2.5 Conclusions

Anomalous $\Delta^{17}O$ values of bones and teeth of small terrestrial mammals may be erased during diagenetic recrystallisation of the biogenic apatite. Thus, triple oxygen isotope analysis of fossil bioapatite from small terrestrial mammals can be used as a diagenetic proxy. Pronounced negative $\Delta^{17}O$ values preserved in fossil tooth enamel of Middle Eocene to Miocene rodents support the preservation of the in vivo oxygen isotopic compositions. In contrast, the lack of a ^{17}O anomaly in dentine of the same teeth suggests the diagenetic alteration of this dental tissue by isotope exchange with non-anomalous diagenetic fluids, due to its higher liability to diagenetic alteration. This underscores that at least for Neogene and older fossil skeletal remains, only tooth enamel should be used for oxygen isotope analysis of mammalian bioapatite.

In contrast to other indirect diagenetic proxies applied so far, such as rare earth element concentrations, apatite crystallinity, $\delta^{18}O_{CO3}$-$\delta^{18}O_{PO4}$-offset, this new approach using the bioapatite triple oxygen isotope composition (^{16}O, ^{17}O and ^{18}O) directly targets the oxygen isotope composition within the PO_4 group and its alteration.

However, changing $\Delta^{17}O$ values of air oxygen over geologic time (Luz et al., 1999; Bao et al., 2008), uncertainties in physiological parameters of the mammals as well as intra- and interspecific variations have to be taken into account and need to be better constrained. Although, it may not be possible to exclude partial changes of the pristine oxygen isotope composition in fossil bioapatite, the approach will at least allow rejecting those samples that entirely have lost their in vivo oxygen isotope composition such as all the dentine samples analysed in this study.

This novel triple oxygen isotope approach enhances the knowledge of oxygen isotope systematics in modern and fossil bioapatite. It has the potential to become a new geochemical tool to detect diagenesis of the phosphate oxygen isotope composition of biogenic apatite in small mammals. Therefore, triple oxygen isotope analysis will help to improve terrestrial palaeoclimate reconstructions based on the oxygen isotope composition of bioapatite of fossil mammals.

Acknowledgments

The authors are grateful to K. Heissig, T. Lehmann, G. Rößner and S. Schaal for providing fossil samples as well as M. Böhme for the help in assigning absolute ages to some of the sample localities.

For the assistance in the sample preparation and isotope measurements, the authors would like to thank N. Albrecht and M. Kröger. Further thanks are due to R. Przybilla for the technical support at the mass spectrometry line. Finally, the authors would like to thank the reviewers H. Bao and C. Lécuyer, who have greatly improved the present paper with their comments and suggestions. A. G. and T. T. were supported by the German National Science Foundation DFG grant PA909/5-1 (A.P.) and DFG grant TU148/2-1 (T.T., Emmy Noether-Group “Bone Geochemistry”).

References

Ayliffe, L.K., Chivas, A.R. (1990). Oxygen isotope composition of bone phosphate of Australian kangoroos: potential as a palaeoenvironmental recorder. *Geochimica et Cosmochimica Acta* **54**, 2603-2609.

Ayliffe, L.K., Lister, A.M., Chivas, A.R. (1992). The preservation of glacial-interglacial climatic signatures in the oxygen isotopes of elephant skeletal phosphate. *Palaeogeography, Palaeoclimatology, Palaeoecology* **99**, 179-191.

Bao, H., Lyons, J., Zhou, C. (2008). Triple oxygen isotope evidence for elevated CO_2 levels after a Neoproterozoic glaciation. *Nature* **453**, 504-506.

Barkan, E., Luz, B. (2005). High precision measurements of $^{17}O/^{16}O$ and $^{18}O/^{16}O$ ratios in H_2O. *Rapid Communications in Mass Spectrometry* **19**, 3737-3742.

Bender, M., Sowers, T., Labeyrie, L. (1994). The Dole effect and its variations during the last 130,000 years as measured in the Vostok ice core. *Global Biogeochemical Cycles* **8**, 363-376.

Blunier, T., Barnett, B., Bender, M.L., Hendricks, M.B. (2002). Biological oxygen productivity during the last 60,000 years from triple oxygen isotope measurements. *Global Biogeochemical Cycles* **16**, 1-15.

Bryant, J.D., Luz, B., Froelich, P.N. (1994). Oxygen isotopic composition of fossil horse tooth phosphate as a record of continental paleoclimate. *Palaeogeography, Palaeoclimatology, Palaeoecology* **107**, 303-316.

Chenery, C., Müldner, G., Evans, J., Eckardt, H., Lewis, M. (2010). Strontium and stable isotope evidence for diet and mobility in Roman Gloucester, UK. *Journal of Archaeological Science* **37**, 150-163.

Chritz, K.L., Dyke, G.J., Zazzo, A., Lister, A.M., Monaghan, N.T., Sigwart, J.D. (2009). Palaeobiology of an extinct Ice Age mammal: Stable isotope and cementum analysis of giant deer teeth. *Palaeogeography, Palaeoclimatology, Palaeoecology* **282**, 133-144.

Clayton, R.N., Mayeda, T.K. (1983). Oxygen isotopes in eucrites, shergottites, nakhlites, and chassignites. *Earth and Planetary Science Letters* **62**, 1-6.

D'Angela, D., Longinelli, A. (1990). Oxygen isotopes in living mammal's bone phosphate: further results. *Chemical Geology* **86**, 75-82.

Dansgaard, W. (1964). Stable isotopes in precipitation. *Tellus* **16**, 436-468.

Delgado Huertas, A., Iacumin, P., Stenni, B., Sánchez Chillón, B., Longinelli, A. (1995). Oxygen isotope variations of phosphate in mammalian bone and tooth enamel. *Geochimica et Cosmochimica Acta* **59**, 4299-4305.

Fricke, H.C. (2003). Investigation of early Eocene water-vapor transport and paleoelevation using oxygen isotope data from geographically widespread mammal remains. *Geological Society of America Bulletin* **115**, 1088-1096.

Fricke, H.C., O'Neil, J.R. (1999). The correlation between $^{18}O/^{16}O$ ratios of meteoric water and surface Temperature: its use in investigating terrestrial climate change over geologic time. *Earth and Planetary Science Letters* **170**, 181-196.

Gaboardi, M., Deng, T., Wang, Y. (2005). Middle Pleistocene climate and habitat change at Zhoukoudian, China, from the carbon and oxygen isotopic record from herbivore tooth enamel. *Quaternary Research* **63**, 329-338.

Grimes, S.T., Collinson, M.E., Hooker, J.J., Mattey, D.P. (2008). Is small beautiful? A review of the advantages and limitations of using small mammal teeth and the direct laser fluorination analysis technique. *Palaeogeography, Palaeoclimatology, Palaeoecology* **266**, 39-50.

Grimes, S.T., Hooker, J.J., Collinson, M.E., Mattey, D.P. (2005). Summer temperatures of late Eocene to early Oligocene freshwaters. *Geology* **33**, 189-192.

Grimes, S.T., Mattey, D.P., Collinson, M.E., Hooker, J.J. (2004). Using mammal tooth phosphate with freshwater carbonate and phosphate palaeoproxies to obtain mean palaeotemperatures. *Quaternary Science Reviews* **23**, 967-976.

Grimes, S.T., Mattey, D.P., Hooker, J.J., Collinson, M.E. (2003). Eocene-Oligocene palaeoclimate reconstruction using oxygen isotopes: problems and solutions from the use of multiple palaeoproxies. *Geochimica et Cosmochimica Acta* **67**, 4033-4047.

Héran, M.A., Lécuyer, C., Legendre, S. (2010). Cenozoic long-term terrestrial climatic evolution in Germany tracked by $\delta^{18}O$ of rodent tooth phosphate. *Palaeogeography, Palaeoclimatology, Palaeoecology* **285**, 331-342.

Hofmann, M.E.G., Pack, A. (2010). Technique for High-Precision Analysis of Triple Oxygen Isotope Ratios in Carbon Dioxide. *Analytical Chemistry* **82**, 4357-4361.

Iacumin, P., Bocherens, H., Mariotti, A., Longinelli, A. (1996). Oxygen isotope analyses of co-existing carbonate and phosphate in biogenic apatite: a way to monitor diagenetic alteration of bone phosphate? *Earth and Planetary Science Letters* **142**, 1-6.

Kleiber, M. (1947). Body size and metabolic rate. *Physiological Reviews* **27**, 511-541.

Koch, P.L., Fisher, D.C., Dettman, D. (1989). Oxygen Isotope variation in the tusks of extinct proboscideans: A Measure of season of death and seasonality. *Geology* **17**, 515-519.

Kohn, M.J. (1996). Predicting animal $\delta^{18}O$: accounting for diet and physiological adaption. *Geochimica et Cosmochimica Acta* **60**, 4811-4829.

Kohn, M.J., Cerling, T.E. (2002). Stable Isotope Compositions of Biological Apatite. *Reviews in Mineralogy and Geochemistry* **48**, 455-488.

Kohn, M.J., Schoeninger, M.J., Valley, J.W. (1998). Variability in oxygen isotope compositions of herbivore teeth: reflections of seasonality or developmental physiology. *Chemical Geology* **152**, 97-112.

Landais, A., Barkan, E., Luz, B. (2008). Record of $\delta^{18}O$ and ^{17}O-excess in ice from Vostok Antarctica during the last 150,000 years. *Geophysical Research Letters* **35**, L02709.

Levin, N.E., Cerling, T.E., Passey, B.H., Harris, J.M., Ehleringer, J.R. (2006). A stable isotope aridity index for terrestrial environments. *Proceedings of the National Academy of Sciences* **103**, 11201-11205.

Lindars, E.S., Grimes, S.T., Mattey, D.P., Collinson, M.E., Hooker, J.J., Jones, T.P. (2001). Phosphate $\delta^{18}O$ determination of modern rodent teeth by direct laser fluorination: An appraisal of methodology and potential application to palaeoclimate reconstruction. *Geochimica et Cosmochimica Acta* **65**, 2535-2548.

Longinelli, A. (1984). Oxygen isotopes in mammal bone phosphate: a new tool for paleohydrological and paleoclimatological research? *Geochimica et Cosmochimica Acta* **48**, 385-390.

Longinelli, A., Iacumin, P., Davanzo, S., Nikolaev, V. (2003). Modern reindeer and mice: revised phosphate-water isotope equations. *Earth and Planetary Science Letters* **214**, 491-498.

Longinelli, A., Nuti, S. (1973). Revised phosphate-water isotopic temperature scale. *Earth and Planetary Science Letters* **19**, 373-376.

Luz, B., Barkan, E., Bender, M.L., Thiemens, M.H., Boering, K.A. (1999). Triple-isotope composition of atmospheric oxygen as a tracer of biosphere productivity. *Nature* **400**, 547-550.

Luz, B., Kolodny, Y. (1985). Oxygen isotope variations in phosphate of biogenic apatites, IV. Mammal teeth and bones. *Earth and Planetary Science Letters* **75**, 29-36.

Luz, B., Kolodny, Y., Horowitz, M. (1984). Fractionation of oxygen isotopes between mammalian bone phosphate and environmental drinking water. *Geochimica et Cosmochimica Acta* **48**, 1689-1693.

Martin, C., Bentaleb, I., Kaandorp, R., Iacumin, P., Chatri, K. (2008). Intra-tooth study of modern rhinoceros enamel $\delta^{18}O$: Is the difference between phosphate and carbonate $\delta^{18}O$ a sound diagenetic test? *Palaeogeography, Palaeoclimatology, Palaeoecology* **266**, 183-187.

Meijer, H.A.J., Li, W.J. (1998). The use of electrolysis for accurate $\delta^{17}O$ and $\delta^{18}O$ isotope measurements in water. *Isotopes in Environmental and Health Studies* **34**, 349-369.

Miller, M.F. (2002). Isotopic fractionation and the quantification of ^{17}O anomalies in the oxygen three-isotope system: an appraisal and geochemical significance. *Geochimica et Cosmochimica Acta* **66**, 1881-2055.

Mosbrugger, V., Utescher, T., Dilcher, D.L. (2005). Cenozoic continental climatic evolution of Central Europe. *Proceedings of the National Academy of Sciences* **102**, 14964-14969.

Navarro, N., Lécuyer, C., Montuire, S., Langlois, C., Martineau, F. (2004). Oxygen isotope compositions of phosphate from arvicoline teeth and Quaternary climatic changes, Gigny, French Jura. *Quaternary Research* **62**, 172-182.

Pack, A., Süssenberger, A., Gehler, A., Wotzlaw, J. (2009). Tracing the oxygen triple isotopic composition of tropospheric molecular oxygen in biogenic apatite – a new tool for palaeoclimatology. *Geophysical Research Abstracts* **11**, EGU2009-10706.

Pack, A., Toulouse, C., Przybilla, R. (2007). Determination of oxygen triple isotope ratios of silicates without cryogenic separation of NF_3 — technique with application to analyses of technical O_2 gas and meteorite classification. *Rapid Communications in Mass Spectrometry* **21**, 3721-3728.

Pellegrini, M., Lee-Thorp, J.A., Donahue, R.E. (2011). Exploring the variation of the $\delta^{18}O_p$ and $\delta^{18}O_c$ relationship in enamel increments. *Palaeogeography, Palaeoclimatology, Palaeoecology* **310**, 71-83.

Robert, F., Rejou-Michel, A., Javoy, M. (1992). Oxygen isotope homogeneity of the Earth: new evidence. *Earth and Planetary Science Letters* **108**, 1-9.

Royer, D.L. (2006). CO_2-forced climate thresholds during the Phanerozoic. *Geochimica et Cosmochimica Acta* **70**, 5665-5675.

Rozanski, K., Johnsen, S.J., Schotterer, U., Thompson, L.G. (1997). Reconstruction of past climates from stable isotope records of palaeo-precipitation preserved in continental archives. *Hydrological Sciences* **42**, 725-745.

Ruddy, M. (2008). Water vole incisors as records of palaeoclimate. *Quaternary Newsletter* **116**, 51-54.

Rumble, D., Miller, M.F., Franchi, I.A., Greenwood, J.P. (2007). Oxygen three-isotope fractionation lines in terrestrial silicate minerals: an inter-laboratory comparison for hydrothermal quartz and eclogite garnet. *Geochimica et Cosmochimica Acta* **71**, 3592-3600.

Schmidt-Nielsen, K., 1984. *Scaling: why is animal size so important?*. Cambridge University Press (Cambridge), 241 pp.

Shemesh, A., Kolodny, Y., Luz, B. (1988). Isotope geochemistry of oxygen and carbon in phosphate and carbonate of phosphorite francolite. *Geochimica et Cosmochimica Acta* **52**, 2565-2572.

Thiemens, M.H. (2006). History and Applications of Mass-Independent Isotope Effects. *Annual Review of Earth and Planetary Sciences* **34**, 217-262.

Tütken, T., Furrer, H., Vennemann, T.W. (2007). Stable isotope compositions of mammoth teeth from Niederweningen, Switzerland: Implications for the Late Pleistocene climate, environment, and diet. *Quaternary International* **164-65**, 139-150.

Tütken, T., Vennemann, T. (2009). Stable isotope ecology of Miocene large mammals from Sandelzhausen, southern Germany. *Paläontologische Zeitschrift* **83**, 207-226.

Tütken, T., Vennemann, T.W., Janz, H., Heizmann, E.P.J. (2006). Palaeoenvironment and palaeoclimate of the Middle Miocene lake in the Steinheim Basin, SW Germany: A reconstruction from C, O, and Sr isotopes of fossil remains. *Palaeogeography, Palaeoclimatology, Palaeoecology* **241**, 457-491.

Young, E.D., Galy, A., Nagahara, H. (2002). Kinetic and equilibrium mass-dependent isotope fractionation laws in nature and their geochemical and cosmochemical significance. *Geochimica et Cosmochimica Acta* **66**, 1095-1104.

Yung, Y.L., DeMore, W.B., Pinto, J.P. (1991). Isotopic exchange between carbon dioxide and ozone via O(^{1}D) in the stratosphere. *Geophysical Research Letters* **18**, 13-16.

Zanazzi, A., Kohn, M.J. (2008). Ecology and physiology of White River mammals based on stable isotope ratios of teeth. *Palaeogeography, Palaeoclimatology, Palaeoecology* **257**, 22-37.

Zazzo, A., Lécuyer, C., Sheppard, S.M.F., Grandjean, P., Mariotti, A. (2004). Diagenesis and the reconstruction of palaeoenvironments: a method to restore original $\delta^{18}O$ values of carbonate and phosphate from fossil tooth enamel. *Geochimica et Cosmochimica Acta* **68**, 2245-2258.

3. Manuscript II

Exploring the usability of isotopically anomalous oxygen in bones and teeth as palaeo-CO_2-barometer

Andreas Pack[a], Alexander Gehler[a] & Annette Süssenberger[a]

[a]Georg-August-Universität, Geowissenschaftliches Zentrum, Abteilung Isotopengeologie, Goldschmidtstr. 1, D-37077 Göttingen, Deutschland

in press, Geochimica et Cosmochimica Acta, http://dx.doi.org/10.1016/j.gca.2012.10.017

Abstract

Fluctuations in atmospheric pCO_2 may have played the key role in global climate throughout Earth's history. For the quantification of past variations in atmospheric pCO_2, several geological proxy approaches and geochemical models have been developed. Here, we evaluate a new CO_2 proxy approach that is based on the triple oxygen isotope composition (^{16}O, ^{17}O, ^{18}O) of skeletal apatite of terrestrial mammals. Our approach utilizes the relation between an anomaly in ^{17}O of tropospheric air O_2 and atmospheric pCO_2. The anomaly is transferred from inhaled air O_2 to skeletal apatite of mammals. Hence, triple oxygen isotope data of mammalian bioapatite provide information regarding pCO_2 during the animal's lifetime. The approach was calibrated with a detailed mass balance model that was verified by analyses on a set of recent mammals. We evaluate the potential of this new independent terrestrial palaeo-CO_2 proxy in a case study including Eocene to Miocene samples. The present investigation provides promising results that are in good agreement with existing proxy- and model data. The uncertainty intrinsic to the proxy is mainly due to uncertainties in physiological parameters.

3.1 Introduction

3.1.1 Atmospheric carbon dioxide – Climate and proxies

Arrhenius (1896) suggested that atmospheric carbon dioxide (CO_2) played a major role in fluctuations of global temperature throughout Earth's history. Only a look back into the Earth's climate history can test this hypothesis. Determination of past pCO_2 is important in order to understand if CO_2 was the cause of large temperature fluctuations during Earth's history (Royer et al., 2001) or if these fluctuations were caused by other factors (e.g., Veizer et al., 2000).

A close coupling of atmospheric CO_2 partial pressure (pCO_2) and global temperature derived from $^{18}O/^{16}O$-ratios of Arctic and Antarctic precipitates is well documented from air inclusions in ice cores for the past 800,000 years (Petit et al., 1999; Lüthi et al., 2008). Because no ice core data are available beyond the 800,000 years limit, geochemical modelling (Berner, 2006a; Berner, 2006b; 2008), the $^{13}C/^{12}C$-ratio of pedogenic minerals, the $^{13}C/^{12}C$-ratios of phytoplankton, stomatal density and stomatal index of land plants and the $^{11}B/^{10}B$-ratios of planktonic foraminifera (Royer et al., 2001, and references therein) have been used to indirectly estimate pCO_2 throughout geological time. However, all of these proxies have specific limitations (Royer et al., 2001; Pagani et al., 2005; Roth-Nebelsick, 2005; Kürschner et al., 2008; Pearson et al., 2009; Breecker et al., 2010; Beerling and Royer, 2011).

Recently, Bao et al. (2008) used the triple oxygen isotope composition (^{16}O, ^{17}O, ^{18}O) of sedimentary sulphate to suggest high pCO_2 of ~12,000 ppmv after the Marinoan Snowball Earth 635 million years ago. The sulfate formed by oxidative weathering of sulfide in air. Tropospheric O_2 has an oxygen isotope anomaly that is related to photoreactions in the stratosphere. The magnitude of the anomaly is thought to be a function of atmospheric pCO_2 (Luz et al., 1999; Bao et al., 2008). The sulphate analysed by Bao et al. (2008) inherited information about the isotope anomaly of air O_2 at the time of its formation by subaerial oxidation of sulfide.

In this contribution, we demonstrate that the triple oxygen isotope composition of skeletal apatite ($Ca_5[PO_4, CO_3, F]_3[OH, F, Cl, CO_3]$) of terrestrial mammals inherits anomalous oxygen from inhaled O_2. It is tested if the triple oxygen isotope composition of bioapatite can be used as CO_2-barometer.

Mammals are heterotrophic and inhale air O_2 to oxidatively respire fats, carbohydrates and proteins. The reaction products (mainly H_2O, CO_2, and $C_5H_4N_4O_3$ [uric acid]) mix and equilibrate with body water and transfer the ^{17}O anomaly of inhaled air to the body. The anomaly is then transferred to bone and tooth apatite that precipitates in isotopic equilibrium with body water (Longinelli and Nuti, 1973; Longinelli, 1984; Luz et al., 1984; Bryant and Froelich, 1995; Kohn, 1996). Knowledge of the oxygen isotope anomaly of inhaled O_2 from triple oxygen isotope analyses of bone and tooth apatite may allow reconstructing pCO_2 during the animal's lifetime.

3.2 Triple oxygen isotope systematics

3.2.1 Nomenclature

Variations in oxygen isotope ratios ($^{17}O/^{16}O$, $^{18}O/^{16}O$) are expressed in δ-notation. The $\delta^{18}O$ and $\delta^{17}O$ values are defined as:

$$\delta^{17}\mathrm{O}(‰) = \left(\frac{\left(\frac{^{17}\mathrm{O}}{^{16}\mathrm{O}}\right)_{\mathrm{sample}}}{\left(\frac{^{17}\mathrm{O}}{^{16}\mathrm{O}}\right)_{\mathrm{VSMOW}}} - 1 \right) \times 1000 \qquad \text{Eq. 3.1}$$

$$\delta^{18}\mathrm{O}(‰) = \left(\frac{\left(\frac{^{18}\mathrm{O}}{^{16}\mathrm{O}}\right)_{\mathrm{sample}}}{\left(\frac{^{18}\mathrm{O}}{^{16}\mathrm{O}}\right)_{\mathrm{VSMOW}}} - 1 \right) \times 1000 \qquad \text{Eq. 3.2}$$

VSMOW denotes the international reference material Vienna Standard Mean Ocean Water. The linearised form of the δ-notation ($\delta'^{18}O$, $\delta'^{17}O$, Hulston and Thode, 1965) is defined as:

$$\delta'^{17}\mathrm{O} = 1000 \ln\left(\frac{\delta^{17}\mathrm{O}}{1000} + 1 \right) \qquad \text{Eq. 3.3}$$

$$\delta'^{18}\mathrm{O} = 1000 \ln\left(\frac{\delta^{18}\mathrm{O}}{1000} + 1 \right) \qquad \text{Eq. 3.4}$$

The triple oxygen isotope fractionation between phases (A, B) is described by the fractionation factor α_{A-B} and the triple isotope fractionation exponent θ_{A-B} (Young et al., 2002, Eq. 3.5).

$$\alpha_{A-B}^{17/16} = \left(\alpha_{A-B}^{18/16}\right)^{\theta_{A-B}} \qquad \text{Eq. 3.5}$$

The fractionation factors $\alpha_{A-B}^{17/16}$ and $\alpha_{A-B}^{18/16}$ are the ratios of $^{17}O/^{16}O$ and $^{18}O/^{16}O$ of coexisting phases. Each equilibrium fractionation process is characterized by an individual θ value (sometimes also termed β or λ). The θ value is function of phases involved and, in general, of temperature. So far, it has only been experimentally determined for 2 cases of oxygen isotope equilibrium: (i) for the water to vapor fractionation, θ was experimentally determined to 0.529 (Barkan and Luz, 2005). This coincides with the high-T equilibrium approximation of θ for oxygen by Young et al. (2002). (ii) For the CO_2-water equilibrium ($2 \leq t \leq 37$ °C), Hofmann et al. (2012) experimentally determined a θ value of 0.522. The experimental data demonstrate that θ can significantly deviate from the high-T approximation.

Oxygen isotope anomalies are expressed in form of the $\Delta^{17}O$ notation. In a $\delta'^{17}O$ vs. $\delta'^{18}O$ diagram, $\Delta^{17}O$ is defined by the deviation of a sample in $\delta'^{17}O$ from a given reference line (RL) with:

$$\Delta^{17}O_{RL}^{sample} = \delta'^{17}O_{VSMOW}^{sample} - \lambda_{RL} \times \delta'^{18}O_{VSMOW}^{sample} - \gamma_{RL} \qquad \text{Eq. 3.6}$$

The reference line (RL) is defined by slope λ_{RL} and intercept γ_{RL}. For the slope of the reference line we use λ_{RL} and not θ as it is not controlled by a single physical process, but likely a mixture of high- and low-T equilibrium and kinetic effects. It is important to note that not only the slope but also the intercept must be given for comparability of $\Delta^{17}O$ values from studies using different reference lines. Intercepts other than zero indicate that VSMOW does not fall on the chosen RL, i. e. $\Delta^{17}O_{RL}^{VSMOW} \neq 0$. Depending on the scientific question, various studies on the triple oxygen isotope compositions use different reference lines with different slopes and intercepts (e.g., Clayton et al., 1973; Luz et al., 1999; Wiechert et al., 2004; Landais et al., 2006; 2007; Pack et al., 2007; Hofmann and Pack, 2010; Tanaka and Nakamura, 2012).

No consensus has yet been reached on which reference line should be chosen for defining $\Delta^{17}O$. In this study, we used rocks and minerals along with NBS-28 quartz to define the RL (terrestrial fractionation line, TFL). We have analysed 1071 terrestrial rocks and minerals in the time between April 2008 and June 2011. Our reference O_2 was analysed by Eugeni Barkan (Earth Science Institute, The Hebrew University, Jerusalem) relative to VSMOW. Rocks and minerals fall on a line with $\lambda_{TFL} = 0.5251 \pm 0.0007$ (1σ). The slope λ_{TFL} is, within error, identical to the slopes reported by Miller (2002), Pack et al. (2007), and Rumble et al. (2007). The slope of the TFL of 0.5251 is likely the mean exponent for the isotope fractionation between melts, minerals and fluids at various temperatures and pressures. We determined the intercept by high-T equilibration of CeO_2 with air O_2 (air data from Barkan and Luz, 2011) and successive analysis of the CeO_2 to γ_{TFL} = –0.036 ± 0.018‰ (details will be presented elsewhere). Kusakabe and Matsuhisa (2008) report a $\Delta^{17}O$ of NBS-28, which is 0.056‰ higher than the value suggested here. The uncertainty in $\delta^{17}O$, however, is given as ± 0.06‰. Recently, Tanaka and Nakamura (2012) reported high-precision data of $\Delta^{17}O$ of NBS-28 (recalculated relative to our TFL) of –0.051 ± 0.005‰. For this study, we adopt a weighted mean from our laboratory and from Tanaka and Nakamura (2012) of γ_{TFL} = –0.048‰.

3.3 Oxygen mass balance model for mammals

3.3.1 Fluxes

In order to understand the quantitative relation between $\Delta^{17}O_{TFL}$ of inhaled air O_2, body mass M_b and $\Delta^{17}O_{TFL}$ of skeletal apatite, we have developed an oxygen mass balance model for $\Delta^{17}O_{TFL}$ of mammalian bioapatite. The model is based on the approach of Bryant and Froelich (1995) and considers oxygen in- (F_i) and outfluxes (F_j). We adopt values for fluxes $F_{i,j}$ and isotopic compositions for central Germany as most of the recent mammals lived there.

Mammals exchange oxygen with the environment mainly in the form of O_2, H_2O, CO_2, and oxygen bound in organic food compounds.

$$F_{i,j} = a_{i,j} (M_b)^{b_{i,j}} \qquad \text{Eq. 3.7}$$

The fluxes $F_{i,j}$ scale with the logarithmic body mass M_b (Eq. 3.7). The variables $a_{i,j}$ and $b_{i,j}$ are the allometric scaling parameters. Fluxes are given in mol O_2 per day, M_b is given in kg.

We consider drinking water (DW), water in food (FW), oxygen in organic food compounds (F) and respired O_2 (A) as influxes F_i. Outfluxes F_j are transcutaneous water vapor (TR), water vapor in exhaled breath (BR), water in urine, feces and sweat (LW), and exhaled CO_2 (CO2). Allometric scaling parameters $a_{i,j}$ and $b_{i,j}$ are available for the total water flux (F_{TW}), respired O_2 (F_A) and the total evaporative water loss (F_{EVA}). The total water flux scales with M_b to $F_{TW} = 3.78\ M_b^{0.86}$. The allometric scaling function was calculated for non-desert terrestrial herbivores from the dataset of Nagy and Peterson (1988, $M_b \leq 300$ kg). The uncertainty of F_{TW} is $1\sigma(\log_{10}F_{TW}) = \pm 0.24$. The amount of inhaled O_2 for terrestrial herbivores scales with M_b with $F_A = 1.49\ M_b^{0.65}$ (Nagy et al., 1999). The uncertainty of F_A is $1\sigma(\log_{10}F_A) = \pm 0.14$. For the evaporative water flux we adopt $F_{EVA} = 1.088\ M_b^{0.88}$ from Bryant and Froelich (1995). The uncertainty of F_{EVA} is estimated to $1\sigma(\log_{10}F_{EVA}) = \pm 0.27$.

Fluxes F_{DW}, F_{FW}, F_F, F_{TR}, F_{BR}, F_{LW} and F_{CO2} can be derived from F_{TW}, F_A and F_{EVA} using Eqs. 3.8 - 3.14 (Bryant and Froelich, 1995).

$$(F_{DW} + F_{FW}) = F_{TW} - 0.5 \times R_q \times F_A \qquad \text{Eq. 3.8}$$

$$F_{DW} = X_{DW} \times (F_{TW} - 0.5 \times R_q \times F_A) \qquad \text{Eq. 3.9}$$

$$F_F = F_A \times (1.5 \times R_q - 1) \qquad \text{Eq. 3.10}$$

$$(F_{TR} + F_{BR}) = F_{EVA} \qquad \text{Eq. 3.11}$$

$$F_{TR} = X_{TR} - F_{EVA} \qquad \text{Eq. 3.12}$$

$$F_{LW} = X_{TW} - F_{EVA} \qquad \text{Eq. 3.13}$$

$$F_{CO_2} = R_q \times F_A \qquad \text{Eq. 3.14}$$

The respiratory quotient R_q is the molar ratio of respired O_2 to exhaled CO_2. For herbivores, it is 0.9 (Bryant and Froelich, 1995). We assume an uncertainty of ± 0.05. The ratios $X_{DW} = F_{DW}/(F_{DW} + F_{FW})$ and $X_{TR} = F_{TR}/(F_{TR} + F_{BR})$ are estimated to be 0.8 ± 0.1 (Bryant and Froelich, 1995; Podlesak et al., 2008) and 0.21 ± 0.05 (Kohn, 1996), respectively. Even though X_{DW} is variable within mammals, it has only minor influence on the model result because both, F_{DW} and F_{FW} have a $\Delta^{17}O_{TFL}$ close to zero.

3.3.2 Isotope compositions

Each source *i* is given a $\delta^{18}O^{i}$ and a $\Delta^{17}O_{TFL}$. For each sink *j*, the isotopic fractionation in $^{18}O/^{16}O$ (expressed as $\Delta^{18}O_{j-BW} = \delta^{18}O^{j} - \delta^{18}O^{BW}$) and in $\Delta^{17}O_{TFL}$ between outflux *j* and body water (BW) is considered.

Drinking water (DW) is considered to have the $\delta^{18}O$ value of local meteoric water (MW). For northern and central Europe, a value of –8 ± 2‰ for $\delta^{18}O^{DW}$ has been adopted (IAEA, 2011). Meteoric water falls on a line (MWL) with $\lambda_{MWL} = 0.528 \pm 0.0001$ (Meijer and Li, 1998; Barkan and Luz, 2005; Luz and Barkan, 2010) and an intercept of $\gamma_{MWL} = +0.033 \pm 0.003‰$ (Luz and Barkan, 2010). This gives $\Delta^{17}O_{TFL}^{DW} = (0.528 \pm 0.0001 - 0.5251) \times -8 \pm 2‰ + 0.048‰ + 0.033 \pm 0.003 = 0.058 \pm 0.007‰$.

In temperate regions, leaf water, i.e. food water (FW), is enriched by 6.5‰ in ^{18}O relative to local meteoric water (Kohn, 1996). We assume an uncertainty of ±2‰ for the fractionation between leaf water and local meteoric water. The λ-value for the leaf water fractionation line is $\lambda_{FW} = 0.5216 \pm 0.0008 - 0.0078 \pm 0.0026 \times h$, where h is the atmospheric relative humidity ($0.3 \le h \le 1$; Landais et al., 2006). This gives $\Delta^{17}O_{TFL}^{FW} = \Delta^{17}O_{TFL}^{DW} + (\lambda_{FW} - 0.5251) \times 6.5 \pm 2‰ = -0.00 \pm 0.03‰$ for $h = 0.72 \pm 0.05$.

Oxygen in organic food compounds (F) is released as combustion products in the form of CO_2 and H_2O to the body water. For herbivores, $\delta^{18}O^{F}$ can be approximated from the isotope composition of cellulose, which is 27‰ higher than the $\delta^{18}O$ of leaf water (Bryant and Froelich, 1995, and references therein), i.e. $\delta^{18}O^{F} \approx 25.5‰$. We assume that this value has an uncertainty of ±10‰. As an approximation, a $\theta_{F\text{-}FW}$ value in the range $0.525 \le \theta \le 0.53$ ($\theta_{F\text{-}FW} = 0.5275$) is assumed for the cellulose(F)-water(FW) equilibrium isotope fractionation. This results in a $\Delta^{17}O_{TFL}^{F} = \Delta^{17}O_{TFL}^{FW} + ([0.525…0.53] - 0.5251) \times 27 \pm 10‰ = 0.07 \pm 0.14‰$.

The $\delta^{18}O$ and the $\delta^{17}O$ of air O_2 are 23.88‰ and 12.03‰, respectively (Barkan and Luz, 2011). According to Eq. 3.6, this results in a $\Delta^{17}O_{TFL}$ of –0.39‰ for air O_2. The $\delta^{18}O$ value of respired O_2 (A) is lower than ambient O_2 due to preferential diffusive uptake of light O_2 (Epstein and Zeiri, 1988). The average $\delta^{18}O^{A}$ value of respired O_2 of 15‰ is adopted from Kohn (1996) with an estimated uncertainty of ±2‰. The associated $\theta_{A\text{-}air}$ of 0.5179 ± 0.0006 is taken from Luz and Barkan (2005), which is assumed to be valid as a

general value for mammals. This gives $\Delta^{17}O^{A}_{TFL}$ = –0.39 ‰ + (0.5179 ± 0.0006 – 0.5251) × (15 ± 2‰ – 23.88‰) = –0.32 ± 0.01‰.

The fractionation in $^{18}O/^{16}O$ between transcutaneous water vapor (TR) and body water (BW) is adopted from Bryant and Froelich (1995) with $\Delta^{18}O_{TR\text{-}BW}$ = –19‰ with an assumed uncertainty of ±5‰. As an approximation for $\lambda_{TR\text{-}BW}$ for the fractionation between transcutaneous water vapor and body water, the slope for plant respiration at an atmospheric relative humidity of h = 0.72 ± 0.05 ($\lambda_{TR\text{-}BW}$ = 0.516 ± 0.002) has been adopted from Landais et al. (2006). This gives $\Delta^{17}O^{TR}_{TFL} = \Delta^{17}O^{BW}_{TFL}$ + (0.516 ± 0.002 – 0.5251) × –19 ± 5‰ = $\Delta^{17}O^{BW}_{TFL}$ + 0.17 ± 0.06‰.

Water vapor in exhaled air is in isotope equilibrium with body water with $\Delta^{18}O_{BR-BW}$ = –8.44‰ (Horita and Wesolowski, 1994) with an estimated uncertainty of ±2 ‰. The θ value for the water-to-water vapor equilibrium is 0.529 ± 0.001 (Barkan and Luz, 2005), which gives $\Delta^{17}O^{BR}_{TFL} = \Delta^{17}O^{BW}_{TFL}$ + (0.529 ± 0.001 – 0.5251) × –8.44 ± 2‰ = $\Delta^{17}O^{BW}_{TFL}$ – 0.03 ± 0.01‰. Liquid water in urine, feces and sweat (LW) is not fractionated relative to body water, i.e. $\Delta^{17}O^{LW}_{TFL} = \Delta^{17}O^{BW}_{TFL}$. Exhaled CO_2 (CO2) in equilibrium with body water (t = 37°C) has $\delta^{18}O^{CO2} = \delta^{18}O^{BW}$ + 38.8 ± 0.05‰ (Brenninkmeijer et al., 1983). The associated $\theta_{CO2\text{-}BW}$ = 0.522 ± 0.001 has been determined by Hofmann et al. (2012). The $\Delta^{17}O_{TFL}$ value of exhaled CO_2 is $\Delta^{17}O^{CO_2}_{TFL} = \Delta^{17}O^{BW}_{TFL}$ + (0.522 ± 0.001 – 0.5251) × 38.8 ± 0.05‰ = $\Delta^{17}O^{BW}_{TFL}$ – 0.12 ± 0.04‰.

The oxygen isotope ratios in skeletal apatite (AP) are fractionated relative to body water with $\Delta^{18}O_{AP\text{-}BW}$ = 17.3 ± 0.2‰ (t = 37 °C; Longinelli and Nuti, 1973; Longinelli, 1984; Luz et al., 1984). The related equilibrium $\theta_{AP\text{-}water}$ value of 0.523 ± 0.002 has been determined in the present study using triple oxygen isotope data from a rostrum of a harbour porpoise (*Phocoena phocoena*, see section 3.5.1). This gives $\Delta^{17}O_{AP} = \Delta^{17}O_{BW}$ + (0.523 ± 0.002 – 0.5251) × 17.1 ± 0.3‰ = $\Delta^{17}O_{BW}$ – 0.04 ± 0.04‰.

Table 3.1: List of model parameters used in the mass balance and error calculation.

Flux F in mol O_2 day^{-1}	Description	*a*	*b*	1σ (log_{10}F)	References
F_{TW}	total water flux, allometric scaling	3.73	0.78	± 0.24	Nagy and Peterson (1988)
F_A	flux of inhaled O_2, allometric scaling	1.44	0.61	± 0.14	Nagy et al. (1999)
F_{EVA}	evaporative flux, allometric scaling	1.088	0.88	± 0.27	Bryant and Froelich (1995)

Parameter		Values ± 1σ	
λ_{TFL}	slope of reference line	0.5251 ± 0.0007	this study
γ_{TFL}	intercept of reference line	-0.048‰	this study, Tanaka and Nakamura (2012)
R_q	respiratory quotient	0.9 ± 0.05	Bryant and Froelich (1995)
X_{DW}	fraction of drinking water	0.8 ± 0.1	Bryant and Froelich (1995), Podlesak et al., 2008)
X_{TR}	fraction of transpired water	0.21 ± 0.05	Kohn (1996)
$\delta^{18}O_{DW}$	$^{18}O/^{16}O$ of drinking water	-8 ± 2‰	IAEA (2011)
λ_{MWL}	slope of meteoric water line	0.5281 ± 0.0001	Meijer and Li (1998), Barkan and Luz (2005), Luz and Barkan (2010)
γ_{MWL}	intercept of meteoric water line	0.03 ± 0.003‰	Luz and Barkan (2010)
$\Delta^{18}O_{FW\text{-}DW}$	fractionation between food and drinking water	6.5 ± 2‰	Kohn (1996)
h	average relative humidity	0.72 ± 0.05	temperate region
$D^{18}O_{F\text{-}FW}$	equilibrium fractionation between food (e.g., cellulose) and leaf water	27 ± 10‰	Bryant and Froelich (1995) and references therein
$\theta_{F\text{-}FW}$	equilibrium fractionation exponent (food - leaf water)	0.5275 ± 0.0025	no data available
$\delta^{18}O^{Air}$	$^{18}O/^{16}O$ of air relative to SMOW	23.88‰	Barkan and Luz (2011)
$\Delta^{17}O_{Air}$	isotope anomaly of air O_2 (present)	-0.39‰	Barkan and Luz (2011) and TFL from this study
$\Delta^{18}O_{A\text{-}Air}$	fractionation between respired O_2 and air	8.9 ± 2‰	Kohn (1996)
$\lambda_{A\text{-}Air}$	fractionation exponent between respired and air O_2	0.5179 ± 0.0006	Luz and Barkan (2005)
$\Delta^{18}O_{TR\text{-}BW}$	fractionation between transpired and body water	-19 ± 10‰	Bryant and Froelich (1995)
$\lambda_{TR\text{-}BW}$	fractionation exponent between transpired and body water	0.516 ± 0.002	Landais et al. (2006)
$\Delta^{18}O_{BR\text{-}BW}$	fractionation between breath vapor and body water	-8.44 ± 2‰	Horita and Wesolowski (1994)
$\theta_{BR\text{-}BW}$	fractionation exponent between water and vapor	0.529 ± 0.001	Barkan and Luz, 2005
$\Delta^{18}O_{LW\text{-}BW}$	fractionation between excrements and body water	0	Bryant and Froelich (1995)
$\Delta^{18}O_{CO2\text{-}BW}$	fractionation between CO_2 and water	38.8 ± 0.05‰	Brenninkmeijer et al. (1983)
$\theta_{CO2\text{-}BW}$	fractionation exponent for the CO_2 water equilibrium	0.522 ± 0.001	Hofmann et al. (2012)
$\Delta^{18}O_{AP\text{-}BW}$	fractionation between apatite and body water	17.3 ± 0.2‰	Longinelli and Nuti (1973), Longinelli (1984), Luz et al. (1984)
$\theta_{AP\text{-}BW}$	fractionation exponent for the apatite water equilibrium	0.523 ± 0.002	this study

The $\Delta^{17}O^{AP}_{TFL}$ of biogenic apatite is calculated according to Eq. 3.15. Outfluxes F_j in Eq. 3.15 are characterised by their $\Delta^{17}O^{j}_{BW} = \Delta^{17}O^{j}_{TFL} - \Delta^{17}O^{BW}_{TFL}$.

$$\Delta^{17}O^{AP}_{TFL} = \frac{\sum F_i^{in} \times \Delta^{17}O^{i}_{TFL} - \sum F_j^{out} \times \Delta^{17}O^{BW}_{j}}{\sum F_j^{out}} + \theta_{AP-BW} - \lambda_{TFL} \times 17.3‰ \qquad \text{Eq. 3.15}$$

The uncertainty of the model was calculated by propagating the errors of the individual parameters (see Table 3.1). The error propagation was conducted by means of a Monte Carlo simulation with independent random numbers generated according to the

distribution of the error (log-normal distribution [for fluxes], normal distribution, or random distribution in a given interval [for $\theta_{F\text{-}FW}$]). We used WOLFRAM MATHEMATICA 7.0 for all computations.

3.4 Materials and Methods

3.4.1 Bioapatite of modern mammals

In this study, the triple oxygen isotope compositions of skeletal apatite of 17 different species (19 individual specimens) of modern terrestrial herbivorous, omnivorous and carnivorous mammals with body masses ranging from ~2 g to ~5000 kg were analysed (Table 3.2). Preferably, samples from mammalian families with a long geologic range have been selected. With the exception of two elephant species (*Elephas maximus*, *Loxodonta africana*) and a kangaroo rat (*Dipodomys* sp., New Mexico, USA) all samples originate from German localities. The Etruscan shrew (*Suncus etruscus*) has been bred in captivity; all other specimens were wild animals (see Table 3.2 for details).

Table 3.2: List of recent species that were analysed for their triple oxygen isotope composition. The body masses Mb are from Mohr (1950), Niethammer and Krapp (1978-2005) and Grzimek (1990).

Taxon	**Order**	M_b **in kg**	**Sample locality**
Capreolus capreolus (male)	Artiodactyla	23 ± 8	NW Germany
Cervus elaphus (male)	Artiodactyla	130 ± 35	52°48'N, 09°49'E
Dama dama (male)	Artiodactyla	93 ± 10	53°02'N, 10°08'E
Sus scrofa (male)	Artiodactyla	98 ± 35	52°25'N, 07°10'E
Phocoena phocoena	Cetacea	58 ± 30	53°38'N, 08°02'E
Crocidura leucodon	Eulipotyphla	0.01 ± 0.004	51°30'N, 09°56'E
Suncus etruscus	Eulipotyphla	0.0018 ± 0.0006	52°30'N, 13°20'E
Oryctolagus cuniculus	Lagomorpha	1.4 ± 0.4	52°44'N, 07°17'E
Homo sapiens (male)	Primates	80 ± 10	NW Germany
Elephas maximus (male, subadult)	Proboscidea	2000 ± 200	unknown
Loxodonta africana	Proboscidea	5000 ± 500	Africa
Apodemus flavicollis	Rodentia	0.032 ± 0.006	52°20'N, 12°39'E
Apodemus sylvaticus (1)	Rodentia	0.0195 ± 0.002	51°30'N, 09°56'E
Apodemus sylvaticus (2)	Rodentia	0.0195 ± 0.002	51°44'N, 06°56'E
Cricetus cricetus	Rodentia	0.34 ± 0.12	51°30'N, 09°56'E
Dipodomys sp.	Rodentia	0.1 ± 0.04	USA, New Mexico
Mus musculus domesticus	Rodentia	0.021 ± 0.005	50°06'N, 11°26'E
Rattus norvegicus (juvenile)	Rodentia	0.2 ± 0.07	51°44'N, 06°56'E
Sciurus vulgaris (1)	Rodentia	0.225 ± 0.025	51°30'N, 09°56'E
Sciurus vulgaris (2)	Rodentia	0.225 ± 0.025	50°59'N, 11°20'E

Table 3.2: Triple oxygen isotope data from bioapatite of recent mammals. Except the *Phocoena phocoena*, all mammals were terrestrial. Given is the 1σ uncertainty. The number of analyses (n) is indicated.

Taxon	Order	Sampled material	$\delta^{18}O_{VSMOW}$ (‰)	$\Delta^{17}O_{TFL}$ (‰)		n
Capreolus capreolus (male)	Artiodactyla	tooth & bone	15.6 ± 0.2	-0.02 ± 0.02	±0.02	5
Cervus elaphus (male)	Artiodactyla	bone & antler	14.7 ± 0.5	-0.06 ± 0.02	±0.02	4
Dama dama (male)	Artiodactyla	bone	16.8 ± 0.3	0.02 ± 0.01	±0.01	6
Sus scrofa (male)	Artiodactyla	tooth	16.0 ± 0.3	0.04 ± 0.02	±0.02	4
Phocoena phocoena	Cetacea	bone	17.1 ± 0.3	0.01 ± 0.01	±0.01	4
Crocidura leucodon	Eulipotyphla	tooth & bone	18.0 ± 0.3	-0.06 ± 0.01	±0.01	5
Suncus etruscus	Eulipotyphla	tooth & bone	17.2 ± 0.9	-0.12 ± 0.02	±0.02	3
Oryctolagus cuniculus	Lagomorpha	tooth & bone	19.8 ± 0.2	0.02 ± 0.01	±0.01	4
Homo sapiens (male)	Primates	tooth	15.7 ± 0.2	-0.02 ± 0.02	±0.02	4
Elephas maximus (male, subadult)	Proboscidea	dentine (tusk)	17.9 ± 0.1	-0.01 ± 0.01	±0.01	5
Loxodonta africana	Proboscidea	tooth enamel	19.7 ± 0.1	0.03 ± 0.01	±0.01	13
Apodemus flavicollis	Rodentia	tooth enamel	17.3 ± 0.4	-0.11 ± 0.03	±0.03	3
Apodemus sylvaticus (1)	Rodentia	tooth & bone	18.0 ± 0.4	-0.15 ± 0.01	±0.01	4
Apodemus sylvaticus (2)	Rodentia	tooth enamel	17.1 ± 0.4	-0.09 ± 0.04	±0.04	2
Cricetus cricetus	Rodentia	tooth	17.1 ± 0.2	-0.05 ± 0.02	±0.02	4
Dipodomys sp.	Rodentia	tooth enamel	20.3 ± 0.4	-0.11 ± 0.03	±0.03	3
Mus musculus domesticus	Rodentia	tooth enamel	15.5 ± 0.5	-0.12 ± 0.02	±0.02	3
Rattus norvegicus (juvenile)	Rodentia	tooth enamel	19.4 ± 0.2	-0.12 ± 0.02	±0.02	4
Sciurus vulgaris (1)	Rodentia	tooth enamel	12.0 ± 0.2	-0.14 ± 0.02	±0.02	5
Sciurus vulgaris (2)	Rodentia	tooth enamel	17.6 ± 0.5	-0.10 ± 0.05	±0.05	1

3.4.2 Bioapatite of fossil mammals

We selected a set of teeth from Neogene and Palaeogene fossil small rodents with estimated M_b ranging from 0.1 to 0.6 kg. All samples originate from German localities (see Table 3.4 for details). We have sampled only tooth enamel as it is less prone to diagenetic alteration as compared to dentine or bone material (Kohn and Cerling, 2002). In a recent study, Gehler et al. (2011) compare the $\Delta^{17}O$ of enamel and dentine of fossil mammals. They demonstrate that tooth enamel can preserve the original $\Delta^{17}O$, whereas the $\Delta^{17}O$ of dentine in the investigated samples has been reset during diagenesis.

3.4.3 Sample preparation

Organic matter was removed from modern samples by a treatment with H_2O_2 (30%). The samples were subsequently heated for 10 - 15 minutes in an Ar-flushed horizontal tube furnace at 1000 °C. All samples were cooled down to <100 °C in Ar atmosphere before they were immediately stored in a desiccator. This procedure removes remaining organic matter, sorbed water, structural carbonate and OH^- groups (Lindars et al., 2001). A dry Ar gas atmosphere is used to avoid exchange with atmospheric moisture.

3.4.4 Triple oxygen isotope analysis

Oxygen isotope analyses were carried out by means of infrared laser fluorination (Sharp, 1990) in combination with gas chromatography isotope ratio monitoring gas mass spectrometry (GC-CF-IRMS; Hofmann and Pack, 2010; Gehler et al., 2011; Hofmann et al., 2012). Between 0.3 and 1.5 mg of bioapatite was loaded along with NBS-28 quartz, NBS-120c Florida phosphate rock and other terrestrial rocks and minerals with a $\delta^{18}O$-range from 0 to 24‰ into an 18-pit polished Ni metal sample holder. After evacuation and heating of the sample chamber to 70 °C overnight, materials were reacted in a ~20 - 30 mbar atmosphere of purified F_2 gas (Asprey, 1976) by means of heating with a SYNRAD 50 W CO_2-laser. Usually, the first sample of a tray had to be discarded due to its incorrect $\delta^{18}O$ and $\Delta^{17}O$. Liberated O_2 was cleaned from excess F_2 by reacting with heated NaCl (~180 °C) and cryotrapping of Cl_2. The released O_2 was first cryofocused on a ¼-inch stainless steel molecular sieve trap at –196 °C (liquid N_2). The sample O_2 was then released by heating to ~120 °C and transported with He carrier gas through a second molecular sieve trap, where a fraction of the sample gas was again cryofocused at –196 °C. The sample O_2 was then released at 92 ± 2 °C (tempered hot water bath) back into the He carrier gas stream and transported through a 5 Å molecular sieve GC column of a THERMO SCIENTIFIC GasBench-II. The column separated NF_3 from O_2, which is important when analysing $\delta^{17}O$ (e.g., Pack et al., 2007). Purified sample O_2 was then injected via an open split valve of the GasBench-II into the source of a THERMO MAT 253 gas mass spectrometer. The signals of $^{16}O/^{16}O$, $^{17}O/^{16}O$ and $^{18}O/^{16}O$ were simultaneously monitored on 3 Faraday cups. The m/z = 33 signal was amplified with a 10^{12} Ω feedback resistor. Bell-shaped sample peaks had an amplitude of ~25 - 30 V (m/z = 32) and a full width at half maximum of ~20 s. Reference O_2 was injected for 40 s two times before the sample through a second open split valve of the GasBench-II. The amplitudes (m/z = 32) of the reference gas peaks were ~25 V.

For measurements of reference O_2 vs. reference O_2 an external reproducibility of ±0.04‰ in $\delta^{18}O$ and ±0.03‰ in $\Delta^{17}O$ was achieved. The uncertainty in $\delta^{18}O$ of silicates and oxides was ±0.25‰, determined from replicate analyses of the same material. The corresponding external reproducibility in $\Delta^{17}O_{TFL}$ was ±0.03 - ±0.05‰. An example for the results from one analytical session is displayed in Fig. 3.1. Tests have shown that the uncertainty in $\Delta^{17}O$ considerably increases when analysing the materials with peaks <15 V

(m/z = 32). The larger uncertainty in $\delta^{18}O$ of sample measurements compared to reference gas measurements can be explained in terms of mass-dependent fractionation during sample gas extraction. The slightly larger uncertainty in $\Delta^{17}O$ of samples compared to reference gas is likely due to differences in peak shape and peak amplitude between reference gas and sample O_2.

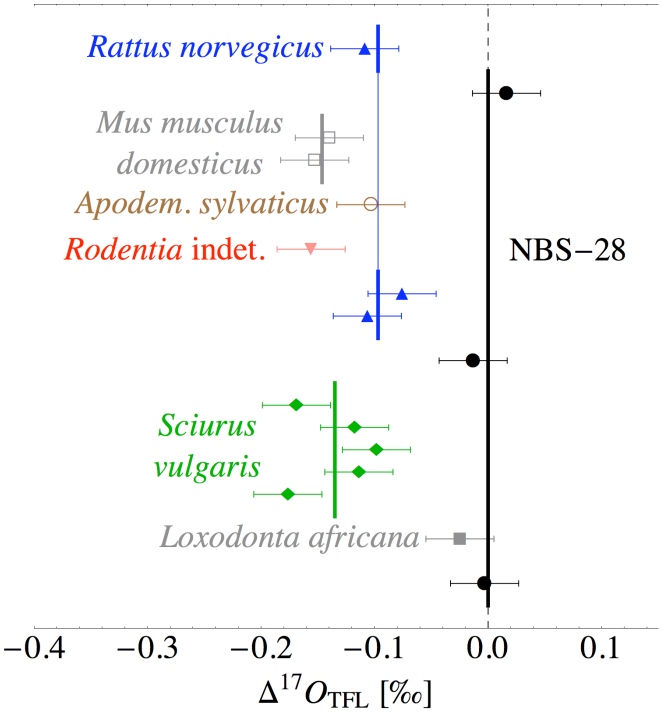

Fig. 3.1: Variation diagram showing the results in $\Delta^{17}O$ for one analytical session. The data points are vertically arranged in the order they have been obtained (from bottom to top). The mean data for the same samples are connected by thin vertical lines. The bars indicate the 1σ standard deviation.

Table 3.4: List of fossil tooth enamel samples. Absolute ages are from Böhme and Ilg (2003). The errors are 1σ.

Taxon	Location	Age (10^6 years)	$\delta^{18}O_{VSMOW}$ (‰)	$\Delta^{17}O_{TFL}$ (‰)	n	M_b (kg)	GPP_t/GPP_0 (A)	GPP_t/GPP_0 (B)	GPP_t/GPP_0 (C)	p_{CO2} (A) (ppmv)	p_{CO2} (B) (ppmv)	p_{CO2} (C) (ppmv)
Palaeosciurus sp.	Petersbuch 31 (Miocene, MN7)	13.6 ± 0.1	17.6 ± 0.5	-0.08 ± 0.05	2	0.3 ± 0.10	1.0	1.4	1.0	240 ± 250	330 ± 340	250 ± 265
Rodentia indet.	Steinberg, Ries (Miocene, MN6)	14.4 ± 0.9	18.1 ± 0.5	-0.07 ± 0.05	1	0.1 ± 0.05	1.0	1.4	1.1	140 ± 195	190 ± 265	140 ± 205
Rodentia indet.	Walda (Miocene, MN5)	16.2 ± 0.2	16.7 ± 0.5	-0.07 ± 0.05	2	0.1 ± 0.05	1.0	1.4	1.1	140 ± 195	190 ± 275	140 ± 205
Rodentia indet.	Sandelzhausen (Miocene, MN5)	16.4 ± 0.1	18.0 ± 0.5	-0.09 ± 0.05	1	0.1 ± 0.05	1.0	1.4	1.1	210 ± 215	300 ± 310	230 ± 235
Archaeomys sp.	Herrlingen (Oligocene, MP25-30)	25.7 ± 2.7	18.8 ± 0.5	-0.10 ± 0.05	2	0.6 ± 0.10	1.0	1.7	1.2	400 ± 330	670 ± 545	480 ± 395
Rodentia indet.	Burgmagerbein 2 (Oligocene, MP24/25)	28.5 ± 0.8	21.9 ± 0.5	-0.13 ± 0.05	2	0.1 ± 0.05	1.0	1.7	1.3	390 ± 270	670 ± 475	490 ± 345
Rodentia indet.	Bernloch 1 (Oligocene, MP23)	30.9 ± 0.6	16.8 ± 0.5	-0.10 ± 0.05	1	0.1 ± 0.05	1.0	1.8	1.3	260 ± 235	470 ± 420	350 ± 310
Pseudosciurus suevicus	Ronheim 1 (Oligocene, MP 22)	30.9 ± 0.6	20.9 ± 0.5	-0.10 ± 0.05	1	0.3 ± 0.10	1.0	1.8	1.3	340 ± 290	610 ± 515	450 ± 380
Rodentia indet.	Moehren 13 (Oligocene, MP22)	32.3 ± 0.8	20.1 ± 0.5	-0.10 ± 0.05	1	0.1 ± 0.05	1.0	1.8	1.4	260 ± 235	480 ± 430	360 ± 320
Masillamys sp.	Messel (Eocene, MP11)	47.0 ± 0.3	18.1 ± 0.5	-0.18 ± 0.05	1	0.3 ± 0.10	1.0	2.2	2.1	740 ± 430	1630 ± 955	1520 ± 890

3.5 Results and Discussion

3.5.1 The θ value of the apatite-water equilibrium fractionation at 37 °C

The interpretation of the $\Delta^{17}O$ of skeletal apatite requires knowledge of the triple oxygen isotope exponent θ for the equilibration between water and apatite at 37 °C. The rostral bone of a harbour porpoise (*P. phocoena*) from the North Sea has a $\delta^{18}O^{AP}$ value of 17.1 ± 0.3‰ and $\Delta^{17}O_{TFL}$ = 0.010 ± 0.013‰ (Table 3.3). The body water of cetaceans is not fractionated in $^{18}O/^{16}O$ with respect to the environmental seawater they live in (Yoshida and Miyazaki, 1991). The observed values of 17.1 ± 0.3‰ agrees within error with the expected value of 17.3‰ from apatite-water fractionation with $\delta^{18}O$ = 0‰.

Seawater has a $\delta^{18}O$ value of ~0‰ and a $\Delta^{17}O_{TFL}$ value of +0.051‰ (Luz and Barkan, 2010). This gives an equilibrium exponent for the apatite water fractionation (t = 37 °C) of θ_{AP-H_2O} = 0.523 ± 0.002.

This value is significantly lower than the high-T equilibrium value of 0.529 (Young et al., 2002) and demonstrates that the equilibrium θ can deviate from theoretical approximations. It is, however, in the same range as the θ values for the CO_2-water (0.522; Hofmann et al., 2012) isotope equilibrium (2 °C ≤ t ≤ 37 °C). A similar λ value is reported for the TFL (this study; Miller, 2002; Pack et al., 2007; Rumble et al., 2007), which may be explained by a θ for the equilibrium fractionation between minerals and fluids that is in the range of 0.525. Only the water-to-water vapor θ value (Barkan and Luz, 2005) is identical to the high-T approximation of Young et al. (2002). The result demonstrates that, when dealing with triple oxygen isotope fractionation, θ must be experimentally determined for each fractionation process.

3.5.2 The oxygen mass balance in comparison with the isotope composition of recent mammals

The mass balance equation predicts that the $\Delta^{17}O_{TFL}$ of biogenic apatite decreases with decreasing M_b and with decreasing $\Delta^{17}O_{TFL}^{air}$. The model predicts that small recent mammals have a $\Delta^{17}O_{TFL}$ down to –0.15‰. For mammals with M_b >10 kg the predicted $\Delta^{17}O_{TFL}$ of bioapatite approaches zero.

The mass balance model suggests that skeletal apatite of small mammals contains a higher proportion of anomalous oxygen from inhaled air O_2 than bioapatite of large mammals. This can be understood in terms of the high specific metabolic rates of small

mammals (Kleiber, 1947; Schmidt-Nielsen 1972, 1984). The present isotope anomaly of tropospheric O_2 ($\Delta^{17}O_{TFL}$ = –0.39‰) (Barkan and Luz, 2011) can be identified in the bioapatite of mammals with M_b <1 kg. The oxygen isotope composition of mammals with M_b exceeding 1 kg is largely controlled by isotopically normal drinking and food water, respectively.

Data from recent mammals (Table 3.3) are used to verify the prediction from the mass balance model. The $\Delta^{17}O_{TFL}$ value of skeletal apatite varies between –0.15 ± 0.01‰ (long-tailed field mouse, *Apodemus sylvaticus*) and 0.04 ± 0.02‰ (wild boar, *Sus scrofa*; Table 3.3, Fig. 3.2). The corresponding $\delta^{18}O$ values range from 12 to 20‰. The $\Delta^{17}O_{TFL}$ of mammalian apatite, indeed, shows a systematic decrease with decreasing body mass M_b (Fig. 3.2). The $\Delta^{17}O$ data of recent mammals are within error in agreement with the prediction from the mass balance (Fig. 3.2). Even the data of mammals from very different locations (elephants, kangaroo rat) overlap within uncertainty with the mass balance model. The data clearly demonstrate that the isotope anomaly of inhaled O_2 is transferred to the body water and from there to tooth and bone apatite.

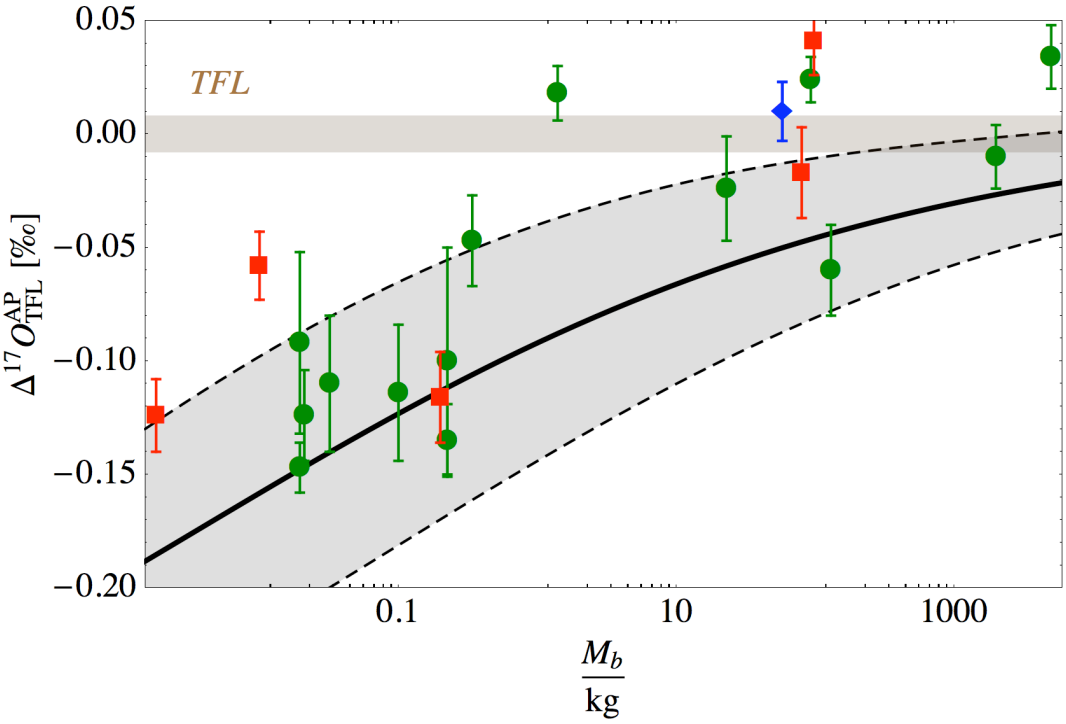

Fig. 3.2: Plot of $\Delta^{17}O_{TFL}$ of skeletal apatite of modern terrestrial mammals and a harbour porpoise vs. body mass M_b. Circles: herbivores; squares: omnivores and carnivores; diamond: harbour porpoise *(Phocoena phocoena).* Error bars are 1σ. The solid curve is the mass balance model (= $\Delta^{17}O_{TFL}^{air}$ –0.39 ‰, 380 ppmv CO_2). The dashed curves outline the gray shaded 1σ uncertainty interval (Monte Carlo simulation, for details, see Section 3.3). Data and model are in excellent agreement. The fact that slightly more than 68% of all data fall within the 1σ error envelope suggests that the error estimate is likely too conservative and that variations in physiological parameters F_{TW} and F_A may actually be smaller than estimated from field data.

The data indicate that carnivorous shrews record a slightly lower proportion of inhaled O_2 than herbivores of the same body mass (Fig. 3.2). This can be explained by a higher specific water flux F_{TW} in shrews. The only shrews (*Blarina brevicauda*, 4 individuals) included in the study of Nagy and Peterson (1988) have a 4 - 8 times higher water flux than the average total water flux rate predicted for eutherian mammals of the same body mass. A higher water uptake of carnivores can be related to their N-rich protein diet and the need for keeping the uric acid concentration under control. Therefore, herbivores may be more suitable as pCO_2 proxy than omnivores and carnivores.

The large portion of anomalous atmospheric O_2 in the body water of small mammals with M_b <1 kg makes their skeletal apatite a potential tracer for the $\Delta^{17}O$ of past atmospheric molecular O_2.

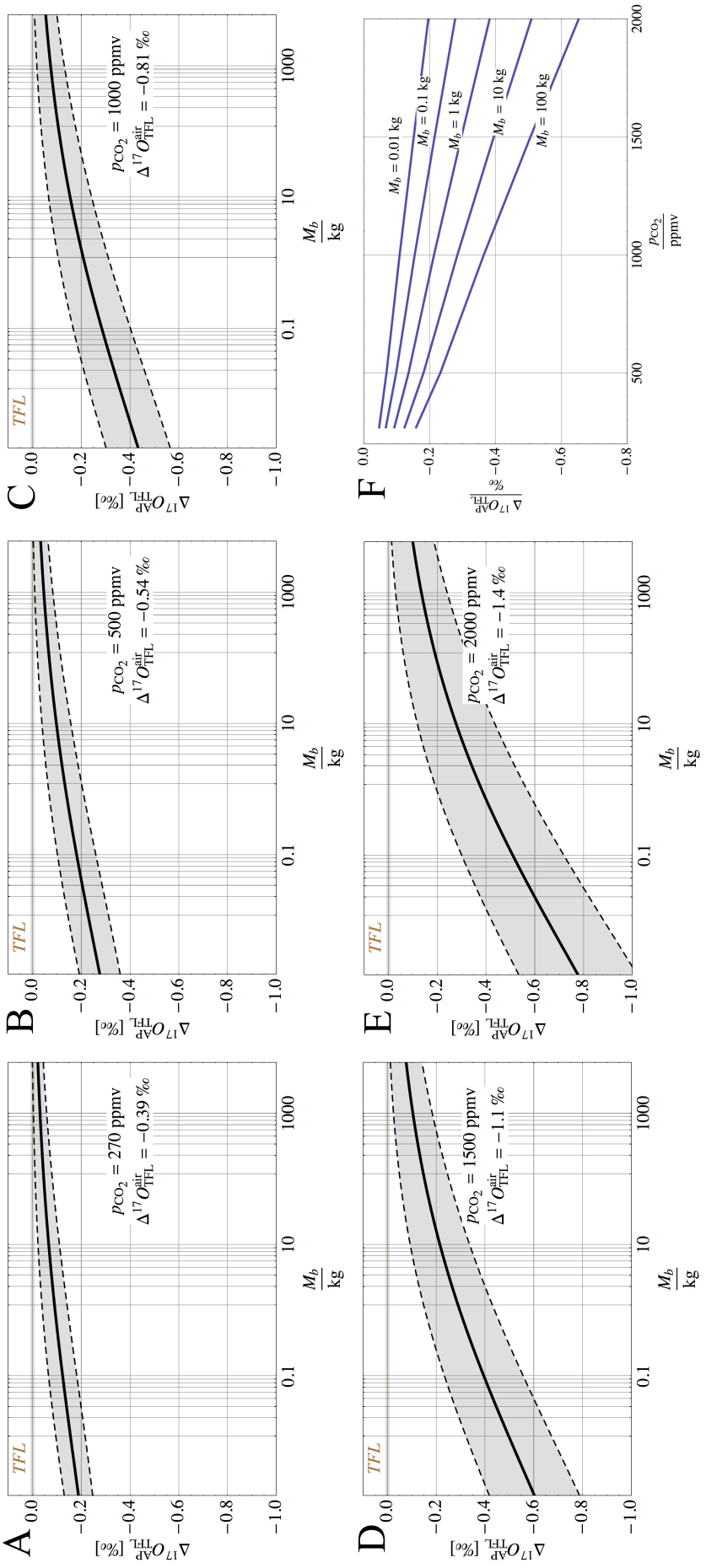

Fig. 3.3: (A – E) Plots of $\Delta^{17}O_{TFL}$ of bioapatite (AP) as function of body mass (M_b) for p_{CO2} between 270 (A) and 2000 ppmv (E). The gray shaded area outlines the 1σ error interval of the mass balance model. (F) Plot of the relation between $\Delta^{17}O_{TFL}$ of bioapatite and p_{CO2} for M_b between 10 g and 100 kg.

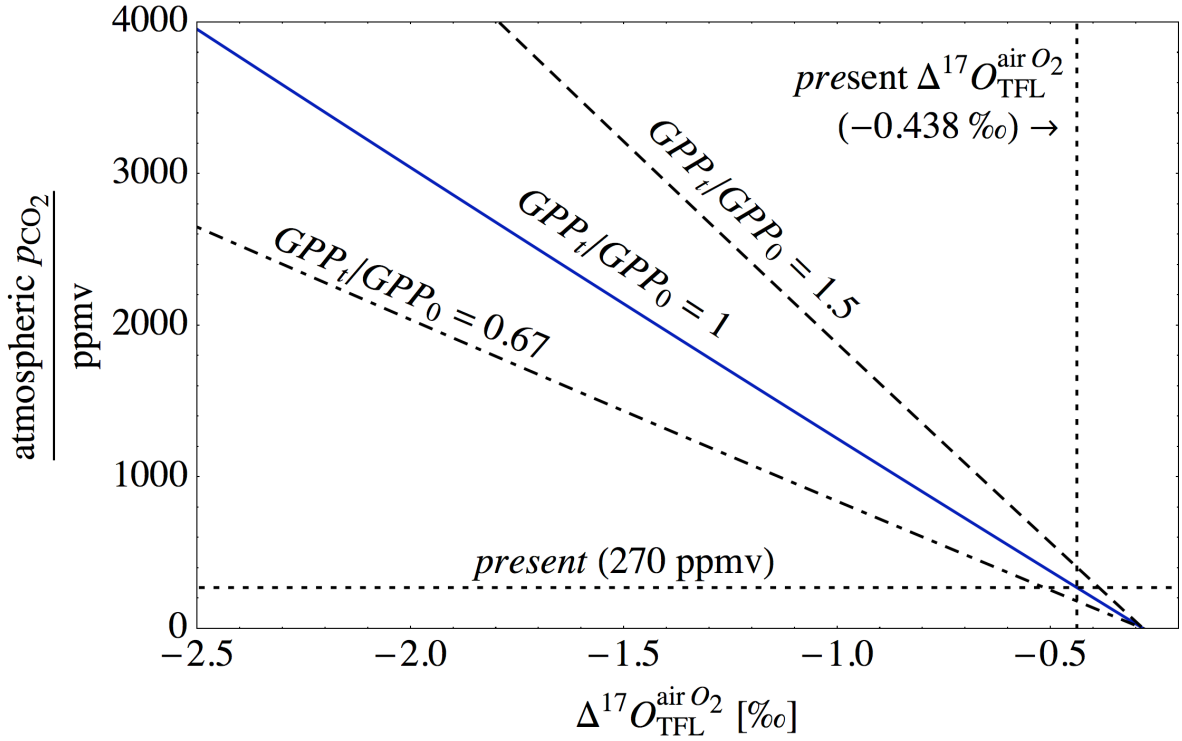

Fig. 3.4: Plot of p_{CO2} vs. $\Delta^{17}O_{TFL}$ of tropospheric O_2. The relation is taken from Bao et al. (2008). Shown are relations for GPP_t/GPP_0 of 0.67, 1.0 and 1.5 (see Luz et al., 1999).

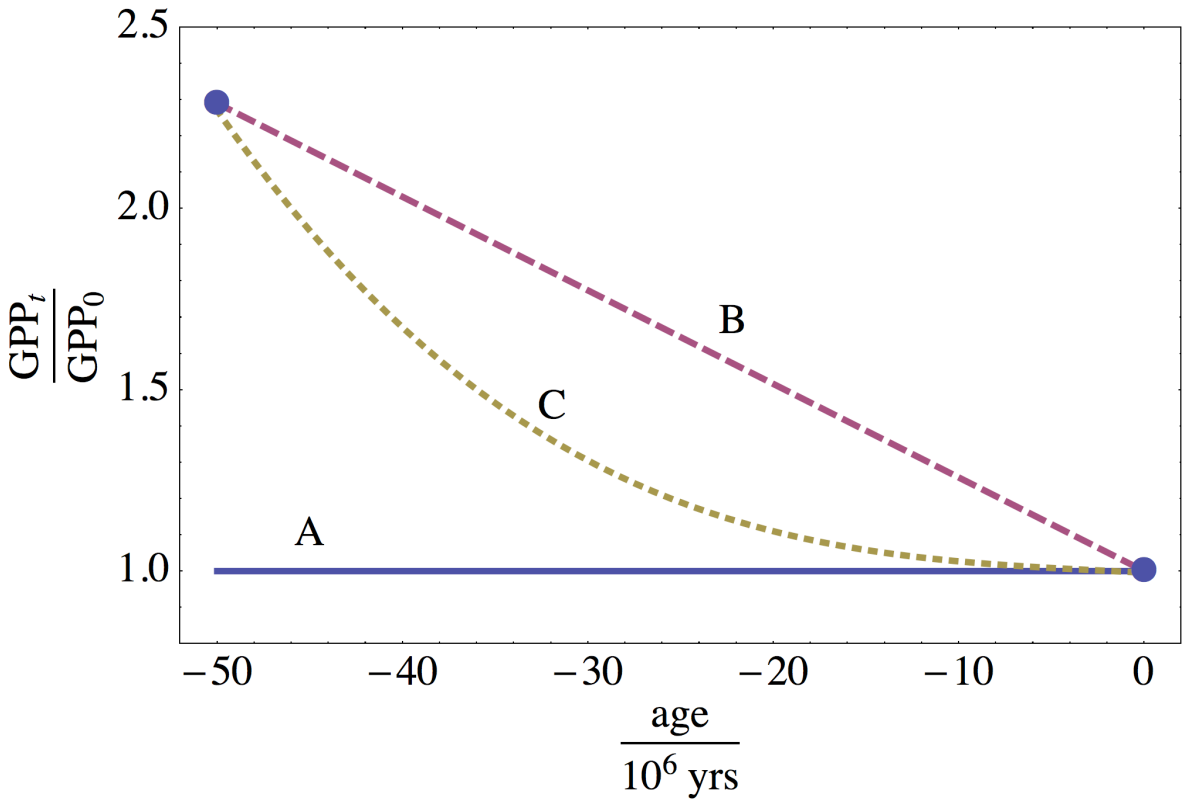

Fig. 3.5: Plot showing 3 different scenarios (A, B, C) for GPP_t/GPP_0 for the past 50 Ma. The data point for 50 Ma is from the estimate of Beerling (1999).

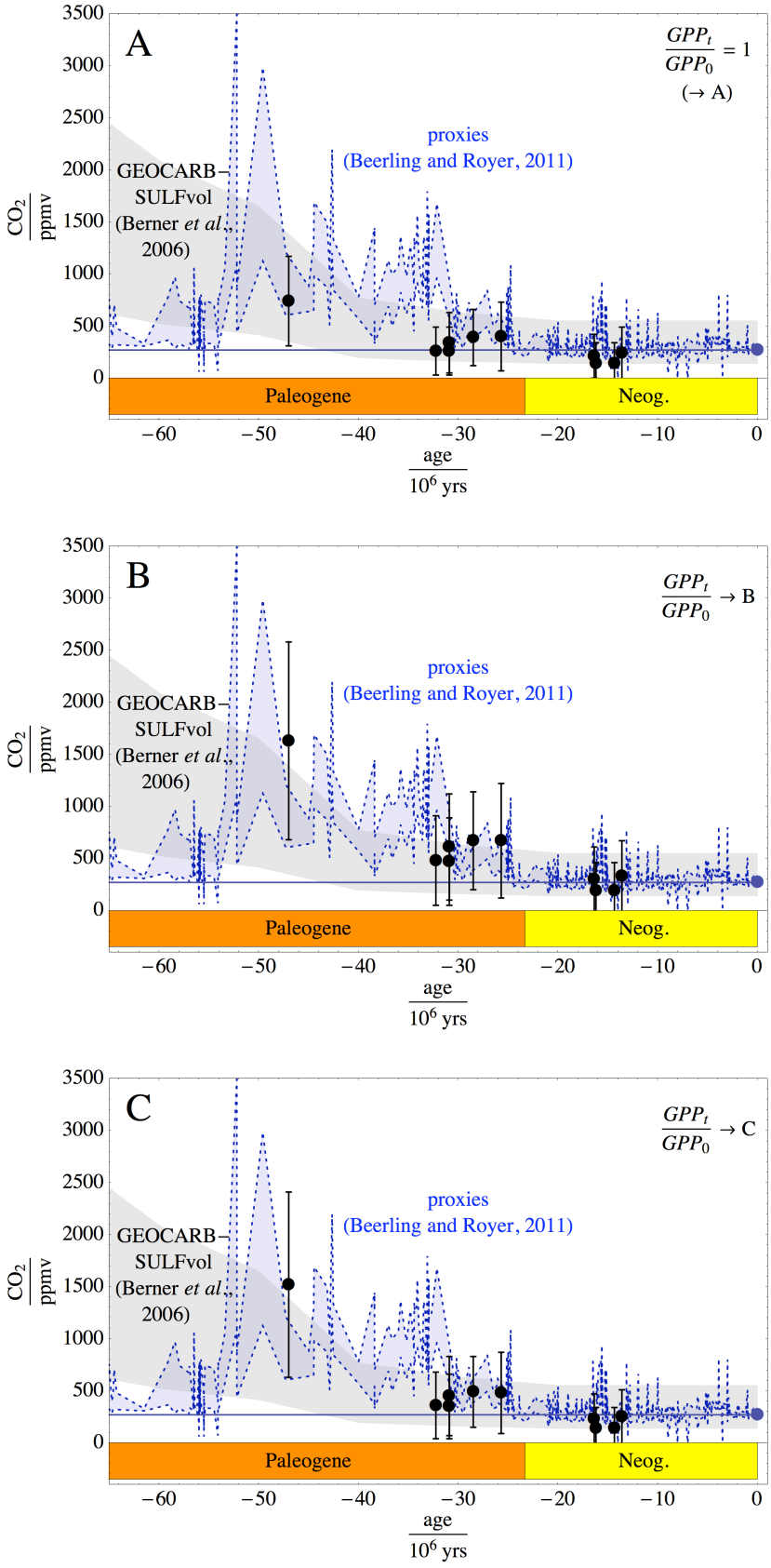

Fig. 3.6: Plot of p_{CO2} vs. time from a compilation of available proxies (Beerling and Royer, 2011) and from the GEOCARBSULFvol mass balance model (grey shaded area, Berner 2006a; 2006b; 2008). The data from this study are shown as solid black circles for the 3 different scenarios of for GPP_t/GPP_0 (Fig. 3.5). The best agreement with other proxies is obtained with a *GPP* that was similar to the present (A).

3.5.3 Error analysis

We have considered uncertainties for most of the parameters used in the mass balance. Comparison between data from recent mammals and the mass balance model shows that more than 68% of the measured data fall within the error envelope of the model. This suggests that the error calculation is rather conservative and that the actual uncertainty of the model is slightly smaller. The variation in the total water flux (F_{TW}) accounts for 51% of the uncertainty of the model. The variations in the flux of respired oxygen (F_A) and the evaporative water flux (F_{EVA}) account for 27 and 3.4% of the total uncertainty of the model. The estimated uncertainty intrinsic to the respiratory quotient (R_q) accounts for 3.1% of the total error of the model. The uncertainties intrinsic to all other parameters have little influence (<3%) on the uncertainty of the model.

The error analysis demonstrates that the variations in physiological parameters dominate the uncertainty intrinsic to the prediction of palaeo-CO_2.

3.5.4 Is $\Delta^{17}O$ of fossil bioapatite a suitable CO_2 proxy?

The relation between $\Delta^{17}O$ of bioapatite, M_b and $\Delta^{17}O$ of inhaled air can be used to determine the $\Delta^{17}O$ of past tropospheric O_2. The $\Delta^{17}O$ of tropospheric O_2 is, in turn, related to pCO_2 and gross primary production (GPP, Luz et al., 1999; Bao et al., 2008) with:

$$\frac{pCO_2}{\text{ppmv}} = (-377 - 1717 \times \Delta^{17}O_{TFL}^{air} + 23.6 \times (\Delta^{17}O_{TFL}^{air})^2) \times \frac{GPP_t}{GPP_0} \qquad \text{Eq. 3.16}$$

The ratio GPP_t/GPP_0 is the gross primary production (GPP) at time t normalised to the present GPP. The curve ($GPP_t/GPP_0 = 1$) passes through the pre-industrial pCO_2 = 270 ppmv and the present $\Delta^{17}O_{TFL}^{air}$ = –0.39‰ (Barkan and Luz, 2011). The relation between $\Delta^{17}O_{AP}$, M_b and $\Delta^{17}O_{TFL}^{air}$ is illustrated in Fig. 3.3 for CO_2 mixing ratios between 270 and 2000 ppmv.

For the Cenozoic, Beerling (1999) suggested an increase of GPP from GPP_0 = 31 Pmol O_2 yr^{-1} to $GPP_{50\,Ma}$ = 71 Pmol O_2 yr^{-1}. We calculate pCO_2 according to 3 different scenarios with respect to GPP over the last 50 Ma (Fig. 3.5). In a first scenario (A), GPP is assumed to have been constant over the past 50 Ma. In a second scenario (B), a linear decrease in GPP by a factor of ~2 over the past 50 Ma is assumed. In a third

scenario (C), a curved decrease is assumed for the past 50 Ma.

At given *GPP*, $\Delta^{17}O_{TFL}^{air}$ can be estimated from $\Delta^{17}O_{TFL}^{AP}$, and thus pCO_2 can be determined from triple oxygen isotope analyses of fossil tooth enamel of small mammals with known M_b.

Recently, Sansjofre et al. (2011) demonstrated that the O_2 concentration also influences the relation shown in Eq. 3.16. The effect of pO_2, however, is neglected in this study as variations in pO_2 were much smaller (Berner, 1999) compared to those discussed in Sansjofre et al. (2011). For the time interval studied here, pO_2 varied only between ~20 and ~25 vol.% (Berner, 1999).

The tooth enamel of the selected fossil small mammals has $\delta^{18}O$ values between 17 and 22‰ with $\Delta^{17}O_{TFL}$ varying between –0.18‰ (*Masillamys* sp; Eocene, Lutetian; Messel, Germany) and –0.07‰ (Rodentia indet.; Miocene, Langhian; Steinberg/Ries, Germany; Table 3.4). CO_2 concentrations are listed in Table 3.4.

The data suggest a decrease in pCO_2 over the past 50 Ma (Fig. 3.6). The data for scenario A (i.e. $GPP_t/GPP_0 = 1$ over the past 50 Ma) are in best agreement with other proxies (Beerling and Royer, 2011) as well as the GEOCARBSULFvolc mass balance model (Berner 2006a, b, 2008). The scenarios with a linear (B) and with a curved (C) increase in GPP from present to the elevated GPP as predicted by (Beerling, 1999) for the time 50 Ma ago would imply higher pCO_2 (e.g. ~1700 ppmv) for the Middle Eocene (Messel, 47 Ma). Other proxies and geochemical modelling suggests only ~750 ppmv for the same time. The large uncertainty intrinsic to our approach does not allow us to distinguish between the different GPP scenarios for the Oligocene and Miocene samples (Fig. 3.6).

3.6 Conclusions

- Laser fluorination in combination with GC-CF-IRMS is a suitable method for analysing $\Delta^{17}O$ of silicates, oxides and apatite with a precision of ± 0.03 - 0.05‰ (1σ, SD, single analysis).
- Bioapatite of recent mammals inherits a portion of the isotope anomaly of inhaled air O_2. It is analytically resolvable in the apatite of small (<1 kg) terrestrial mammals.
- The triple oxygen isotope exponent for the apatite-water fractionation is $\theta_{apatite\text{-}water} = 0.523 \pm 0.002$ (t = 37 °C) and deviates from the high-T approximation of θ for oxygen. The datum shows that when dealing with complex isotope fractionation networks, equilibrium exponents have to be determined for each fractionation process.
- Mass balance calculation for recent mammals supports that the isotope anomaly of inhaled air O_2 is partially transferred to bone and tooth phosphate. The largest uncertainty in the oxygen mass balance with respect to $\Delta^{17}O^{AP}$ is due to the variability in physiological parameters of the total water flux (F_{TW}), the metabolic rate (F_A), the evaporative water flux (F_{EVA}).
- The $\Delta^{17}O^{AP}$ of tooth enamel of small fossil mammals can be used as palaeo-CO_2-barometer. Data from Cenozoic mammals agree within uncertainty with other proxies and geochemical modelling if GPP was similar to today.
- When considering all possible uncertainties and applying rigorous error calculation, we obtain an uncertainty of the pCO_2 reconstruction that is comparable to other proxies and mass balance modelling. Comparison between model and data suggest that the variations of the physiological parameters (total water flux F_{TW}, respiration rate F_A) may actually be smaller than inferred from measured field data.
- At given pCO_2 (e.g. from other proxies), triple oxygen isotope analyses of small mammals can also be used to obtain information on the GPP.

Acknowledgements

The authors wish to express their gratitude to Armin Pack (Meppen) who provided most of the samples of the recent fauna. Additional samples of modern mammals were provided by M. Brecht, B. von Bülow, F. Mayer, L. Maul, M. Reich and B. Wuntke. Further thanks are due to K. Heissig, T. Lehmann, G. Rößner, M. Rummel, S. Schaal and T. Tütken who provided the fossil samples. M .E. G. Hofmann and B. Horváth are thanked for inspiring discussions. Z. D. Sharp provided skeletal material of a New Mexican kangaroo rat and is thanked for inspiring discussions. For the assistance in the sample preparation and isotope measurements, the authors would like to thank N. Albrecht and M. Kröger. R. Przybilla is thanked for his technical support at the mass spectrometer and the extraction line. Reviews by H. Bao and a number of anonymous reviewers led to improvements of this and the earlier versions of the manuscript. Editorial handling and helpful suggestions by E. Schauble are acknowledged. A. G. was supported by the German National Science Foundation DFG grant PA909/5-1 (A.P.).

References

Arrhenius, S. (1896). On the influence of carbonic acid in the air upon the temperature on the ground. *Philosophical Magazine* **41**, 237-279.

Asprey, L.B. (1976). The preparation of very pure F_2 gas. *Journal of Fluorine Chemistry* **7**, 359-361.

Bao, H., Lyons, J., Zhou, C. (2008). Triple oxygen isotope evidence for elevated CO_2 levels after a Neoproterozoic glaciation. *Nature* **453**, 504-506.

Barkan, E., Luz, B. (2005). High precision measurements of $^{17}O/^{16}O$ and $^{18}O/^{16}O$ ratios in H_2O. *Rapid Communications in Mass Spectrometry* **19**, 3737-3742.

Barkan, E., Luz, B. (2011). The relationships among the three stable isotopes of oxygen in air, seawater and marine photosynthesis. *Rapid Communications in Mass Spectrometry* **25**, 2367-2369.

Beerling, D. (1999). Quantitative estimates of changes in marine and terrestrial primary productivity over the past 300 million years. *Proceedings Of the Royal Society Of London B* **266**, 1821-1827.

Beerling, D.J., Royer, D.L. (2011). Convergent Cenozoic CO_2 history. *Nature Geoscience* **4**, 418-420.

Berner, R.A. (1999). Atmospheric oxygen over Phanerozoic time. *Proceedings of the National Academy of Sciences* **96**, 10955-10957.

Berner, R. (2006a). GEOCARBSULF: a combined model for Phanerozoic atmospheric O_2 and CO_2. *Geochimica et Cosmochimica Acta* **70**, 5653-5664.

Berner, R.A. (2006b). Inclusion of the weathering of volcanic rocks in the GEOCARBSULF model. *American Journal of Science* **306**, 295-302.

Berner, R.A. (2008). Addendum to "Inclusion of the weathering of volcanic rocks in the GEOCARBSULF model" (V. 306, p. 295-302, 2006). *American Journal of Science*

308, 100-103.

Böhme, M., Ilg, A. (2003). Online Database of Vertebrates: Fossil Fishes, Amphibians, Reptiles, and Birds (fosFARbase), <http://www.wahre-staerke.com/>.

Breecker, D.O., Sharp, Z.D., McFadden, L.D. (2010). Atmospheric CO_2 concentrations during ancient greenhouse climates were similar to those predicted for A.D. 2100. *Proceedings of the National Academy of Sciences* **107**, 576-580.

Brenninkmeijer, C.A.M., Kraft, P., Mook, W.G. (1983). Oxygen isotope fractionation between CO_2 and H_2O. *Chemical Geology* **41**, 181-190.

Bryant, J.D., Froelich, P.N. (1995). A model of oxygen isotope fractionation in body water of large mammals. *Geochimica et Cosmochimica Acta* **59**, 4523-4537.

Clayton, R.N., Grossman, L., Mayeda, T.K. (1973). A component of primitive nuclear composition in carbonaceous meteorites. *Science* **182**, 485-488.

Epstein, S., Zeiri, L. (1988). Oxygen and carbon isotopic compositions of gases respired by humans and plants. *Proceedings of the National Academy of Sciences* **85**, 1727-1731.

Gehler, A., Tütken, T., Pack, A. (2011). Triple oxygen isotope analysis of bioapatite as tracer for diagenetic alteration of bones and teeth. *Palaeogeography, Palaeoclimatology, Palaeoecology* **310**, 84-91.

Grzimek, B. (Ed.), (1990). *Grzimek's Encyclopedia of Mammals*. New York City (McGraw-Hill), 3250 pp.

Hofmann, M.E.G., Horváth, B., Pack, A. (2012). Triple oxygen isotope equilibrium fractionation between carbon dioxide and water. *Earth and Planetary Science Letters* **319-320**, 159-164.

Hofmann, M.E.G., Pack, A. (2010). Technique for high-precision analysis of triple oxygen isotope ratios in carbon dioxide. *Analytical Chemistry* **82**, 4357-4361.

Horita, J., Wesolowski, D.J. (1994). Liquid-vapor fractionation of oxygen and hydrogen isotopes of water from the freezing to the critical temperature. *Geochimica et Cosmochimica Acta* **58**, 3425-3437.

Hulston, J.R., Thode, H.G. (1965). Variations in the S^{33}, S^{34}, and S^{36} contents of meteorites and their relation to chemical and nuclear effects. *Journal of Geophysical Research* **70**, 3475-3484.

IAEA (2011). Water Isotope System for Data Analysis, Visualization, and Electronic Retrieval (WISER). IAEA: International Atomic Energy Agency.

Kleiber, M. (1947). Body size and metabolic rate. *Physiological Reviews* **27**, 511-541.

Kohn, M.J. (1996). Predicting animal $\delta^{18}O$: accounting for diet and physiological adaption. *Geochimica et Cosmochimica Acta* **60**, 4811-4829.

Kohn, M.J., Cerling, T.E. (2002). Stable isotope compositions of biological apatite. *Reviews in Mineralogy and Geochemistry* **48**, 455-488.

Kürschner, W.M., Kvacek, Z., Dilcher, D.L. (2008). The impact of Miocene atmospheric carbon dioxide fluctuations on climate and the evolution of terrestrial ecosystems. *Proceedings of the National Academy of Sciences* **105**, 449-453.

Kusakabe, M., Matsuhisa, Y. (2008). Oxygen three-isotope ratios of silicate reference materials determined by direct comparison with VSMOW-oxygen. *Geochemical Journal* **42**, 309-317.

Landais, A., Barkan, E., Yakir, D., Luz, B. (2006). The triple isotopic composition of oxygen in leaf water. *Geochimica et Cosmochimica Acta* **70**, 4105-4115.

Landais, A., Lathiere, J., Barkan, E., Luz, B. (2007). Reconsidering the change in global biosphere productivity between the Last Glacial Maximum and present day from the triple oxygen isotopic composition of air trapped in ice cores. *Global Biogeochemical Cycles* **21**, GB1025.

Lindars, E.S., Grimes, S.T., Mattey, D.P., Collinson, M.E., Hooker, J.J., Jones, T.P. (2001). Phosphate $\delta^{18}O$ determination of modern rodent teeth by direct laser fluorination: an appraisal of methodology and potential application to palaeoclimate reconstruction. *Geochimica et Cosmochimica Acta* **65**, 2535-2548.

Longinelli, A. (1984). Oxygen isotopes in mammal bone phosphate: a new tool for paleohydrological and paleoclimatological research? *Geochimica et Cosmochimica Acta* **48**, 385-390.

Longinelli, A., Nuti, S. (1973). Revised phosphate-water isotopic temperature scale. *Earth and Planetary Science Letters* **19**, 373-376.

Lüthi, D., Le Floch, M., Bereiter, B., Blunier, T., Barnola, J.-M., Siegenthaler, U., Raynaud, D., Jouzel, J., Fischer, H., Kawamura, K., Stocker, T.F. (2008). High-resolution carbon dioxide concentration record 650,000-800,000 years before present. *Nature* **453**, 379-382.

Luz, B., Barkan, E. (2005). The isotopic ratios $^{17}O/^{16}O$ and $^{18}O/^{16}O$ in molecular oxygen and their significance in biogeochemistry. *Geochimica et Cosmochimica Acta* **69**, 1099-1110.

Luz, B., Barkan, E. (2010). Variations of $^{17}O/^{16}O$ and $^{18}O/^{16}O$ in meteoric waters. *Geochimica et Cosmochimica Acta* **74**, 6276-6286.

Luz, B., Barkan, E., Bender, M.L., Thiemens, M.H., Boering, K.A. (1999). Triple-isotope composition of atmospheric oxygen as a tracer of biosphere productivity. *Nature* **400**, 547-550.

Luz, B., Kolodny, Y., Horowitz, M. (1984). Fractionation of oxygen isotopes between mammalian bone phosphate and environmental drinking water. *Geochimica et Cosmochimica Acta* **48**, 1689-1693.

Meijer, H.A.J., Li, W.J. (1998). The use of electrolysis for accurate $\delta^{17}O$ and $\delta^{18}O$ isotope measurements in water. *Isotopes in Environmental and Health Studies* **34**, 349-369.

Miller, M.F. (2002). Isotopic fractionation and the quantification of ^{17}O anomalies in the oxygen three-isotope system: an appraisal and geochemical significance. *Geochimica et Cosmochimica Acta* **66**, 1881-2055.

Mohr, E. (1950). *Die freilebenden Nagetiere Deutschlands und der Nachbarländer*. Jena (Gustav Fischer), 212 pp.

Nagy, K.A., Girard, I.A., Brown, T.K. (1999). Energetics of free-ranging mammals, reptiles, and birds. *Annual Review of Nutrition* **19**, 247-277.

Nagy, K.A., Peterson, C.C. (1988). *Scaling of Water Flux Rate in Animals*. Berkeley (University of California Press), 172 pp.

Niethammer, J., Krapp, F. (Eds.), (1978-2005). *Handbuch der Säugetiere Europas*. Aula-Verlag, Wiebelsheim, 6300 pp.

Pack, A., Toulouse, C., Przybilla, R. (2007). Determination of oxygen triple isotope ratios of silicates without cryogenic separation of NF_3 — technique with application to analyses of technical O_2 gas and meteorite classification. *Rapid Communications in Mass Spectrometry* **21**, 3721-3728.

Pagani, M., Zachos, J.C., Freeman, K.H., Tipple, B., Bohaty, S. (2005). Marked decline in atmospheric carbon dioxide concentrations during the Paleogene. *Science* **309**, 600-603.

Pearson, P.N., Foster, G.L., Wade, B.S. (2009). Atmospheric carbon dioxide through the Eocene-Oligocene climate transition. *Nature* **461**, 1-4.

Petit, J.R., Jouzel, J., Raynaud, D., Barkov, N.I., Barnola, J.-M., Basile, I., Bender, M., Chappellaz, J., M. Davisk, Delaygue, G., Delmotte, M., Kotlyakov, V.M., Legrand, M., Lipenkov, V.Y., Lorius, C., Pépin, L., Ritz, C., Saltzmank, E., Stievenard, M. (1999). Climate and atmospheric history of the part 420,000 years from the Vostok ice core, Antarctica. *Nature* **399**, 429-436.

Podlesak, D.W., Torregrossa, A., Ehleringer, J., Dearing, M., Passey, B., Cerling, T.E. (2008). Turnover of oxygen and hydrogen isotopes in the body water, CO_2, hair, and enamel of a small mammal. *Geochimica et Cosmochimica Acta* **72**, 19-35.

Roth-Nebelsick, A. (2005). Reconstructing atmospheric carbon dioxide with stomata: possibilities and limitations of a botanical pCO_2-sensor. *Trees - Structure and Function* **19**, 251-265.

Royer, D.L., Berner, R., Beerling, D.J. (2001). Phanerozoic atmospheric CO_2 change: evaluating geochemical and paleobiological approaches. *Earth-Science Reviews* **54**, 349-392.

Rumble, D., Miller, M.F., Franchi, I.A., Greenwood, J.P. (2007). Oxygen three-isotope fractionation lines in terrestrial silicate minerals: an inter-laboratory comparison for hydrothermal quartz and eclogite garnet. *Geochimica et Cosmochimica Acta* **71**, 3592-3600.

Sansjofre, P., Adler, M., Trindade, R.I.F., Elie, M., Lyons, J., Cartigny, P., Nogueira, A.C.R. (2011). A carbon isotope challange to the snowball Earth. *Nature* **478**, 93-96.

Schmidt-Nielsen, B. (1984). *Scaling, why is animal size so important?*. Cambridge (Cambridge University Press), 241 pp.

Schmidt-Nielsen, K. (1972). *How animals work*. New York (Cambridge University Press), New York, 114 pp.

Sharp, Z.D. (1990). A laser-based microanalytical method for the *in situ* determination of oxygen isotope ratios of silicates and oxides. *Geochimica et Cosmochimica Acta* **54**, 1353-1357.

Tanaka, R., Nakamura, E. (2012). Kinetic isotope fractionation effect observed in oxygen triple isotope ratios in terrestrial silicate minerals, Sixth International Symposium on Isotopomers. Carnegie Institution of Washington, Washington (DC), p. 88.

Veizer, J., Godderis, Y., Francois, L.M. (2000). Evidence for decoupling of atmospheric CO_2 and global climate during the Phanerozoic eon. *Nature* **408**, 698-701.

Wiechert, U.H., Halliday, A.N., Palme, H., Rumble, D. (2004). Oxygen isotope evidence for rapid mixing of the HED meteorite parent body. *Earth and Planetary Science Letters* **221**, 373-382.

Yoshida, N., Miyazaki, N. (1991). Oxygen isotope correlation of cetacean bone phosphate with environmental water. *Journal of Geophysical Research* **96**, 815-820.

Young, E.D., Galy, A., Nagahara, H. (2002). Kinetic and equilibrium mass-dependent isotope fractionation laws in nature and their geochemical and cosmochemical significance. *Geochimica et Cosmochimica Acta* **66**, 1095-1104.

4. Manuscript III

Temperature and atmospheric CO_2-concentration changes across the Palaeocene-Eocene Thermal Maximum (PETM) – new insights from triple oxygen isotope analysis of mammalian bioapatite

Alexander Gehler[a], Philip D. Gingerich[b] & Andreas Pack[a]

[a]Georg-August-Universität, Geowissenschaftliches Zentrum, Abteilung Isotopengeologie, Goldschmidtstr. 1, D-37077 Göttingen, Deutschland

[b]Museum of Paleontology, The University of Michigan, Ann Arbor, MI 48109-1079, United States of America

In preparation, not yet approved by the coauthors for submission

Abstract

One of the most remarkable environmental and climatic events during the Cenozoic is the Palaeocene-Eocene Thermal Maximum (PETM), whose detailed understanding might also improve our knowledge of future climate change. It is marked by a large negative carbon isotope excursion (CIE) contemporaneous with a rapid temperature increase about 56 Ma ago. Whereas the CIE and the temperature rise are well-documented by a number of terrestrial and marine proxies, the carbon source responsible for the CIE as well as the quantities of the greenhouse gases CO_2 and CH_4, which contributed to global warming, are poorly constrained by proxy data and still highly debated. The present study for the first time combines an established method to estimate palaeotemperature change with a newly developed proxy approach that aims to quantify ancient CO_2 concentrations, both from the oxygen composition of mammalian bioapatite. Here we present triple oxygen isotope data of tooth enamel from the genus *Ectocion* (Mammalia, Condylarthra, Phenacodontidae) from PETM strata of the Clarks Fork Basin (Wyoming, USA) with the intent to help towards an enhanced understanding of this „ancient carbon mystery“, as it has been referred to by an earlier study. Our results are consistent with existing estimates of PETM temperature change but do not suggest any extremely large fluctuations in pCO_2, supporting the hypothesis of methane clathrate as primary carbon source that induced the CIE.

4.1 Introduction

The Palaeocene-Eocene transition at about 56 Ma (Westerhold et al., 2009) is marked by an abrupt climate change in conjunction with a large negative carbon isotope excursion (CIE), ocean acidification and enhanced terrestrial runoff during a period lasting less than 200,000 years (McInerney and Wing, 2011 and refs. therein). Within this period, a global temperature increase of 5 to 8°C has been inferred from a variety of marine and terrestrial proxies (Dickens, 2011 and refs. therein; McInerney and Wing, 2011 and refs. therein) which led to the frequently-used term "Palaeocene-Eocene Thermal Maximum" (PETM) for the respective time interval.

The CIE is well-documented by proxy data and it is largely accepted that it was caused by the addition of several Gt of ^{13}C-depleted carbon into the exogenic carbon cycle (McInerney and Wing, 2011 and refs. therein). Considering the atmospheric CIE to be between –4 and –5‰ (Diefendorf et al., 2010; Cui et al., 2011; McInerney and Wing, 2011 and refs. therein), the suggested amount of carbon needed to cause this negative carbon isotope shift ranges between 2200 and 153,000 Gt, primarily depending on the isotope composition of its carbon source and secondarily on the used model approach (Panchuk et al., 2008; Zeebe et al., 2009; Cui et al., 2011; Dickens, 2011 and refs. therein; McInerney and Wing, 2011 and refs. therein). Possible carbon sources are biogenic methane (i.e. methane clathrates, $\delta^{13}C \sim -60‰$), thermogenic methane or permafrost soil carbon ($\delta^{13}C \sim -30‰$), carbon released due to wildfires or by desiccation and oxidation of organic matter due to drying of epicontinental seas ($\delta^{13}C \sim -22‰$) and mantle CO_2 ($\delta^{13}C \sim -5‰$) (Higgins and Schrag, 2006; McInerney and Wing, 2011 and refs. therein).

A massive release of methane clathrates by thermal dissociation (Dickens et al., 1995 and refs. therein) has been the most convincing hypothesis to explain the CIE for years but after the emergence of substantial scepticism it is still debated controversially and evidence for the involvement of other carbon sources – exclusively or additional – is discussed critically (e.g. Higgins and Schrag, 2006; Dickens, 2011 and refs. therein; McInerney and Wing, 2011 and refs. therein).

However, the contemporaneous global warming, also well-documented by marine and terrestrial proxy data (McInerney and Wing, 2011 and refs. therein), unquestionably has been induced by radiative forcing due to increased concentrations of greenhouse gases,

most likely CO_2 and/or CH_4, and accessory phenomena such as aerosol forcing and reduced cloudiness (Dickens, 2011; Kurtén et al., 2011).

Strongly differing CO_2 scenarios have been discussed for the PETM. Depending from the proposed magnitude of the CIE and the associated carbon source, mass balance estimates range from an atmospheric CO_2 concentration increase of less than 100 to several 10,000 ppm (e.g. Schmidt and Shindell, 2003; Shellito et al., 2003; Zachos et al., 2003; Renssen and Beets, 2004; Pagani et al., 2006; Panchuk et al., 2008; Zeebe et al., 2009; Cui et al., 2011; McInerney and Wing, 2011 and refs. therein).

Existing proxy data for CO_2 concentrations in the relevant time slice (50 to 60 Ma) suggest a pCO_2 between 100 and 1900 ppm (Beerling and Royer, 2011 and refs. therein), but only a single estimate (Royer et al., 2001) is roughly correlated to PETM strata.

In an alternative approach, Currano et al. (2008; 2011) try to connect increased insect herbivory during the PETM to three to four times increased atmospheric CO_2 levels but cannot convincingly prove that this is not an effect of higher insect diversity and population density due to the elevated temperatures.

Here we report triple oxygen isotope data of tooth enamel bioapatite of the genus *Ectocion* (Mammalia, Condylarthra, Phenacodontidae) from the Late Clarkforkian and Early Wasatchian of the Clarks Fork Basin (Wyoming, USA). The analysed samples originate from strata shortly before, within and after CIE and PETM, with the attempt to expand the current knowledge of temperature and CO_2 concentration change through the Palaeocene-Eocene transition. Our approach enables to record both, temperature and CO_2 fluctuations, from a single proxy. It is (1) based on the well-studied connection between the oxygen composition of mammalian bioapatite and air temperature (e.g. Longinelli, 1984; Luz et al., 1984) and (2) on a recently published finding of a relation between the triple oxygen composition of mammalian bioapatite and atmospheric CO_2 concentrations (Pack et al., in press).

4.2 Definitions

Variations in the oxygen isotope ratios ($^{17}O/^{16}O$, $^{18}O/^{16}O$) are usually reported relative to the international isotope reference standard Vienna Standard Mean Ocean Water (VSMOW) in terms of the δ-notation as ‰-variations. The $\delta^{17}O$ and $\delta^{18}O$ values are defined as:

$$\delta^{17}\mathrm{O}(‰) = \left(\frac{\left(\frac{^{17}\mathrm{O}}{^{16}\mathrm{O}}\right)_{\mathrm{sample}}}{\left(\frac{^{17}\mathrm{O}}{^{16}\mathrm{O}}\right)_{\mathrm{VSMOW}}} - 1 \right) \times 1000 \qquad \text{Eq. 4.1}$$

$$\delta^{18}\mathrm{O}(‰) = \left(\frac{\left(\frac{^{18}\mathrm{O}}{^{16}\mathrm{O}}\right)_{\mathrm{sample}}}{\left(\frac{^{18}\mathrm{O}}{^{16}\mathrm{O}}\right)_{\mathrm{VSMOW}}} - 1 \right) \times 1000 \qquad \text{Eq. 4.2}$$

In mass dependent (equilibrium or kinetic) fractionation processes, $\delta^{18}O$ is correlated to $\delta^{17}O$ by

$$\left(\frac{\left(\frac{^{17}\mathrm{O}}{^{16}\mathrm{O}}\right)_{\mathrm{sample}}}{\left(\frac{^{17}\mathrm{O}}{^{16}\mathrm{O}}\right)_{\mathrm{VSMOW}}} \right) = \left(\frac{\left(\frac{^{18}\mathrm{O}}{^{16}\mathrm{O}}\right)_{\mathrm{sample}}}{\left(\frac{^{18}\mathrm{O}}{^{16}\mathrm{O}}\right)_{\mathrm{VSMOW}}} \right)^{\lambda} \qquad \text{Eq. 4.3}$$

where λ indicates the slope of a specific fractionation slope which varies slightly around 0.52 in nearly all terrestrial fractionation processes.

Oxygen isotope compositions diverging from this reference line (RL) are denominated as anomalous. For an accurate quantification of these ^{17}O anomalies, the linearised form of the δ-notation ($\delta'^{17}O$, $\delta'^{18}O$) must be used (Hulston and Thode, 1965; Miller, 2002), which is defined as:

$$\delta'^{17}O = 1000 \times \ln\left(\frac{\delta^{17}O}{1000} + 1\right) \quad \text{Eq. 4.4}$$

$$\delta'^{18}O = 1000 \times \ln\left(\frac{\delta^{18}O}{1000} + 1\right) \quad \text{Eq. 4.5}$$

Typically, ^{17}O anomalies are expressed as $\Delta^{17}O$ values. In a $\delta'^{17}O$ vs. $\delta'^{18}O$ diagram, $\Delta^{17}O$ is defined by the deviation of a sample in $\delta'^{17}O$ from a RL with:

$$\Delta^{17}O_{RL}^{sample} = \delta'^{17}O_{VSMOW}^{sample} - \lambda_{RL} \times \delta'^{18}O_{VSMOW}^{sample} - \gamma_{RL} \quad \text{Eq. 4.6}$$

where λ denotes the slope of the RL and γ the intercept of the RL. In the present study, we used the Terrestrial Fraction Line (TFL) with a slope λ of 0.5251 and an intercept γ of –0.048 (Pack et al., in press and refs. therein).

4.3 Oxygen isotopes in mammalian bioapatite and its palaeoclimatic relevance

The oxygen isotope composition of mammalian body water is determined by its different oxygen sources and sinks. The main oxygen input sources for mammals are drinking water, food water and inhaled air O_2. The fractionation between $\delta^{18}O$ of body water and $\delta^{18}O$ of bioapatite in mammals is constant due to a constant body temperature of ~37°C, and it has been demonstrated that it is possible to relate the $\delta^{18}O$ of mammalian bioapatite to the oxygen isotope composition of drinking water (i.e. environmental surface water, $\delta^{18}O_{SW}$) by empirically developed calibration equations or by modeling approaches (Longinelli, 1984; Luz et al., 1984; Luz and Kolodny, 1985; D'Angela and Longinelli, 1990; Bryant and Froelich, 1995; Kohn, 1996). Due to the strong correlation between the oxygen isotope composition of $\delta^{18}O_{SW}$ and mean annual (air) temperatures (MAT) (Dansgaard, 1964), it is in turn possible to infer palaeotemperatures using the reconstructed oxygen isotope composition of $\delta^{18}O_{SW}$ from $\delta^{18}O$ of mammalian bioapatite, which was first applied extensively by Bryant et al. (1994).

Studies relying on this principle already exist for the Paleocene-Eocene transition in the Clarks Fork and Bighorn Basin (Wyoming, USA) on various mammalian taxa, targeting either the carbonate oxygen component ($\delta^{18}O_{CO3}$) of mammalian tooth enamel, the

phosphate oxygen component (phosphate ($\delta^{18}O_{PO4}$) or both in a combined approach (Koch et al., 1995; Fricke et al., 1998; Fricke, 2003; Fricke and Wing, 2004; Secord et al., 2008; Secord et al., 2010; Secord et al., 2012).

Those studies can rely solely on $\delta^{18}O$, because in nearly all terrestrial fractionation processes, $\delta^{18}O$ is correlated to $\delta^{17}O$ by the equation $\delta^{17}O \sim 0.52 \times \delta^{18}O$ (Eq 3, e.g. Sharp, 2007 and refs. therein).

However, a fractionation slope of ~0.52 is not valid for a number of atmospheric gas species such as CO, CO_2, O_3 and N_2O (e.g. Thiemens, 2006 and refs. therein) due to mass independent fractionation effects resulting in a ^{17}O-anomaly, which is typically expressed as $\Delta^{17}O$ (Eq. 6). A small ^{17}O-anomaly in atmospheric O_2 was first proposed by M. Thiemens (in Bender et al., 1994) and was later confirmed and quantified in detail by Luz et al. (1999) and Luz and Barkan (2005; 2011). The ^{17}O-anomaly of air oxygen is a function of the atmospheric CO_2 concentration and global gross primary productivity (GPP) (Luz et al., 1999; Bao et al., 2008). The $\Delta^{17}O$ of modern air oxygen in relation to the TFL used here (see chapter 4.2) is –0.39‰.

Recently, Pack et al. (in press) demonstrated that a portion of this anomaly can be detected in mammalian skeletal tissue due to transfer from inhaled air to body water and respectively to bioapatite. The magnitude of the ^{17}O-anomaly in mammalian bioapatite is connected to the fraction of inhaled anomalous air O_2 in relation to the other oxygen sources. For physiological reasons, the anomaly increases in mammalian skeletal tissue with decreasing body mass (Pack et al., in press).

In the same study, Pack et al. (in press) evaluated the potential of $\Delta^{17}O$ values from fossil mammalian bioapatite as a proxy to estimate palaeo-CO_2 concentrations by reconstructing the $\Delta^{17}O$ of ancient tropospheric O_2, which is linearly related to the atmospheric pCO_2 (Bao et al., 2008). The most suitable taxa for an application of this method should have a body weight as small as possible (to ensure a high portion of inhaled anomalous air oxygen in respect to the other oxygen sources) but large enough (with respect to fossil samples) to provide an adequate amount of diagenetically unaltered sample material (i.e. tooth enamel, see section 4.4.1).

4.4 Materials and Methods

4.4.1 Samples

We have sampled teeth from jaws as well as isolated teeth from the phenacodontid genus *Ectocion* (*E*. *osbornianus* and *E*. *parvus*) from the Clarks Fork Basin (Sand Coulee area) in north-western Wyoming, USA (e.g. Gingerich and Smith, 2006). The samples cover a time interval of several mammalian biozones, from the Late Clarkforkian (Cf-3) to the Early Wasatchian (Wa-2), encompassing the PETM. All samples were acquired from the collections of the Museum of Paleontology at the University of Michigan, Ann Arbor (localities SC-002, SC-011, SC-067, SC-107, SC-138 and SC-161) and were casted before the destructive sampling. Only second molars (M2) were used for the present study to obtain highest possible comparability.

Due to its higher resistance to post-depositional diagenetic alteration (e.g. Kohn and Cerling, 2002; Gehler et al., 2011 and refs. therein), only tooth enamel carefully hand-picked under a binocular prior to the pretreatment was used for the present study.

4.4.2 Sample pretreatment

To ensure analysis of the phosphate oxygen isotope composition ($\delta^{18}O_{PO4}$) only, other oxygen bearing components of the sample material (e.g. organic matter, sorbed water, structural carbonate, OH^- groups) were removed by treating the tooth enamel in an argon-flushed horizontal tube furnace for 10 to 15 minutes at 1000°C. Subsequently, the samples were cooled down to below 100°C still in an Ar atmosphere followed by an immediate storage in a desiccator until analysis (Pack et al., in press). This procedure follows Lindars et al. (2001), who demonstrated a safe removal of all these compounds at temperatures between 850 and 1000 °C. The argon is used to avoid exchange with atmospheric water which was reported to be a problem by Lindars et al. (2001) when heating their samples to 1000°C in ambient air.

4.4.3 Triple oxygen isotope analysis

The oxygen was released from the samples by infrared (IR) laser fluorination (Sharp, 1990) and analysed by gas chromatography isotope ratio monitoring gas mass spectrometry in continuous flow mode (GC-CF-IRMS) (e.g. Pack et al., 2007). Typically ~0.3 mg of pretreated fossil tooth enamel were loaded into an 18-pit polished Ni sample holder along with ~0.3 mg of pretreated tooth enamel from a modern African Elephant

(*Loxodonta africana*) as an internal standard and ~0.2 mg NBS 28 quartz. Following evacuation and heating of the sample chamber to 70°C for at least 12 hours, fluorination was implemented by heating the samples with a SYNRAD 50 W CO_2-laser in a ~20 - 30 mbar atmosphere of F_2 gas, purified according to Asprey (1976). Liberated excess F_2 was reacted with heated NaCl (~180°C) to NaF and Cl_2, the latter was cryotrapped by liquid N_2 until all samples were analysed. Sample O_2 was then cryofocused on a molecular sieve trap at –196°C (liquid N_2), afterwards expanded into a stainless steel capillary and transported with He as carrier gas through a second molecular sieve trap, where a fraction of the sample gas was again cryofocused at –196°C. After releasing it back into the He carrier gas stream by heating it in a hot water bath (~92°C), the sample O_2 was purified by passing it through a 5 Å molecular sieve GC-column of a Thermo Scientific GasBench II and injected via an open split valve of the GasBench II into the source of a Thermo MAT 253 gas mass spectrometer. The signals of $^{16}O^{16}O$, $^{17}O^{16}O$ and $^{18}O^{16}O$ were simultaneously monitored on 3 Faraday cups. Reference O_2 was injected before each sample through a second open split valve of the GasBench II. Sample and reference gas peaks (m/z = 32) had an amplitude of 20 - 30 V.

The standard deviation for replicates of the same bioapatite samples from different runs is typically better than $\pm$ 0.5‰ in $\delta^{18}O$ and $\pm$ 0.05‰ in $\Delta^{17}O$.

4.5 Results and Discussion

A total of 72 single laser fluorination analyses from 14 different *Ectocion* tooth enamel samples has been conducted, covering the Late Clarkforkian and Early Wasatchian biozones Cf-3, Wa-0 and Wa-2 (Table 4.1).

Table 4.1: Analytical results (±1σ) of $\delta^{18}O_{PO4}$ and $\Delta^{17}O$ of tooth enamel from 2nd molars of *Ectocion osbornianus* and *Ectocion parvus* from the Clarks Fork Basin (Sand Coulee area) in north-western Wyoming, USA.

Species	biozone	m level	locality	sample number	$\delta^{18}O$ (‰)	$\Delta^{17}O$ (‰)	n
Ectocion osbornianus	Wa-2	1720	Sc-002	85906	13.0±0.4	-0.08±0.04	5
Ectocion osbornianus	Wa-2	1720	Sc-002	66572 (sample A)	12.4±0.3	-0.10±0.02	8
Ectocion osbornianus	Wa-2	1720	Sc-002	66572 (sample B)	13.0±0.5	-0.10±0.03	7
mean					**12.9**	**-0.09**	
Ectocion osbornianus	Wa-2	1665	Sc-161	80705	13.5±0.4	-0.05±0.02	3
Ectocion osbornianus	Wa-2	1665	Sc-161	98404	13.2±0.3	-0.04±0.03	4
Ectocion osbornianus	Wa-2	1665	Sc-161	68200	12.3±0.3	-0.06±0.03	4
mean					**13.0**	**-0.05**	
Ectocion parvus	Wa-0	1520	Sc-067	83478	14.3±0.3	-0.05±0.04	2
Ectocion parvus	Wa-0	1520	Sc-067	87354	14.3±0.6	-0.08±0.03	5
Ectocion parvus	Wa-0	1520	Sc-067	86572 (sample A)	15.1±0.2	-0.07±0.03	7
Ectocion parvus	Wa-0	1520	Sc-067	86572 (sample B)	14.4±0.3	-0.05±0.03	2
mean					**14.5**	**-0.06**	
Ectocion osbornianus	Cf-3	1502	Sc-107	66621	11.0±0.5	-0.06±0.03	11
Ectocion osbornianus	Cf-3	1495	Sc-138	67243 (sample A)	13.7±0.3	-0.07±0.03	7
Ectocion osbornianus	Cf-3	1495	Sc-138	67243 (sample B)	13.8±0.6	-0.10±0.05	4
Ectocion osbornianus	Cf-3	1485	Sc-011	64726	12.1±0.3	-0.05±0.02	3
mean					**12.3**	**-0.07**	

4.5.1 PETM temperature change inferred from $\delta^{18}O$ of *Ectocion* tooth enamel

Considering the mean values of each mammalian biozone, the oxygen isotope composition of tooth enamel phosphate ($\delta^{18}O_{PO4}$) of the investigated *Ectocion* specimens increases from the Late Clarkforkian (Cf-3) to the CIE within the Early Wasatchian (Wa-0) by 2.2‰. From Wa-0 to Wa-2, a decrease in $\delta^{18}O_{PO4}$ of 1.6‰ is observed (Fig. 4.1; Tables 4.1; 4.2)[1]. This is in good agreement with previous data on $\delta^{18}O_{PO4}$ (Fricke et al., 1998; Secord et al., 2010) as well as on $\delta^{18}O_{CO3}$ (Koch et al., 1995; Fricke et al., 1998; Secord et al., 2010) from mammals covering in part the biozones of the present study within the region. To estimate the change of $\delta^{18}O_{SW}$ from $\delta^{18}O_{PO4}$, Secord et al. (2010) used the relationship $\Delta^{18}O_{SW} = 1.32 \times \Delta^{18}O_{PO4}$ for modern herbivorous mammals adapted from Kohn (1996) as a general basis.

[1] Due to nearly identical mean values (12.9 and 13.0‰ respectively), no discrimination regarding $\delta^{18}O_{PO4}$ has been made between the results from both considerably different stratigraphic levels (1665 and 1720 m) within Wa-2.

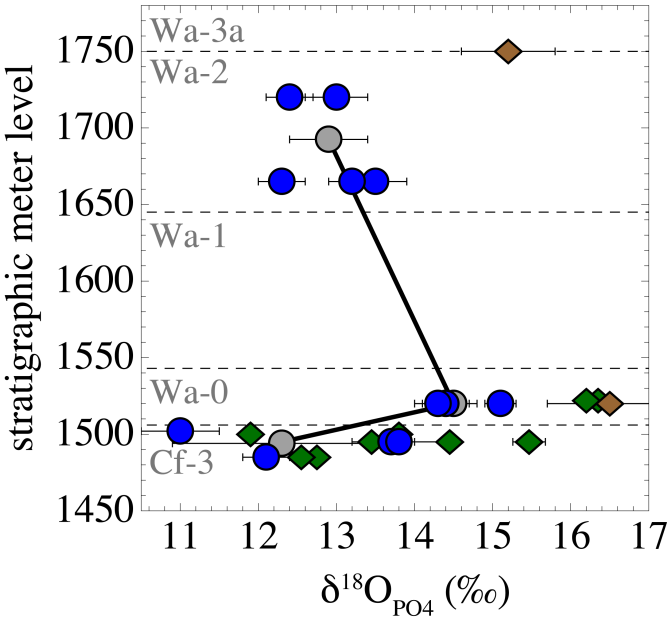

Fig. 4.1: Analytical results of $\delta^{18}O_{PO4}$ (±1σ) of *Ectocion* (blue dots, this study; Table 4.1), *Phenacodus* (green diamonds; Secord et al., 2010) and *Coryphodon* specimens (brown diamonds; Fricke et al., 1998). Grey dots represent mean biozone values of *Ectocion* (this study). Missing error bars indicate single analyses. The stratigraphic meter level is expressed in meters above the K-T boundary in the Clarks Fork Basin.

Applying this to our data, $\delta^{18}O_{LW}$ became enriched by 2.9‰ from Cf-3 to Wa-0 followed by a depletion of 2.1‰ until Wa-2 (Table 4.2).

As the $\delta^{18}O_{LW}$/MAT slope is sensitive to the latitudinal gradient and other factors (e.g. Fricke and O'Neil, 1999) an important precondition to estimate the corresponding change in temperature is to adapt this slope as well as possible to early Cenozoic conditions. The modern temperature dependence within a MAT of 0 to 20°C ranges between 0.5 and 0.6‰ per °C (Rozanski et al., 1992; Rozanski et al., 1993; Gourcy et al., 1997). With respect to conditions in the Bighorn Basin during the Palaeocene-Eocene transition, Secord et al. (2010) proposed $\delta^{18}O_{LW}$/MAT slopes of 0.39 and 0.36 (‰ per °C), based on two different approaches.

For our data on *Ectocion*, this implies an increase of 7.4°C (8.1°C) from Cf-3 to Wa-0 and a decrease of 5.4°C (5.8°C) from Wa-0 to Wa-2 (the value in brackets refers to the slope of 0.36). These results are in general agreement with previous studies from Fricke et al. (1998) and Secord et al. (2010) based on tooth enamel $\delta^{18}O_{PO4}$ of *Coryphodon* and *Phenacodus*, respectively. Calculated on the same basis, the data from Fricke et al. (1998) indicate a temperature increase of 6.2°C (6.7°C) from Cf-2 to Wa-0 and a decrease of 4.6°C (5.0°C) from Wa-0 to Wa-3[2]. The data from Secord et al. (2010) suggest a temperature increase of 7.2°C (7.8°C) from Cf-3 to Wa-0, if mean biozone values were taken into account (Table 4.2).

[2] Fricke et al. (1998) assign sample no. 83517 to Wa-1. However, if the sample number is correct it belongs to the 1750 m level and consequently should be assigned to Wa-3a.

Table 4.2: Estimated change in $\delta^{18}O_{LW}$ and temperature at the Palaeocene-Eocene transition in the Clarks Fork and Bighorn Basin, based on $\delta^{18}O_{PO4}$ of *Ectocion* (this study), *Phenacodus* (Secord et al., 2010) and *Coryphodon* (Fricke et al., 1998), for three different MAT/$\delta^{18}O_{LW}$ slopes (the modern and two calculated values for Early Eocene conditions from Secord et al., 2010).

Biozone interval	$\Delta^{18}O_{PO4}$ (‰)	$\Delta^{18}O_{LW}$ (‰)	ΔT (0.58‰/°C)	ΔT (0.39‰/°C)	ΔT (0.36‰/°C)
this study					
Wa-0 to Wa-2	-1.6	-2.1	-3.6	-5.4	-5.8
Cf-3 to Wa-0	+2.2	+2.9	+5.0	+7.4	+8.1
Secord et al. (2010)					
Cf-3 to Wa-0	+2.1	+2.8	+4.8	+7.2	+7.8
Fricke et al. (1998)					
Wa-0 to Wa-3a	-1.4	-1.8	-3.1	-4.6	-5.0
Cf-2 to Wa-0	+1.8	+2.4	+4.1	+6.2	+6.7

4.5.2 PETM CO_2 levels inferred from $\Delta^{17}O$ of *Ectocion* tooth enamel

Tooth enamel of the investigated *Ectocion* specimens has a small but distinct ^{17}O anomaly, ranging between –0.04 and –0.1‰ (Table 4.1). Using the model of Pack et al. (in press), which has been developed for terrestrial herbivorous mammals, it is possible to estimate the $\Delta^{17}O$ of inhaled, isotopically anomalous air oxygen. Body weights of *E. osbornianus* and *E. parvus* have been assigned to be 9 and 5 kg, respectively (e.g. Gingerich, 2003; Gingerich, 2006), for the model input.

Combining the approach of Pack et al. (in press) with the linear relationship of Bao et al. (2008), the suggested mean pCO_2 values are 250, 190, 130 and 460 ppm for Cf-3 (1485 to 1502 m level), Wa-0 (1520 m level), Wa-2 (1665 m level) and Wa-2 (1720 m level) respectively (Fig. 4.2a, Table 4.3). However, these data are based on modern O_2 and GPP conditions. Whereas pO_2 remains more or less unchanged within the last 60 Ma (Berner, 2001), a considerably different GPP of 2.3 times the modern value has been estimated by Beerling (1999) for the Early Eocene. As a doubling of GPP results in halving of $\Delta^{17}O_{air}$ (Bao et al., 2008; Pack et al., in press), a 2.3 times higher GPP would imply pCO_2 mean values of 580, 450, 300 and 1050 ppm for Cf-3 (1485 to 1502 m level), Wa-0 (1520 m level), Wa-2 (1665 m level) and Wa-2 (1720 m level), respectively (Fig. 4.2b, Table 4.3). All four estimates are identical within the error limit.

The results for the latter scenario agree well with previous proxy data for the time slice between 50 and 60 Ma BP from $\delta^{13}C$ of palaeosols (Koch et al., 1992; Royer et al., 2001; Breecker et al., 2010), leaf stomata (Royer et al., 2001; Greenwood et al., 2003; Royer, 2003; Beerling et al., 2009) and $\delta^{13}C$ of marine phytoplankton (Stott, 1992), which range nearly all between 300 and 800 ppm (Fig. 4.2b). Only a few palaeosol estimates propose a considerably lower pCO_2 of ~100 ppm (Sinha and Stott, 1994; reevaluated by Breecker et al., 2010), and a single estimate from $\delta^{13}C$ of fossil liverworts (Fletcher et al., 2008) suggests a considerably higher pCO_2 of ~1900 ppm for the Early Eocene. Following Beerling and Royer (2011), Palaeocene and Eocene pCO_2 estimates from $\delta^{11}B$ of planktonic foraminifera were not considered for the present comparison. Geochemical modeling (GEOCARBSULFvolc, Berner, 2006a; Berner, 2006b; Berner, 2008) predicts slightly higher pCO_2 than nearly all proxy results. However, the resolution (10 Ma time steps) precludes to track pCO_2 fluctuations within shorter time intervals (Figs. 4.2a; 4.2b).

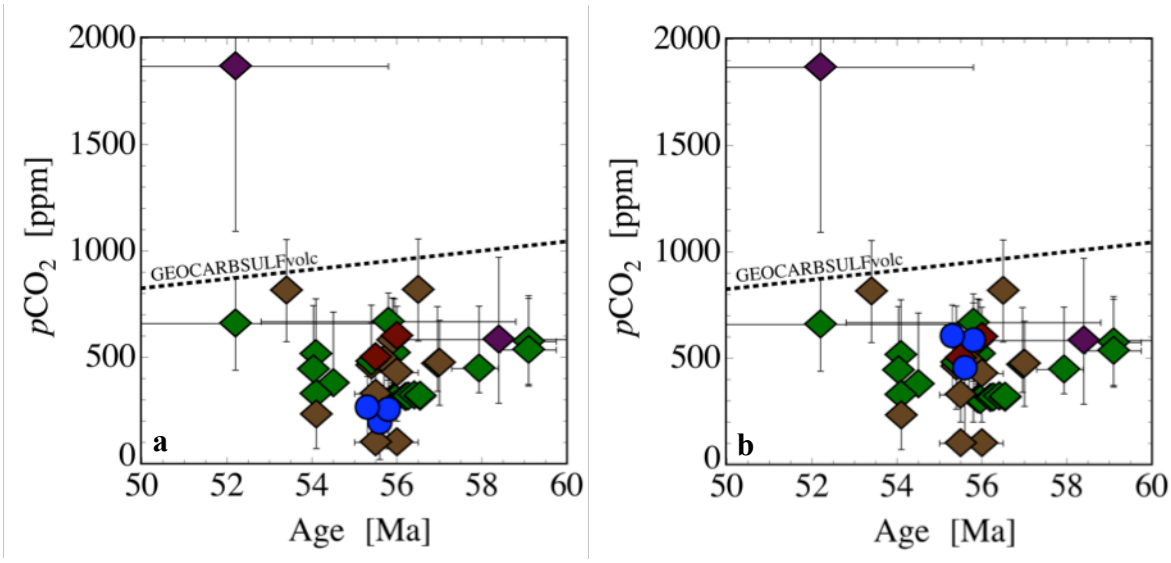

Figures 4.2a (left) and **4.2b** (right)**:** Existing proxy data for pCO_2 between 50 and 60 Ma adapted from the compilation of Beerling and Royer (2011), compared to pCO_2 estimates from $\Delta^{17}O$ of *Ectocion* bioapatite (blue dots, this study). pCO_2 has been calculated for modern GPP conditions (left) and a GPP 2.3 times the modern value (right) as proposed by Berner (2001). Brown diamonds: palaeosols, green diamonds: leaf stomata, red diamonds: marine phytoplankton, purple diamonds: liverworts.

Nearly all previously published proxy data represent either pre- or post-PETM estimates of pCO_2. Only Royer et al. (2001; updated by Beerling et al., 2009; compare also Beerling and Royer, 2011) report a single stomatal index estimate of 670 ppm based on material from the Isle of Mull, UK, that might correlate to the PETM together with slightly lower Late Paleocene and Early Eocene pCO_2 estimates ranging between 300 and 570 ppm.

Thus, the results from the Wa-0 biozone, which for the first time track CO_2 levels directly within the PETM and CIE, are of particular interest and reveal independent new information on the potential carbon source that can be accounted for the CIE.

Table 4.3: Estimated pCO_2 from $\Delta^{17}O$ of *Ectocion* bioapatite (this study), calculated for modern (GPP 1) and Early Eocene (GPP 2.3) GPP conditions as proposed by Berner (2001)., mean errors were calculated according to the equation: $\Delta x = \frac{1}{N}\sqrt{\sum_i \Delta x_i^2}$.

Species	biozone	m level	locality	sample number	pCO_2 (ppm) GPP 1	pCO_2 (ppm) GPP 2.3
Ectocion osbornianus	Wa-2	1720	Sc-002	85906	380±390	670±800
Ectocion osbornianus	Wa-2	1720	Sc-002	66572 (sample A)	540±460	1240±1050
Ectocion osbornianus	Wa-2	1720	Sc-002	66572 (sample B)	540±460	1240±1050
mean					**460±250**	**1050±580**
Ectocion osbornianus	Wa-2	1665	Sc-161	80705	130±270	300±620
Ectocion osbornianus	Wa-2	1665	Sc-161	98404	50±230	110±530
Ectocion osbornianus	Wa-2	1665	Sc-161	68200	210±310	490±710
mean					**130±160**	**300±360**
Ectocion parvus	Wa-0	1520	Sc-067	83478	90±250	220±570
Ectocion parvus	Wa-0	1520	Sc-067	87354	320±350	740±790
Ectocion parvus	Wa-0	1520	Sc-067	86572 (sample A)	240±320	560±710
Ectocion parvus	Wa-0	1520	Sc-067	86572 (sample B)	90±250	220±570
mean					**190±160**	**450±360**
Ectocion osbornianus	Cf-3	1502	Sc-107	66621	210±310	490±710
Ectocion osbornianus	Cf-3	1495	Sc-138	67243 (sample A)	290±350	670±800
Ectocion osbornianus	Cf-3	1495	Sc-138	67243 (sample B)	540±460	1240±1060
Ectocion osbornianus	Cf-3	1485	Sc-011	64726	130±270	300±620
mean					**250±170**	**580±380**

Despite the large uncertainty in pCO_2 for the individual samples, none of them suggests a peak pCO_2 higher than 1550 ppm during PETM and CIE in Wa-0. Considering the proposed increase in pCO_2 associated to the different carbon sources that are discussed to generate a global CIE in a range of –4 to –5‰, our data agree well with a dissociation of ~2500 to ~4500 Gt highly ^{13}C depleted marine methane clathrates, initially suggested by Dickens et al. (1995), which would effect only a moderate pCO_2 increase (e.g. Zeebe et al., 2009; Cui et al., 2011; McInerney and Wing, 2011 and refs. therein).

The model of Zeebe et al. (2009) proposes an increase in pCO_2 from a pre-PETM 1000 pmm baseline to ~1700 ppm during the PETM main phase, based on an initial input of 3000 Gt C from methane clathrates with a $\delta^{13}C$ lighter than –50‰. Furthermore, Zeebe et al. (2009) claim that this 70% increase in pCO_2 is largely independent from the initial pre-PETM pCO_2, suspecting an increase from 500 to ~850 ppm as likewise possible. A similar result is obtained by Cui et al. (2011), if 2500 Gt C from methane clathrates with a $\delta^{13}C$ of –60‰ are assumed as the potential carbon source (increase in pCO_2 from a baseline of 835 ppm to ~1500 ppm). Also the mass balance presented by McInerney and Wing (2011)

estimates a pCO_2 increase to ~1500 ppm, potentially triggered by a release of 4,300 Gt C methane clathrates that are necessary to generate a CIE of –4.6‰.

In contrast, McInerney and Wing (2011) propose a pCO_2 increase to ~3000 ppm if the release of thermogenic methane or permafrost soil carbon (10,000 Gt C, $\delta^{13}C$ ~–30‰) would have induced the same CIE.

For a carbon input with a $\delta^{13}C$ of ~–22‰ from wildfires and/or desiccation and oxidation of organic matter from drying epicontinental seas, the mass balance of McInerney and Wing (2011) suggests CO_2 levels >4000 ppm induced by a release of ~15,400 Gt C. This is nearly identical to the model of Cui et al. (2011), who proposed a release of 13,000 Gt C from the same source, resulting in a pCO_2 increase from 835 to 4200 ppm. An alternative model (Panchuk et al., 2008) suggests a minimum pulse of carbon with a $\delta^{13}C$ of –22‰ to be 6,800 Gt to trigger a CIE of –4‰, associated to an increase in pCO_2 to levels considerably above 2000 ppm.

Those high pCO_2 estimates for CIE carbon sources other than methane clathrates are not supported by the results of the present study, providing new independent evidence for the initial idea of Dickens et al. (1995). Furthermore, a considerable number of doubts that have been proposed for the methane clathrate scenario within the last decade recently turned out to be not well constrained. One of the most discussed arguments is that the respective pCO_2 is insufficient to explain the PETM temperature increase. However, alternative mechanisms, such as direct radiative forcing due to an increased pCH_4 and associated indirect effects (Schmidt and Shindell, 2003; Zeebe et al., 2009; Dickens, 2011; Kurtén et al., 2011) may explain this objection. A proposed too small size of Early Palaeogene methane clathrate reservoirs (Buffet and Archer, 2004), has recently been largely refuted (Dickens, 2011 and refs. therein; Gu et al., 2011). The thesis of an insufficient amount of carbon that would have been released from methane clathrates to explain the observed shoaling of the carbonate compensation depth (CCD) (Zachos et al., 2005) is a further prediction, which nowadays has been discussed critically (Dickens, 2011 and refs. therein).

4.6 Conclusions

Triple oxygen isotope analysis of fossil mammalian bioapatite has the potential to trace fluctuations in temperature and CO_2 levels simultaneously, representing a strong new tool in palaeoclimatological research. Our data agree well with previous temperature change estimates from the oxygen isotope composition of mammalian tooth enamel and other proxies across the Palaeocene-Eocene transition as well as to various existing proxy data for Late Palaeocene and Early Eocene pCO_2. As the analysed samples of *Ectocion* directly derive from pre-, peak- and post-PETM/CIE strata, it has been possible for the first time to gain insight into the respective CO_2 concentration change. The results suggest that PETM CO_2 levels did not exceed 1550 ppm and therefore strongly support the hypothesis that the dissociation of methane clathrates contributed at least the major portion of depleted ^{13}C responsible for the CIE.

Acknowledgements

The authors are grateful to G. Gunnell for support in selection and shipment of the samples and for providing detailed sample information.

For the assistance during sample pretreatment and isotope analysis, the authors would like to thank N. Albrecht, A. Höweling, C. Seidler and M. Troche. Verena Bendel is thanked for technical assistance during preparation of the figures and evaluation of the data, for careful proofreading, the authors are grateful to Vanessa Roden and Wiebke Kallweit. Further thanks are due to Reinhold Przybilla for the technical support at the mass spectrometry line. A. G. was supported by the German National Science Foundation DFG grant PA909/5-1 (A.P.).

References

Asprey, L.B. (1976). The Preparation of Very Pure Fluorine Gas. *Journal of Fluorine Chemistry* **7**, 359-361.

Bao, H., Lyons, J., Zhou, C. (2008). Triple oxygen isotope evidence for elevated CO_2 levels after a Neoproterozoic glaciation. *Nature* **453**, 504-506.

Beerling, D.J. (1999). Quantitative estimates of changes in marine and terrestrial primary productivity over the past 300 million years. *Proceedings of the Royal Society London B* **266**, 1821-1827.

Beerling, D.J., Fox, A., Anderson, C.W. (2009). Quantitative uncertainty analyses of ancient atmospheric CO_2 estimates from fossil leaves. *American Journal of Science* **309**, 775-787.

Beerling, D.J., Royer, D.L. (2011). Convergent Cenozoic CO_2 history. *Nature Geoscience* **4**, 418-420.

Bender, M., Sowers, T., Labeyrie, L. (1994). The Dole effect and its variations during the last 130,000 years as measured in the Vostok ice core. *Global Biogeochemical Cycles* **8**, 363-376.

Berner, R.A. (2001). Modeling atmospheric O_2 over Phanerozoic time. *Geochimica et Cosmochimica Acta* **65**, 685-694.

Berner, R. (2006a). GEOCARBSULF: A combined model for Phanerozoic atmospheric O_2 and CO_2. *Geochimica et Cosmochimica Acta* **70**, 5653-5664.

Berner, R.A. (2006b). Inclusion of the weathering of volcanic rocks in the GEOCARBSULF model. *American Journal of Science* **306**, 295-302.

Berner, R.A. (2008). Addendum to "Inclusion of the weathering of volcanic rocks in the GEOCARBSULF model" (R. A. Berner, 2006, V. 306, p. 295-302). *American Journal of Science* **308**, 100-103.

Breecker, D.O., Sharp, Z.D., McFadden, L.D. (2010). Atmospheric CO_2 concentrations during ancient greenhouse climates were similar to those predicted for A.D. 2100. *Proceedings of the National Academy of Sciences* **107**, 576-580.

Bryant, J.D., Froelich, P.N. (1995). A model of oxygen isotope fractionation in body water of large mammals. *Geochimica et Cosmochimica Acta* **59**, 4523-4537.

Bryant, J.D., Luz, B., Froelich, P.N. (1994). Oxygen isotopic composition of fossil horse tooth phosphate as a record of continental paleoclimate. *Palaeogeography, Palaeoclimatology, Palaeoecology* **107**, 303-316.

Buffet, B., Archer, D. (2004). Global inventory of methane clathrate: sensitivity to changes in the deep ocean. *Earth and Planetary Science Letters* **227**, 185-199.

Cui, Y., Kump, L.R., Ridgwell, A.J., Charles, A.J., Junium, C.K., Diefendorf, A.F., Freeman, K., Urban, N.M., Harding, I.C. (2011). Slow release of fossil carbon during the Palaeocene-Eocene Thermal Maximum. *Nature Geoscience* **4**, 481-485.

Currano, E.D., Kattler, K.R., Flynn, A. (2011). Paleogene insect herbivory as a proxy for pCO_2 and ecosystem stress in the Bighorn Basin, Wyoming, USA. *Berichte der Geologischen Bundes-Anstalt* **85**, 61.

Currano, E.D., Wilf, P., Wing, S.L., Labandeira, C.C., Lovelock, E.C., Royer, D.L. (2008). Sharply increased insect herbivory during the Paleocene-Eocene Thermal Maximum. *Proceedings of the National Academy of Sciences* **105**, 1960-1964.

D'Angela, D., Longinelli, A. (1990). Oxygen isotopes in living mammal's bone phosphate: further results. *Chemical Geology* **86**, 75-82.

Dansgaard, W. (1964). Stable isotopes in precipitation. *Tellus* **16**, 436-468.

Dickens, G.R. (2011). Down the Rabbit Hole: toward appropriate discussion of methane release from gas hydrate systems during the Paleocene-Eocene thermal maximum and other past hyperthermal events. *Climate of the Past* **7**, 831-846.

Dickens, G.R., O'Neil, J.R., Rea, D.K., Owen, R.M. (1995). Dissociation of oceanic methane hydrate as a cause of the carbon isotope excursion at the end of the Paleocene. *Paleoceanography* **10**, 965-971.

Diefendorf, A.F., Mueller, K.E., Wing, S.L., Koch, P., Freeman, K.H. (2010). Global patterns in leaf ^{13}C discrimination and implications for studies of past and future climate. *Proceedings of the National Academy of Sciences* **107**, 5738-5743.

Fletcher, B.J., Brentnall, S.J., Anderson, C.W., Berner, R.A., Beerling, D.J. (2008). Atmospheric carbon dioxide linked with Mesozoic and early Cenozoic climate change. *Nature Geoscience* **1**, 43-48.

Fricke, H.C. (2003). Investigation of early Eocene water-vapor transport and paleoelevation using oxygen isotope data from geographically widespread mammal remains. *Geological Society of America Bulletin* **115**, 1088-1096.

Fricke, H.C., Clyde, W.C., O'Neil, J.R., Gingerich, P.D. (1998). Evidence for rapid climate change in North America during the latest Paleocene thermal maximum: oxygen isotope compositions of biogenic phosphate from the Bighorn Basin (Wyoming). *Earth and Planetary Science Letters* **160**, 193-208.

Fricke, H.C., O'Neil, J.R. (1999). The correlation between $^{18}O/^{16}O$ ratios of meteoric water and surface temperature: its use in investigating terrestrial climate change over geologic time. *Earth and Planetary Science Letters* **170**, 181-196.

Fricke, H.C., Wing, S.L. (2004). Oxygen isotope and paleobotanical estimates of temperature and $\delta^{18}O$-latitude gradients over North America during the Early Eocene. *American Journal of Science* **304**, 612-635.

Gehler, A., Tütken, T., Pack, A. (2011). Triple oxygen isotope analysis of bioapatite as tracer for diagenetic alteration of bones and teeth. *Palaeogeography, Palaeoclimatology, Palaeoecology* **310**, 84-91.

Gingerich, P.D. (2003). Mammalian responses to climate change at the Paleocene-Eocene boundary: Polecat Bench record in the northern Bighorn Basin, Wyoming. In: Wing, S.L., Gingerich, P.D., Schmitz, B., Thomas, E. (Eds.), *Causes and Consequences of Globally Warm Climates in the Early Paleogene* (=Geological Society of America Special Paper **369**). Geological Society of America (Boulder, Colorado), pp. 463-478.

Gingerich, P.D. (2006). Environment and evolution through the Paleocene-Eocene thermal maximum. *Trends in Ecology and Evolution* **21**, 246-253.

Gingerich, P.D., Smith, T. (2006). Paleocene-Eocene land mammals from three new Latest Clarkforkian and Earliest Wasatchian wash sites at Polecat Bench in the northern Bighorn Basin, Wyoming. *Contributions from the Museum of Paleontology, University of Michigan* **31**, 245-303.

Gourcy, L.L., Groening, M., Aggarwal, P.K. (1997). *Stable oxygen and hydrogen isotopes in precipitation, Isotopes in the Water Cycle - Past, Present and Future of a Developing Science*. Springer (Dordrecht), pp. 39-51.

Greenwood, D.R., Scarr, M.J., Christophel, D.C. (2003). Leaf stomatal frequency in the Australian tropical rainforest tree *Neolitsea dealbata* (Lauraceae) as a proxy measure of atmospheric pCO_2. *Palaeogeography, Palaeoclimatology, Palaeoecology* **196**, 375-393.

Gu, G., Dickens, G.R., Bhatnagar, G., Colwell, F.S., Hirasaki, G.J., Chapman, W.G. (2011). Abundant Early Palaeogene marine gas hydrates despite warm deep-ocean temperatures. *Nature Geoscience* **4**, 848-851.

Higgins, J.A., Schrag, D.P. (2006). Beyond methane: Towards a theory for the Paleocene-Eocene Thermal Maximum. *Earth and Planetary Science Letters* **245**, 523-537.

Hulston, J.R., Thode, H.G. (1965). Variations in the S^{33}, S^{34} and S^{36} contents of meteorites and their relation to chemical and nuclear effects. *Journal of Geophysical Research* **70**, 3475-3484.

Koch, P., Zachos, J.C., Dettmann, D.L. (1995). Stable isotope stratigraphy and paleoclimatology of the Paleogene Bighorn Basin (Wyoming, USA). *Palaeogeography, Palaeoclimatology, Palaeoecology* **115**, 61-89.

Koch, P., Zachos, J.C., Gingerich, P.D. (1992). Correlation between isotope records in marine and continental carbon reservoirs near the Palaeocene/Eocene boundary. *Nature* **358**, 319-322.

Kohn, M.J. (1996). Predicting animal $\delta^{18}O$: accounting for diet and physiological adaption. *Geochimica et Cosmochimica Acta* **60**, 4811-4829.

Kohn, M.J., Cerling, T.E. (2002). Stable Isotope Compositions of Biological Apatite. *Reviews in Mineralogy and Geochemistry* **48**, 455-488.

Kohn, M.J., Schoeninger, M.J., Valley, J.W. (1996). Herbivore tooth oxygen isotope compositions: Effects of diet and physiology. *Geochimica et Cosmochimica Acta* **60**, 3889-3896.

Kurtén, T., Zhou, L., Makkonen, R., Merikanto, J., Räisänen, P., Boy, M., Richards, N., Rap, A., Smolander, S., Sogachev, A., Guenther, A., Mann, G.W., Carslaw, K., Kulmala, M. (2011). Large methane releases lead to strong aerosol forcing and reduced cloudiness. *Atmospheric Chemistry and Physics Discussions* **11**, 9057-9081.

Lindars, E.S., Grimes, S.T., Mattey, D.P., Collinson, M.E., Hooker, J.J., Jones, T.P. (2001). Phosphate $\delta^{18}O$ determination of modern rodent teeth by direct laser fluorination: An appraisal of methodology and potential application to palaeoclimate reconstruction. *Geochimica et Cosmochimica Acta* **65**, 2535-2548.

Longinelli, A. (1984). Oxygen isotopes in mammal bone phosphate: a new tool for paleohydrological and paleoclimatological research? *Geochimica et Cosmochimica Acta* **48**, 385-390.

Luz, B., Barkan, E. (2005). The isotopic ratios $^{17}O/^{16}O$ and $^{18}O/^{16}O$ in molecular oxygen and their significance in biogeochemistry. *Geochimica et Cosmochimica Acta* **69**, 1099-1110.

Luz, B., Barkan, E. (2011). The isotopic composition of atmospheric oxygen. *Global Biogeochemical Cycles* **25**, GB3001.

Luz, B., Barkan, E., Bender, M.L., Thiemens, M.H., Boering, K.A. (1999). Triple-isotope composition of atmospheric oxygen as a tracer of biosphere productivity. *Nature* **400**, 547-550.

Luz, B., Kolodny, Y. (1985). Oxygen isotope variations in phosphate of biogenic apatites, IV. Mammal teeth and bones. *Earth and Planetary Science Letters* **75**, 29-36.

Luz, B., Kolodny, Y., Horowitz, M. (1984). Fractionation of oxygen isotopes between mammalian bone phosphate and environmental drinking water. *Geochimica et Cosmochimica Acta* **48**, 1689-1693.

McInerney, F.A., Wing, S.L. (2011). The Paleocene-Eocene Thermal Maximum: A Perturbation of Carbon Cycle, Climate, and Biosphere with Implications for the Future. *Annual Review of Earth and Planetary Sciences* **39**, 489-516.

Miller, M.F. (2002). Isotopic fractionation and the quantification of ^{17}O anomalies in the oxygen three-isotope system: an appraisal and geochemical significance. *Geochimica et Cosmochimica Acta* **66**, 1881-2055.

Pack, A., Gehler, A., Süssenberger, A. (in press). Exploring the usability of isotopically anomalous oxygen in bones and teeth as paleo-CO_2-barometer. *Geochimica et Cosmochimica Acta*, http://dx.doi.org/10.1016/j.gca.2012.10.017.

Pack, A., Toulouse, C., Przybilla, R. (2007). Determination of oxygen triple isotope ratios of silicates without cryogenic separation of NF_3 — technique with application to analyses of technical O_2 gas and meteorite classification. *Rapid Communications in Mass Spectrometry* **21**, 3721-3728.

Pagani, M., Caldeira, K., Archer, D., Zachos, J.C. (2006). An Ancient Carbon Mystery. *Science* **314**, 1556-1557.

Panchuk, K., Ridgwell, A., Kump, L.R. (2008). Sedimentary response to Paleocene-Eocene Thermal Maximum carbon release: A model data comparison. *Geology* **36**, 315-318.

Renssen, H., Beets, J., 2004. Modeling the climate response to a massive methane release from gas hydrates. *Paleoceanography* **19**, PA2010.

Royer, D.L. (2003). Estimating latest Cretaceous and Tertiary atmospheric CO_2 from stomatal indices. In: Wing, S.L., Gingerich, P.D., Schmitz, B., Thomas, E. (Eds.), *Causes and Consequences of Globally Warm Climates in the Early Paleogene* (=Geological Society of America Special Paper **369**). Geological Society of America (Boulder, Colorado), pp. 79-93.

Royer, D.L., Wing, S.L., Beerling, D.J., Jolley, D.W., Koch, P.L., Hickey, L.J., Berner, R.A. (2001). Paleobotanical Evidence for Near Present-Day Levels of Atmospheric CO_2 During Part of the Tertiary. *Science* **292**, 2310-2313.

Rozanski, K., Araguás-Araguás, L., Gonfiantini, R. (1992). Relation between Long-Term Trends of Oxygen-18 Isotope Composition of Precipitation and Climate. *Science* **258**, 981-985.

Rozanski, K., Araguás-Araguás, L., Gonfiantini, R. (1993). Isotopic patterns in modern global precipitation. In: Swart, P.K., Lohmann, K.C., McKenzie, J., Savin, S. (Eds.), *Climate change in continental isotopic records* (= Geophysical Monograph **78**). Washington D. C. (American Geophysical Union), pp. 1-36.

Schmidt, G.A., Shindell, D.T. (2003). Atmospheric composition, radiative forcing, and climate change as a consequence of a massive methane release from gas hydrates. *Paleoceanography* **18**, 1004.

Secord, R., Bloch, J.I., Chester, S.G.B., Boyer, D.M., Wood, A.R., Wing, S.L., Kraus, M.J., McInerney, F.A., Krigbaum, J. (2012). Evolution of the Earliest Horses Driven by Climate Change in the Paleocene-Eocene Thermal Maximum. *Science* **335**, 959-962.

Secord, R., Gingerich, P.D., Lohmann, K.C., MacLeod, K.G. (2010). Continental warming preceding the Palaeocene-Eocene thermal maximum. *Nature* **467**, 955-958.

Secord, R., Wing, S.L., Chew, A. (2008). Stable Isotopes in Early Eocene Mammals as Indicators of Forest Canopy Structure and Resource Partitioning. *Paleobiology* **34**, 282-300.

Sharp, Z. (2007). *Principles of Stable Isotope Geochemistry*. Pearson / Prentice Hall (Upper Saddle River), 344 pp.

Sharp, Z.D. (1990). A laser-based microanalytical method for the *in situ* determination of oxygen isotope ratios of silicates and oxides. *Geochimica et Cosmochimica Acta* **54**, 1353-1357.

Shellito, C.J., Sloan, L.C., Huber, M. (2003). Climate model sensitivity to atmospheric CO_2 levels in the Early-Middle Paleogene. *Palaeogeography, Palaeoclimatology, Palaeoecology* **193**, 113-123.

Sinha, A., Stott, L.D. (1994). New atmospheric pCO_2 estimates from paleosols during the late Paleocene / early Eocene global warming interval. *Global and Planetary Change* **9**, 297-307.

Stott, L.D. (1992). Higher temperatures and lower oceanic pCO_2: A climate enigma at the end of the Paleocene Epoch. *Paleoceanography* **7**, 395-404.

Thiemens, M.H. (2006). History and Applications of Mass-Independent Isotope Effects. *Annual Review of Earth and Planetary Sciences* **34**, 217-262.

Westerhold, T., Röhl, U., McCarren, H.K., Zachos, J.C. (2009). Latest on the absolute age of the Paleocene-Eocene Thermal Maximum (PETM): New insights from exact stratigraphic position of key ash layers +19 and -17. *Earth and Planetary Science Letters* **287**, 412-419.

Zachos, J.C., Röhl, U., Schellenberg, S.A., Sluijs, A., Hodell, D.A., Kelly, D.C., Thomas, E., Nicolo, M., Raffi, I., Lourens, L.J., McCarren, H., Kroon, D. (2005). Rapid Acidification of the Ocean During the Paleocene-Eocene Thermal Maximum. *Science* **308**, 1611-1615.

Zachos, J.C., Wara, M.W., Bohaty, S., Delaney, M.L., Petrizzo, M.R., Brill, A., Bralower, T.J., Premoli-Silva, I. (2003). A Transient Rise in Tropical Sea Surface Temperature During the Paleocene-Eocene Thermal Maximum. *Science* **302**, 1551-1554.

Zeebe, R., Zachos, J.C., Dickens, G.R. (2009). Carbon dioxide forcing alone insufficient to explain Palaeocene-Eocene Thermal Maximum warming. *Nature Geoscience* **2**, 576-580.

5. Manuscript IV

Oxygen and Carbon Isotope Variations in a Modern Rodent Community – Implications for Palaeoenvironmental Reconstructions

Alexander Gehler[a], Thomas Tütken[b] & Andreas Pack[a]

[a]Georg-August-Universität, Geowissenschaftliches Zentrum, Abteilung Isotopengeologie, Goldschmidtstr. 1, D-37077 Göttingen, Deutschland

[b]Rheinische Friedrich-Wilhelms-Universität, Steinmann-Institut für Geologie, Mineralogie und Paläontologie, Emmy Noether-Gruppe Knochengeochemie, Poppelsdorfer Schloss, D-53115 Bonn, Deutschland

Published in PloS ONE **7** (11): e49531 (11 pp.)

Abstract

Background

The oxygen ($\delta^{18}O$) and carbon ($\delta^{13}C$) isotope compositions of bioapatite from skeletal remains of fossil mammals are well-established proxies for the reconstruction of palaeoenvironmental and palaeoclimatic conditions. Stable isotope studies of modern analogues are an important prerequisite for such reconstructions from fossil mammal remains. While numerous studies have investigated modern large- and medium-sized mammals, comparable studies are rare for small mammals. Due to their high abundance in terrestrial ecosystems, short life spans and small habitat size, small mammals are good recorders of local environments.

Methodology/Findings

The $\delta^{18}O$ and $\delta^{13}C$ values of teeth and bones of seven sympatric modern rodent species collected from owl pellets at a single locality were measured, and the inter-specific, intra-specific and intra-individual variations were evaluated. Minimum sample sizes to obtain reproducible population $\delta^{18}O$ means within one standard deviation were determined. These parameters are comparable to existing data from large mammals. Additionally, the fractionation between coexisting carbonate ($\delta^{18}O_{CO3}$) and phosphate ($\delta^{18}O_{PO4}$) in rodent bioapatite was determined, and $\delta^{18}O$ values were compared to existing calibration equations between the $\delta^{18}O$ of rodent bioapatite and local surface water ($\delta^{18}O_{LW}$).

Specific calibration equations between $\delta^{18}O_{PO4}$ and $\delta^{18}O_{LW}$ may be applicable on a taxonomic level higher than the species. However, a significant bias can occur when bone-based equations are applied to tooth-data and vice versa, which is due to differences in skeletal tissue formation times. $\delta^{13}C$ values reflect the rodents' diet and agree well with field observations of their nutritional behaviour.

Conclusions/Significance

Rodents have a high potential for the reconstruction of palaeoenvironmental conditions by means of bioapatite $\delta^{18}O$ and $\delta^{13}C$ analysis. No significant disadvantages compared to larger mammals were observed. However, for refined palaeoenvironmental reconstructions a better understanding of stable isotope signatures in modern analogous communities and potential biases due to seasonality effects, population dynamics and tissue formation rates is necessary.

5.1 Introduction

Stable isotope compositions of mammalian bioapatite are widely used proxies in palaeoenvironmental and palaeodietary studies. Starting with pioneering research on carbon (DeNiro and Epstein, 1978) and oxygen isotopes (Land et al., 1980; Longinelli, 1984; Luz et al., 1984; Luz and Kolodny, 1985) in the 1970s and 1980s, stable isotope analysis of bioapatite from fossil mammals rapidly became an established method for the reconstruction of palaeoclimate and palaeodiet.

The oxygen isotope composition of bioapatite from terrestrial mammals can be used to infer air temperature, climate seasonality, relative humidity or aridity of palaeoenvironments as well as mobility, birth seasonality and drinking behaviour of specific mammal taxa (e.g., Kohn and Cerling, 2002 and references therein; Balasse et al., 2002; 2003; Levin et al., 2006; Tütken et al., 2006; Tütken and Vennemann, 2009). Carbon isotopes can be used to infer the palaeovegetation, vegetation cover, dietary strategies, resource partitioning and habitat use (e.g., Kohn and Cerling, 2002 and references therein; Cerling et al., 2004; MacFadden and Higgins, 2004; Feranec and MacFadden, 2006; Tütken et al., 2006; Drucker et al., 2008; Tütken and Vennemann, 2009).

For various reasons, especially to allow easier sampling and acquisition of sufficient sample material, most studies have focused predominantly on the isotopic analysis of skeletal remains from large mammals. New and improved mass spectrometric techniques

allow oxygen and carbon isotope analysis of (sub)milligram sample amounts of bioapatite, bringing small mammal taxa such as small rodents (with a body mass below 1 kg) into the focus of interest.

So far only a few oxygen and/or carbon isotope studies are based exclusively or partly on fossil small rodents (Rogers and Wang, 2002; Grimes et al., 2003; 2004a; 2004b; 2005; Navarro et al., 2004; Hopley et al., 2006; Yeakel et al., 2007; Tütken et al. 2006; Ruddy, 2008; Heran et al., 2010; Tóth et al., 2010; Hynek et al., 2012). However, for an improved understanding of oxygen and carbon isotope compositions in bioapatite of fossil small rodents, communities of modern analogues have to be studied extensively in order to investigate inter- and intra-specific variabilities. This has been done repeatedly for selected large mammals (e.g., Bocherens et al., 1996; Fricke and O'Neil, 1996; Kohn et al., 1996; Clementz and Koch, 2001; Hoppe et al., 2004; 2005; Hoppe, 2006; Wang et al., 2008) but no comparable study has been conducted on small mammals so far. It is the aim of the present study to investigate such variations for small mammals. Such studies are fundamental in order to evaluate the number of individuals needed for statistically significant results and to ascertain whether species-specific calibrations or calibrations on a higher taxonomic level are suitable for the reconstruction of the oxygen isotope composition of local surface water. Furthermore, the intra-individual variability between bones and permanently growing teeth as well as the intra-jaw variations need to be determined in order to investigate if these skeletal tissues record comparable isotope signatures or are seasonally biased.

We analysed the oxygen ($\delta^{18}O$) and carbon isotope ($\delta^{13}C$) composition (for definitions see Materials and Methods section) of bones and teeth from seven rodent species in multiple individuals. The samples derive from owl pellets of a locality in northwestern Germany, which were accumulated over a 4-year period (1991-1995). Inter-specific, intra-specific, and intra-jaw variations were investigated, as well as variations between teeth and bones from the same individuals. These data were compared to published stable isotope data for large mammals.

Additionally, oxygen isotope analyses of coexisting carbonate ($\delta^{18}O_{CO3}$) and phosphate ($\delta^{18}O_{PO4}$) in rodent bioapatite were conducted on water voles (*Arvicola terrestris*). In order to determine if it is possible to make a correct estimation of the $\delta^{18}O_{LW}$ from the $\delta^{18}O_{CO3}$ values, the data from the other species were converted to $\delta^{18}O_{PO4}$ equivalent

values by using the average offset between $\delta^{18}O_{CO3}$ and $\delta^{18}O_{PO4}$ ($\Delta^{18}O_{CO3\text{-}PO4}$) obtained for *A*. *terrestris*. Then the data were compared to the three published $\delta^{18}O_{PO4}$-$\delta^{18}O_{H2O}$ calibration equations determined for different extant rodent taxa in previous studies (Luz and Kolodny, 1985; Navarro et al., 2004; Longinelli et al., 2003).

With the present study, the authors aim to provide a basic contribution for the enhancement of palaeoenvironmental interpretations of oxygen and carbon isotope data obtained from fossil rodents.

5.2 General considerations

5.2.1 Oxygen isotopes

The oxygen isotope composition of mammalian bioapatite is determined by that of body water, which in turn is controlled by the oxygen isotope compositions of the different oxygen input sources (drinking water, food water, air oxygen, organic food compounds and water vapour in air) and oxygen output fluxes (exhaled CO_2, liquid water in sweat, urine and feces as well as orally, nasally and transcutaneously released water vapour) [(e.g., Luz and Kolodny, 1985; Bryant and Froelich, 1995; Kohn, 1996). The oxygen isotope composition of mammalian body water is linearly related to that of their drinking water (i.e., local surface water) for those mammals with an obligate drinking behaviour (e.g., Longinelli, 1984; D'Angela and Longinelli, 1990). Thus, empirical specific calibration equations relating $\delta^{18}O_{PO4/CO3}$ and $\delta^{18}O_{LW}$ can be developed. Because the oxygen isotope composition of local surface water varies with air temperature and also with the amount of local precipitation and evapotranspiration (e.g., Dansgaard, 1964; Rozanski et al., 1993; 1997; Fricke and O'Neil, 1999), (palaeo-)climatic conditions can be inferred from the oxygen isotope composition of the skeletal remains of fossil mammals (e.g., Tütken and Vennemann, 2009 and references therein).

In bioapatite, oxygen is present in the phosphate, carbonate and the hydroxyl groups (Kohn and Cerling, 2002). The average offset between $\delta^{18}O_{PO4}$ and $\delta^{18}O_{CO3}$ in skeletal apatite of different mammal taxa is around 9‰. This offset ranges from 7.5 to 11.4‰ in the previously investigated modern taxa (Bryant et a., 1996; Iacumin et al., 1996; Shahack-Gross et al., 1999; Zazzo, 2001; Zazzo et al., 2004; Martin et al., 2008; Kirsanow and Tuross, 2011). Both, $\delta^{18}O_{PO4}$ and $\delta^{18}O_{CO3}$, can be used to track the oxygen isotope composition of ingested drinking water. For the offset between $\delta^{18}O_{PO4}$ and oxygen

bound in the hydroxyl group, only a single calculated value of –16.6‰ is known (Jones et al., 1999).

5.2.2 Carbon isotopes

The carbon isotope composition of mammalian bioapatite is controlled by that of ingested food (i.e., plant material in herbivores) (DeNiro and Epstein, 1978) and can therefore be used to investigate dietary preferences. Furthermore, the knowledge of the carbon isotope composition of ingested plant material can mirror specific habitats, type of vegetation cover (i.e., C_3 versus C_4 plants) and density, as well as ecological niches, feeding behaviour and seasonal changes of diet (e.g., Tütken and Vennemann, 2009 and references therein).

Significant differences in the carbon isotope composition of plants are induced by different carbon fixation strategies in plants, i.e., the C_3, C_4 or CAM (Crassulacean Acid Metabolism) photosynthetic pathways (e.g., Bender, 1971; O'Leary, 1988; Farquhar et al. 1989). C_3 plants, which represent about 95% of all terrestrial plant species (e.g., Bowes, 1993), have typical $\delta^{13}C$ values between –36 and –22‰ with an average value of –27‰, whereas the $\delta^{13}C$ values of C_4 plants (mostly warm season grasses and sedges) have –15 to –10‰, with an average value of –13‰ (e.g., Deines, 1980; O'Leary, 1988; Farquhar, 1989; Mariotti, 1991). CAM plants have highly variable $\delta^{13}C$ values within and between specific taxa, overlapping with both C_3 and C_4 plants (e.g., Bender et al., 1973; Deines, 1980; Ting, 1985). However, CAM plants represent only about 4% of all terrestrial plant species (Bowes, 1993) and are mostly succulents (Sayed, 2001), playing a minor role in the nutrition of most herbivorous mammals. Thus, a distinction between browsing and grazing herbivores based on bioapatite $\delta^{13}C$ values is possible, as shown by numerous palaeodietary studies (e.g., Quade et al., 1992; MacFadden et al., 1994; 1999; MacFadden and Cerling, 1996; Cerling et al., 1997; 1999). However, this approach is limited to ecosystems with coexisting C_3 and C_4 plants; the latter were not globally abundant until the late Miocene (Cerling et al., 1993).

Even in a pure C_3 ecosystem, significant differences in the carbon isotopic composition of plants are caused by varying light-, nutrient-, water-, CO_2- and temperature-settings (e.g., Farquhar et al., 1989, Heaton, 1999). Subcanopy plants in humid, shaded environments assimilating CO_2, depleted in ^{13}C by soil respiration, have very low $\delta^{13}C$ values ranging from –36 to –32‰ (Vogel, 1978; Medina and Minchin, 1980; Farquhar et al., 1989; van

der Merwe and Medina, 1989; 1991; Cerling et al., 2004). C_3 plants in arid, open environments have the highest $\delta^{13}C$ values, up to –21‰ (Ehleringer and Cooper, 1988; O'Leary, 1988; Farquhar et al., 1989). Those variations are also visible in the carbon isotope composition of bioapatite from modern and fossil mammals living in C_3-environments and reflect differences in habitat use and/or resource partitioning (e.g., Quade et al., 1995; Harris and Cerling, 2002; Drucker et al., 2003; Cerling et al., 2004; MacFadden and Higgins, 2004; Feranec and MacFadden, 2006; Feranec, 2007; Nelson, 2007; Zanazzi and Kohn, 2008; Tütken and Vennemann, 2009). Terrestrial C_3 plant ecosystems date back to the Palaeozoic and are typical for most parts of the modern northern hemisphere (e.g., Still et al., 2003).

The carbon isotope composition of mammalian bioapatite is enriched by several per mil compared to the respective diet. Reported enrichment factor values range from 9 to 15‰, depending on the digestive physiology of the investigated taxa (e.g., Passey et al., 2005 and references therein).

5.2.3 Stable carbon and oxygen isotopes from bioapatite of fossil small rodents and case studies on modern material

Mammals evolved in the Late Triassic and retained relatively small body size until their radiation after the Cretaceous-Palaeogene transition (Kemp, 2007). Rodents first appear in the Palaeogene fossil record, and fossil rodent remains are widespread in Cenozoic terrestrial deposits, often in high numbers, accumulated predominantly by ancient avian predators. As reviewed by Grimes et al. (2008), one of the main advantages of stable isotope studies on small mammals relative to large taxa is the higher abundance of small mammals in the fossil record, which enhances their availability. Furthermore, small mammals display a rapid evolution of their morphology, and hence small mammal remains are often index fossils for Cenozoic strata that enable a good biostratigraphic resolution. Additionally, most small mammals occupy a very restricted habitat, lacking long distance migratory behaviour, thus reflecting local palaeoenvironmental conditions more precisely than large mammals. Possible disadvantages compared to large mammals concerning the oxygen isotope composition may be a smaller proportion of drinking water in the overall oxygen intake, a more variable physiology (i.e., body temperature), and a possible stronger susceptibility to diagenetic alteration due to smaller, more fragile skeletal elements (Grimes et al., 2008).

Specific calibration equations between $\delta^{18}O_{PO4}$ and $\delta^{18}O_{LW}$ have been developed in the past for laboratory rats (Luz and Kolodny, 1985), wild murids (D'Angela and Longinelli, 1990; Longinelli et al., 2003) and wild arvicolids (Longinelli et al., 2003; Navarro et al., 2004). During the last decade, the oxygen isotope composition of bioapatite of fossil small rodents has been used in an increasing number of studies, targeting Palaeogene (Grimes et al., 2003; 2004b; 2005; Heran et al., 2010), Neogene (Tütken et al., 2006; Heran et al., 2010; Tóth et al., 2010) and Pleistocene (Rogers and Wang, 2002; Navarro et al., 2004, Yeakel et al., 2007; Ruddy, 2008) climate change. Carbon isotope records of fossil small rodents also were used to reconstruct vegetational change and palaeodiets in the Cenozoic (Rogers and Wang, 2003; Yeakel et al., 2007, Grimes et al., 2004a; Hopley et al., 2006; Hynek et al., 2012).

To date, very little is known about the inter- and intra-population variability between individuals from the same locality, as well as about variations between different teeth and bone material within a single individual. Only one study (Lindars et al., 2001) has investigated intra-population and intra-jaw variations ($\delta^{18}O_{PO4}$) in small rodents based on a small number of samples of fat dormice (*Glis glis*, n=3) from Great Missenden (Buckinghamshire, UK) and wood mice (*Apodemus sylvaticus*, n=5) from Dungeness (Kent, UK). From these results, Lindars et al. (2001) concluded that a quantity of >5 different post-weaning teeth should be used for isotope palaeo-thermometry. Further intra-population $\delta^{18}O_{PO4}$ data of multiple bioapatite analyses from small rodents (*Apodemus flavicollis*, *Apodemus sylvaticus*, *Arvicola terrestris*, *Microtus arvalis* and *Pitymus* sp.) are presented in a small quantity (n=3-8) by D'Angela and Longinelli (1990) and Longinelli et al. (2003), but no data for distinct sympatric species from the same locality are available so far.

5.3 Materials and Methods

5.3.1 Material

The samples originate from fresh barn owl (*Tyto alba*) pellets accumulated over a maximum of four years, collected in April 1995 at "Hof Gülker", located in the nature reserve Rhader Wiesen, about 9 km north of Dorsten, North Rhine-Westphalia, Germany (Fig. 5.1) and are part of the original material from Bülow (1997). Long term mean annual local temperatures in this region (IAEA-GNIP station Emmerich) average 10°C, and the mean annual precipitation is 744 mm. The long term weighted mean of the monthly $\delta^{18}O$ record of local precipitation between 1980 and 2005 is –7.3‰. Considering only the period from April 1991 to April 1995 of owl pellet deposition, and hence the most likely time interval when the analysed rodents lived and mineralised their bones and teeth, the respective $\delta^{18}O$ value is –7.7. This is very close to the long-term record (IAEA/WISER, 2011). The seasonal change in monthly precipitation of the sampling area is illustrated in Fig. 5.2.

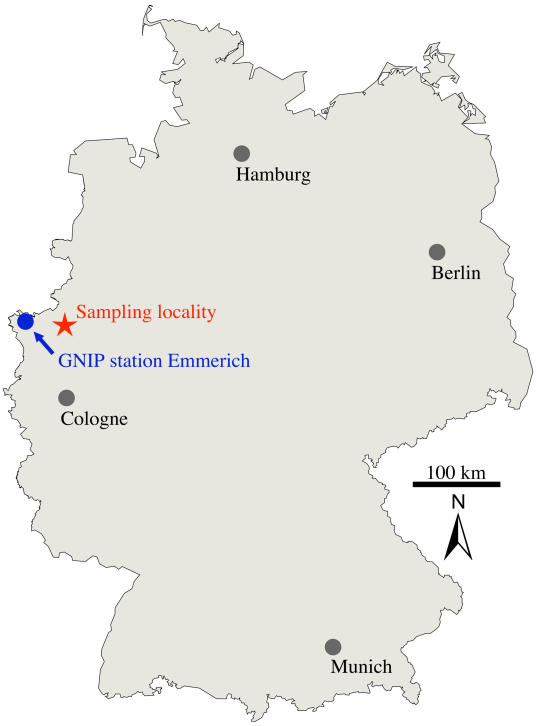

Fig. 5.1: Map showing the sampling locality Rhader Wiesen near Dorsten, North Rhine-Westphalia, Germany (red star) and the closest IAEA-GNIP station to it (blue dot).

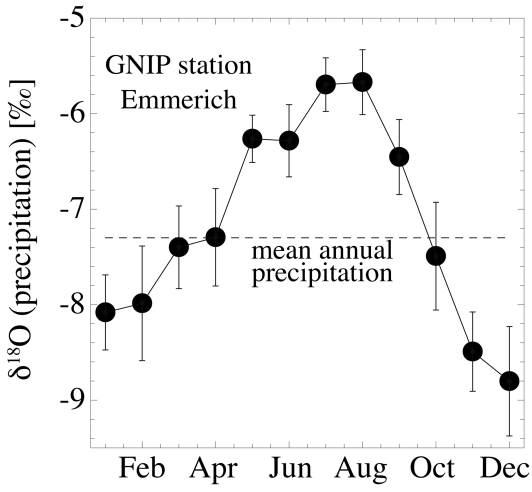

Fig. 5.2: Mean long-term monthly $\delta^{18}O$ record (1980-2005) of local precipitation from the IAEA-GNIP station Emmerich.

The rodent skeletal material belongs to the four arvicolid species *Arvicola terrestris*, *Myodes glareolus*, *Microtus agrestis* and *Microtus arvalis* as well as to the three murid species *Apodemus sylvaticus*, *Mus musculus*, and *Rattus norvegicus*. From the latter species, the owl pellets contained only juvenile individuals. The analysed teeth were permanent growing (arvicolid and murid incisors and most arvicolid molars), thus reflecting the last four to twelve weeks in the life of the respective individual prior to death (Koenigswald and Golenishew, 1979; Klevezal et al., 1990). Bone material comprises stable isotope compositions over a longer time period, approaching the life span of the individual (e.g., Klevezal, 1996), which in the present case is the time until predation by barn owls. None of the analysed taxa hibernate.

The isotope signatures of the skeletal tissue samples are likely to be seasonally biased, because of the different tissue formation and turnover periods and due to the seasonal population dynamics of the rodents and their predators. Population sizes of arvicolids and murids in temperate regions typically increase after a minimum at the end of the winter with the first breed in spring and reach a maximum (partly up to more than one order of magnitude larger than the early spring population) in late summer (e.g., Stubbe, 1982; Bäumler, 1986; Ylönen et al., 1991). Avian predator populations, responsible for pellet accumulations, are positively correlated to populations of their small mammal prey (e.g., Schönfeld and Girbig, 1975; Schönfeld et al., 1977; Salamolard et al., 2000; Norrdahl and Korpimäki, 2002), causing a warm-season biased pellet deposition in modern ecosystems and probably in fossil ecosystems as well. Analogous conditions for modern and fossil samples are an important prerequisite for the development of $\delta^{18}O_{PO4/CO3}$-$\delta^{18}O_{LW}$ calibration equations and their application for palaeoclimate reconstructions (Navarro et al., 2004).

No specific permits were required for the described field studies.

5.3.2 Methods

5.3.2.1 Oxygen and carbon isotope analyses of the carbonate in the bioapatite ($\delta^{18}O_{CO3}$, $\delta^{13}C$)

Only teeth from taxonomically identified jaw specimens were used for stable isotope analysis. Teeth from each species, both upper incisors (in *Arvicola terrestris* and *Rattus norvegicus* only the left upper incisor) of ten individuals, were extracted from the jaw and inspected to ensure that no signs of digestive etching were present. Further $\delta^{18}O_{CO3}$ and

$\delta^{13}C$ analyses were conducted on jaw bone material (derived from the zygomatic region) of five of the ten individuals of each species. In *Arvicola terrestris*, the left upper molars (M1-M3) of the ten specimens were also analysed.

Bulk tooth and bone material was crushed and ground to a fine powder using an agate mortar and pestle. The chemical pretreatment procedure to remove organic matter and adherent carbonates followed Koch et al. (1997). Approximately 10 mg of sample powder were soaked with 30% H_2O_2 (0.1 ml mg^{-1}) for 24 h, rinsed five times with millipore water, soaked for another 24 h with an acetic acid-calcium acetate buffer solution (1 M, pH = 5, 0.05 ml mg^{-1}) and rinsed again five times with millipore water, followed by drying overnight at 50°C. Typically, 1 to 1.3 mg of pretreated sample powder were reacted for 15 min. with 100% H_3PO_4 at 70°C in a Thermo Scientific KIEL IV automated carbonate device. Released CO_2 was measured in dual inlet mode with a Finnigan Delta plus isotope ratio gas mass spectrometer at the stable isotope laboratory of the Geoscience Center at the University of Göttingen. The measured isotope compositions were normalised to the NBS 19 calcite standard, measured in the same runs together with the bioapatite samples. Data are reported in the δ-notation in per mil (‰), relative to the international isotope reference standards Vienna Standard Mean Ocean Water (VSMOW) for $\delta^{18}O$ and Vienna Pee Dee Belemnite (VPDB) for $\delta^{13}C$ (Coplen, 1994).

$$\delta^{18}\mathrm{O} \text{ or } \delta^{13}\mathrm{C}(‰) = \left[\left(R_{sample}/R_{standard}\right) - 1\right] \times 1000,$$

where R_{sample} and $R_{standard}$ are the $^{18}O/^{16}O$ and $^{13}C/^{12}C$ ratios in sample and standard, respectively.

The analytical precision for the NBS 19 was ± 0.1‰ (1σ) in $\delta^{18}O$ and ± 0.04‰ (1σ) in $\delta^{13}C$ (n = 232, analysed between November 2010 and February 2012). For the NBS 120c Florida phosphate rock standard (pretreated as described above), we obtained a $\delta^{18}O$ value of 30.0 ± 0.2‰ (1σ) and a $\delta^{13}C$ value of –6.4 ± 0.04‰ (1σ) (n = 10). Our internal bioapatite standard AG-Lox (African elephant enamel) had a $\delta^{18}O$ value of 30.0 ± 0.08‰ (1σ) and a $\delta^{13}C$ value of –12.0 ± 0.03‰ (1σ) (n = 11). For inter-laboratory comparison, material of our internal AG-Lox enamel standard will be supplied upon request by the authors.

5.3.2.2 Oxygen analyses of the phosphate ($\delta^{18}O_{PO4}$)

Analyses of the phosphate moiety of the bioapatite ($\delta^{18}O_{PO4}$) were conducted on the incisors, M1 and bone material from five of the *Arvicola terrestris* specimens.

Ag_3PO_4 was precipitated from about 4 mg of the pretreated sample powder (see section above), using a method slightly modified after Dettmann et al. (2001) and described in detail by Tütken et al. (2006). For dissolution of the samples, 0.8 ml of HF (2 M) were added, and the sample vials were put on a vibrating table for 12 h. This was followed by centrifugation and transfer to new vials of the supernatant sample solutions, leaving behind the CaF solid residue. After neutralising the HF solution with NH_4OH (25%) in the presence of bromothymol blue as pH-indicator, Ag_3PO_4 was precipitated rapidly by adding 0.8 ml of 2 M silver nitrate ($AgNO_3$) solution. After settling of the small Ag_3PO_4 crystals and centrifugation, the supernatant solution was pipetted off and the Ag_3PO_4 was rinsed twice with 1.8 ml millipore water. The Ag_3PO_4 was then dried overnight in an oven at 50°C.

Ag_3PO_4 aliquots of 0.5 mg were placed into silver capsules and analysed in triplicate by means of high temperature reduction Finnigan TC-EA coupled via a Conflo III to a Finnigan Delta Plus XL GC-IRMS, according to the method of Vennemann et al. (2002).

5.3.2.3 Statistical methods

The statistical analyses were performed using Wolfram Mathematica 7.0 and 8.0. To evaluate if the differences in the mean isotope values among multiple taxa are statistically significant, one-factor analyses of variance (ANOVA) were conducted, followed by posthoc-tests (Tukey) for pairwise comparisons. In one case, the assumptions of the parametric ANOVA were violated (non-normal distribution), therefore we additionally performed a Kruskal-Wallis non-parametric ANOVA that was not in disagreement with the parametric ANOVA results.

Minimum sample sizes to represent the population mean in $\delta^{18}O$ by 95% degree of confidence within ± 1σ were determined by a standard bootstrapping approach according to the method presented by Fox-Dobbs et al. (2007). From the bulk incisor data sets of the seven analysed species (n=10 each), 1,000 randomly selected subsamples (n_{sub}) were generated for every n_{sub} between 2 and n–1. Then, the proportion of subsamples within all random replicates for a given n_{sub} that range between ± 1σ of the mean of the original

datasets was determined, using the average value from 100 repeated evaluations. If the mean values of ≥950 out of 1000 subsamples are in a range between ± 1σ of the analysed dataset, it is indicated that the respective n_{sub} is adequate to estimate the population mean at least by a 95% confidence level.

5.4 Results

5.4.1 Oxygen and carbon isotope data of the carbonate in the bioapatite ($\delta^{18}O_{CO3}$, $\delta^{13}C$)

The data, which are summarised in Table S1, include 135 individual $\delta^{18}O_{CO3}$ and $\delta^{13}C$ analyses of bulk incisor and molar teeth, as well as $\delta^{18}O_{CO3}$ and $\delta^{13}C$ values of bone material from seven modern arvicolid and murid species from a single locality in NW Germany (see Materials and Methods section).

5.4.1.1 Oxygen isotope composition of the incisors

Intra-population variations in $\delta^{18}O_{CO3}$ from 2.0 to 3.9‰ have been observed in the bulk incisor samples (n=10 of each species), with the exception of the arvicolid *M. glareolus*, which has a significantly higher range of 6.7‰. However, if the most extreme value is excluded and considered as an outlier, *M. glareolus* has an intra-population variation of 3.5‰ that falls within the range of variation of the other species (Table 5.1). The mean $\delta^{18}O_{CO3}$ values of the arvicolid incisors are 26.8 ± 1.4‰ (*A. terrestris*), 27.2 ± 1.8‰ (*M. glareolus*), 27.3 ± 1.1‰ (*M. agrestis*) and 27.3 ± 1.2‰ (*M. arvalis*). The murid incisors have mean $\delta^{18}O_{CO3}$ values of 27.9 ± 1.0‰ (*A. sylvaticus*), 28.3 ± 1.0‰ (*M. musculus*) and 29.0 ± 0.7‰ (*R. norvegicus*) (Fig. 5.3, Table 5.1).

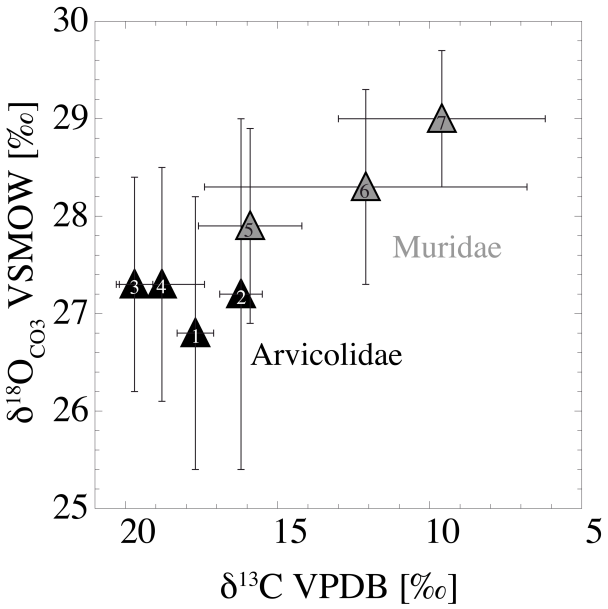

Fig. 5.3: Mean $\delta^{18}O_{CO3}$ and $\delta^{13}C$ values of bulk incisors of the seven analysed rodent species (n=10 in each species) with 1σ error bars. 1: *A. terrestris*, 2: *M. glareolus*, 3: *M. agrestis*, 4: *M. arvalis*, 5: *A. sylvaticus*, 6: *M. musculus*, 7: *R. norvegicus*.

Between the mean $\delta^{18}O_{CO3}$ values of these species, statistically significant differences (one-way ANOVA, F = 3.638, P <0.01) were observed, pair-wise comparison revealed that only *A*. *terrestris* and *R*. *norvegicus* show significantly different values (Tukey test, P <0.01). Within arvicolids, no statistically significant differences in $\delta^{18}O_{CO3}$ were detected (one-way ANOVA, F = 0.304, P = 0.82). Within murids, mean $\delta^{18}O_{CO3}$ values differed significantly (one-way ANOVA, F = 3.654, P <0.05) but only between *A*. *sylvaticus* and *R*. *norvegicus* were significant differences detected by pair-wise comparisons (Tukey test, P <0.05).

Table 5.1: Mean $\delta^{18}O_{CO3}$ and $\delta^{13}C$ values of bulk incisors of the seven analysed rodent species (n=10 in each species) with 1σ error and range of variation (lowest and highest analytical value of the respective species)

Species	material	mean $\delta^{18}O_{CO3}$ (‰ vs. VSMOW)	range of variation in $\delta^{18}O_{CO3}$ values	mean $\delta^{13}C$ (‰ vs. VPDB)	range of variation in $\delta^{13}C$ values	n
Arvicola terrestris	I[1] sin.	26.8±1.4	24.9 to 28.8	-17.7±0.6	-18.5 to -16.7	10
Myodes glareolus	I[1] sin. u. dex.[1]	27.2±1.8	24.7 to 28.2 (31.4)[2]	-16.2±0.7	-17.3 to -15.1	10
Microtus agrestis	I[1] sin. u. dex.	27.3±1.1	26.0 to 28.8	-19.7±0.6	-20.5 to -18.6	10
Microtus arvalis	I[1] sin. u. dex.	27.3±1.2	25.4 to 29.2	-18.8±1.4	-20.8 to -16.8	10
Apodemus sylvaticus	I[1] sin. u. dex.	27.9±1.0	26.0 to 29.1	-15.9±1.7	-17.8 to -12.4	10
Mus musculus	I[1] sin. u. dex.	28.3±1.0	26.4 to 29.7	-12.1±5.3	-17.4 to -4.7	10
Rattus norvegicus	I[1] sin.	29.0±0.7	27.8 to 29.9	-9.6±3.4	-14.7 to -4.5	10

[1] sin. = left, dex. = right, [2] value in brackets excluded as an outlier, see results section

5.4.1.2 Carbon isotope composition of the incisors

The $\delta^{13}C$ values of the incisor samples (n=10 of each species) in three of the four modern arvicolids (*A. terrestris*, *M. glareolus* and *M*. *agrestis*) have very narrow intra-population variations of <2.2‰, with mean values of –17.7 ± 0.6‰, –16.2 ± 0.7‰ and –19.7 ± 0.6‰, respectively. The intra-population $\delta^{13}C$ variations of *M*. *arvalis* and the murid *A*. *sylvaticus* are much larger, with ranges of 4.0‰ and 5.4‰ and mean values of –18.8 ± 1.4‰ and –15.9 ± 1.7‰, respectively. Very large variations were observed in the two murids, *M*. *musculus* and *R*. *norvegicus*, that have an intra-population $\delta^{13}C$ range of 12.7‰ and 10.2‰ with mean values of –12.1 ± 5.3‰ and –9.6 ± 3.4‰, respectively (Fig. 5.3, Table 5.1). Mean $\delta^{13}C$ values differed significantly between the analysed species (one-way ANOVA, F = 20.632, P <0.01). By pair-wise comparison, mean $\delta^{13}C$ values of two murids (*M*. *musculus* and *R*. *norvegicus*) differed significantly from those of all arvicolids as well as from *A. sylvaticus*. The mean $\delta^{13}C$ value of *M*. *agrestis* showed significant differences relative to those of *A*. *sylvaticus* and *M. glareolus* (Tukey test, P <0.05).

Considering the arvicolids separately, differences in the mean $\delta^{13}C$ values between taxa (one-way ANOVA, F = 28.813, P <0.01) were observed. By pair-wise comparisons, significant differences between *M*. *agrestis* and *M. glareolus* themselves and with both other Arvicolidae were detected (Tukey test, P <0.05). Within murids, significant differences among taxa were present as well (one-way ANOVA, F = 7.230, P <0.01), but only *A*. *sylvaticus* and *R*. *norvegicus* show significant differences by pair-wise comparison (Tukey test, P <0.05).

5.4.1.3 Oxygen and carbon isotope compositions of the bones

The bone $\delta^{18}O_{CO3}$ values (n=5 of each species) deviate from the incisor values of of the same individuals by –4.2 to +1.5‰. 85% (30 out of 35 specimens) have higher $\delta^{18}O_{CO3}$ values in their incisors than in their bones (Fig. 5.4, Table S1). Mean values are 25.6 ± 1.2‰ (*A*. *terrestris*), 25.7 ± 1.4‰ (*M. glareolus*), 24.6 ± 1.3‰ (*M. agrestis*) and 26.6 ± 1.3‰ (*M. arvalis*). The murid bones have mean $\delta^{18}O_{CO3}$ values of 25.8 ± 0.8‰ (*A. sylvaticus*), 28.2 ± 1.6‰ (*M. musculus*) and 25.8 ± 1.0‰ (*R*. *norvegicus*) (Table 5.2).

Table 5.2: Mean $\delta^{18}O_{CO3}$ and $\delta^{13}C$ values of bone material of the seven analysed rodent species (n=5 in each species) with 1σ error and range of variation (lowest and highest analytical value of the respective species)

Species	material	mean $\delta^{18}O_{CO3}$ (‰ vs. VSMOW)	range of variation in $\delta^{18}O_{CO3}$ values	mean $\delta^{13}C$ (‰ vs. VPDB)	range of variation in $\delta^{13}C$ values	n
Arvicola terrestris	bone	25.6±1.2	24.6 to 27.7	-17.8±0.9	-19.0 to -16.8	5
Myodes glareolus	bone	25.7±1.4	24.0 to 27.3	-17.7±0.4	-18.3 to -17.3	5
Microtus agrestis	bone	24.6±1.3	23.1 to 26.4	-19.5±0.6	-20.0 to -18.5	5
Microtus arvalis	bone	26.6±1.3	24.8 to 27.9	-18.4±0.8	-19.5 to -17.6	5
Apodemus sylvaticus	bone	25.8±0.8	24.6 to 26.6	-16.4±1.3	-17.3 to -14.1	5
Mus musculus	bone	28.2±1.6	25.5 to 29.5	-11.6±5.5	-16.8 to -5.0	5
Rattus norvegicus	bone	25.8±1.0	24.7 to 26.7	-7.9±2.2	-10.7 to -5.8	5

The different bone-incisor offsets have standard deviations between 0.8 and 1.8‰ within each analysed species, except for the juvenile *R*. *norvegicus* specimen with a standard deviation of only 0.3‰.

The $\delta^{13}C$ of bone material deviates by +1.9 to –1.6‰ from that of the incisors, with the exceptions of one *A*. *sylvaticus* (–2.9‰) and one *M*. *musculus* (+4.3‰). Mean values are –17.8 ± 0.9‰ (*A*. *terrestris*), –17.7 ± 0.4‰ (*M. glareolus*), –19.5 ± 0.6‰ (*M. agrestis*) and –18.4 ± 0.8‰ (*M. arvalis*). The murid bones have higher mean $\delta^{13}C$ values of –16.4 ± 1.3‰ (*A. sylvaticus*), –11.6 ± 5.5‰ (*M. musculus*) and –7.9 ± 2.2‰ (*R*. *norvegicus*). No systematic differences between incisor and bone material can be observed, as it is the case for $\delta^{18}O_{CO3}$ (Fig. 5.5, Table 5.2).

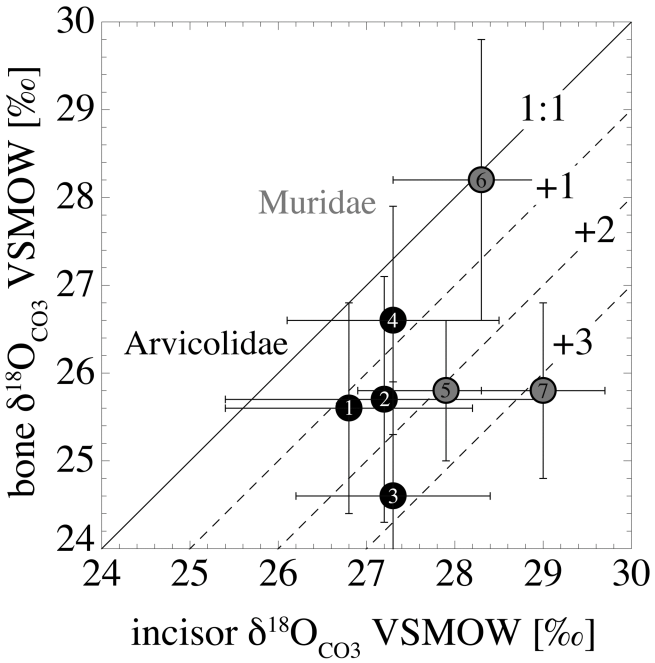

Fig. 5.4: Comparison of incisor and bone $\delta^{13}C$ values from the individuals where both tissues were analysed (n=5 in each species). 1: *A. terrestris*, 2: *M. glareolus*, 3: *M. agrestis*, 4: *M. arvalis*, 5: *A. sylvaticus*, 6: *M. musculus*, 7: *R. norvegicus*. The dashed lines represent the deviation of incisor mean values from bone mean values in ‰ from the 1:1 accordance (solid line).

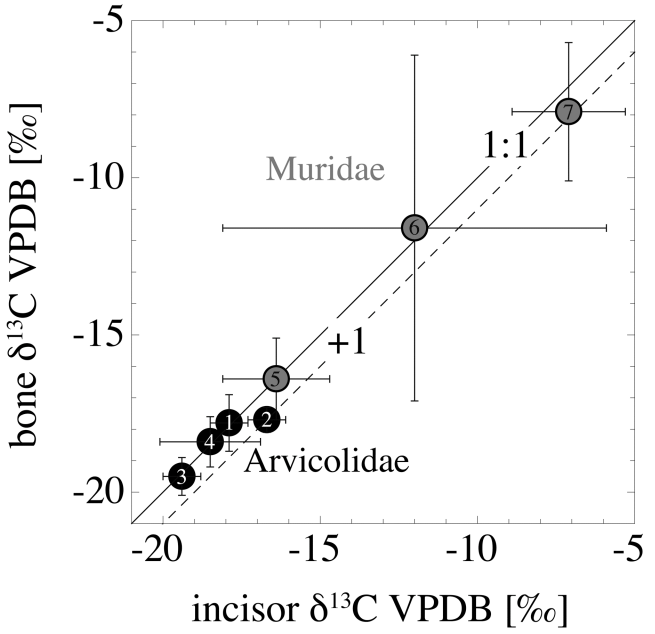

Fig. 5.5: Comparison of incisor and bone $\delta^{18}O_{CO3}$ values from the individuals where both tissues were analysed (n=5 in each species).1: *A. terrestris*, 2: *M. glareolus*, 3: *M. agrestis*, 4: *M. arvalis*, 5: *A. sylvaticus*, 6: *M. musculus*, 7: *R. norvegicus*. The dashed lines represent the deviation of incisor mean values from bone mean values in ‰ from the 1:1 line (solid line).

5.4.1.4 Oxygen and carbon isotope compositions of the molars of *A. terrestris* (intra-jaw variations)

In *A. terrestris* the intra-jaw range (n=10) between the molars (M1-M3) of the same individual is 0.2 to 1.0‰ in $\delta^{18}O_{CO3}$ and 0.1 to 0.6‰ in $\delta^{13}C$. The overall intra-jaw range (I1, M1-M3) varies from 0.3 to 1.9‰ in $\delta^{18}O_{CO3}$, while in most cases the incisors have higher values than the molars (Fig. 5.6, Table S1). In $\delta^{13}C$, nearly all incisors have lower values than the corresponding molars, with overall intra-jaw variations between 0.3 and 1.5‰ (Fig. 5.7, Table S1). Mean values for M1, M2, and M3 are 26.1 ± 1.6‰, 26.1 ± 1.5‰ and 26.2 ± 1.3‰ in $\delta^{18}O_{CO3}$ and –16.9 ± 0.6‰, –16.8 ± 0.6‰ and –16.7 ± 0.5‰, respectively (n=10 of each tooth type).

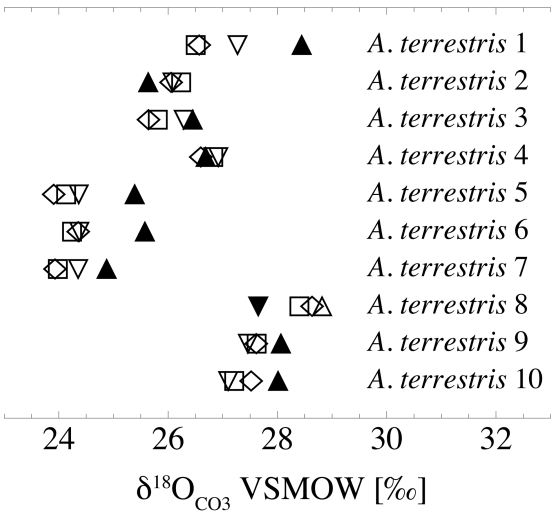

Fig. 5.6: Intra-jaw variations in $\delta^{18}O_{CO3}$ of *Arvicola terrestris*.
Filled triangles = incisors, open diamonds = M1, open squares = M2, open down triangles = M3.

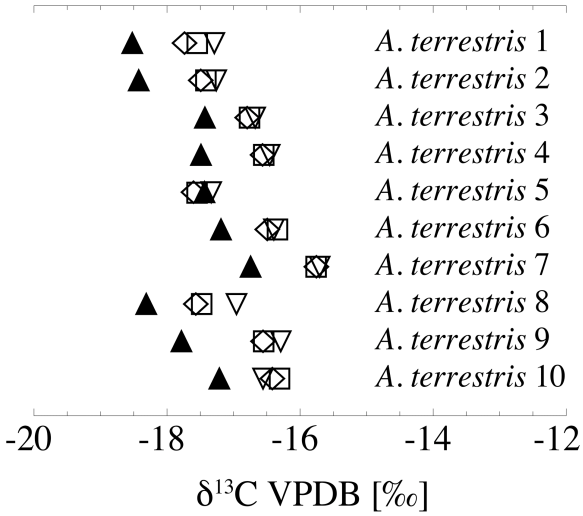

Fig. 5.7: Intra-jaw variations in $\delta^{13}C$ of *Arvicola terrestris*.
Filled triangles = incisors, open diamonds = M1, open squares = M2, open down triangles = M3.

5.4.2 Oxygen isotope analyses of the phosphate in the bioapatite ($\delta^{18}O_{PO4}$) of *A. terrestris*

The mean $\delta^{18}O_{PO4}$ of skeletal apatite from *A. terrestris* are 15.4 ± 1.1‰ (bulk incisors, n=5), 14.9 ± 1.3‰ (bulk M1, n=5) and 14.9 ± 0.8‰ (bone, n=5). The corresponding $\delta^{18}O_{CO3}$ means are 26.5 ± 1.2‰, 25.8 ± 1.1‰ and 25.6 ± 1.2‰, leading to a $\Delta^{18}O_{CO3\text{-}PO4}$ of 11.2 ± 1.0‰ (incisors), 10.9 ± 0.4‰ (M1) and 10.7 ± 0.9‰ (bone), respectively. The overall average $\Delta^{18}O_{CO3\text{-}PO4}$ is 10.9 ± 0.8‰ (Fig. 5.8, Table 5.3).

Table 5.3: $\delta^{18}O_{CO3}$, $\delta^{18}O_{PO4}$ and $\Delta^{18}O_{CO3\text{-}PO4}$ of incisors, first molars and bone material of *A. terrestris* (n=5)

Species	material	$\delta^{18}O_{CO3}$ (‰ vs. VSMOW)	$\delta^{18}O_{PO4}$ (‰ vs. VSMOW)	$\Delta^{18}O_{CO3\text{-}PO4}$ (‰)
Arvicola terrestris 01	I^1 sin.	28.4	15.9	12.5
Arvicola terrestris 01	M^1 sin.	26.6	16.1	10.5
Arvicola terrestris 01	bone	27.7	15.4	12.3
Arvicola terrestris 02	I^1 sin.	25.6	15.6	10.0
Arvicola terrestris 02	M^1 sin.	26.1	15.2	10.9
Arvicola terrestris 02	bone	25.5	15.7	9.8
Arvicola terrestris 03	I^1 sin.	26.4	15.4	11.0
Arvicola terrestris 03	M^1 sin.	25.6	15.2	10.4
Arvicola terrestris 03	bone	25.2	15.0	10.2
Arvicola terrestris 04	I^1 sin.	26.7	16.3	10.4
Arvicola terrestris 04	M^1 sin.	26.6	15.3	11.3
Arvicola terrestris 04	bone	24.6	13.8	10.8
Arvicola terrestris 05	I^1 sin.	25.4	13.6	11.8
Arvicola terrestris 05	M^1 sin.	23.9	12.7	11.2
Arvicola terrestris 05	bone	25.2	14.6	10.6
Mean (I^1)		**26.5±1.2**	**15.4±1.0**	**11.2±1.0**
Mean (M^1)		**25.8±1.1**	**14.9±1.3**	**10.9±0.4**
Mean (bone)		**25.6±1.2**	**14.9±0.7**	**10.7±1.0**
Overall mean				**10.9±0.8**

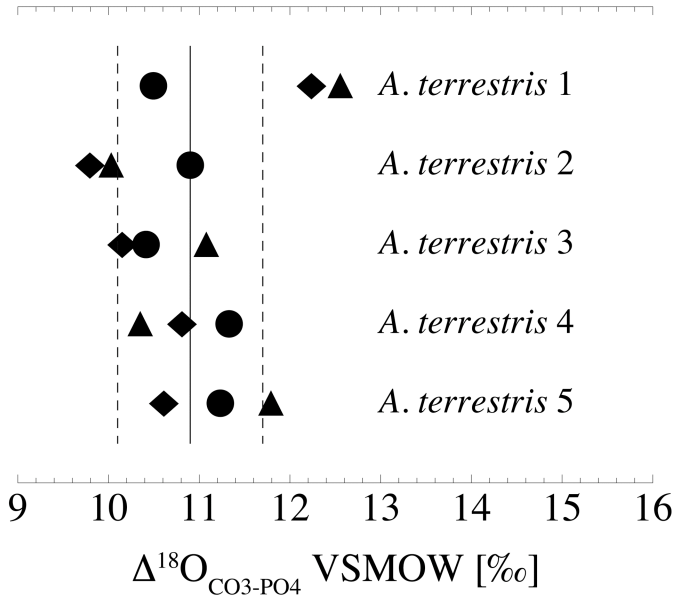

Fig. 5.8: $\Delta^{18}O_{CO3\text{-}PO4}$ of incisors, first molars and bone in *A. terrestris* 1 to 5. Triangles represent the incisors, diamonds the first molars and circles the bones. The average value for all samples is 10.9 ± 0.8‰ (solid and dashed lines)

5.4.3 Minimum sample size calculations

Minimum sample sizes, calculated with the bootstrapping approach used by Fox-Dobbs et al. (2007) are in the same range or smaller than previously published data from large mammals (e.g., Clementz and Koch, 2001; Hoppe et al., 2005; Hoppe, 2006; Wang et al.,

2008; Table 5.4). From all randomly chosen subsamples with n_{sub} ≥4, 95% or more range within 1σ of the mean of the complete data. In the case of a subsample size of n_{sub} ≥7, even a 99% confidence is reached for a range within 1σ of the mean of the whole dataset.

Table 5.4: Results of the bootstrap analysis of $\delta^{18}O_{CO3}$ for rodent incisors (n=10 in each species)

	Number of subsamples out of 1000 random replicates of n_{sub} within 1σ						
	arvicolids (incisors)			murids (incisors)			
n_{sub}	*A. terrestris*	*M. glareolus*	*M. agrestis*	*M. arvalis*	*A. sylvaticus*	*M. musculus*	*R. norvegicus*
2	801	819	831	802	829	842	860
3	918	918	911	909	894	897	936
4	963	951	957	950	955	950	969
5	984	970	982	971	978	968	985
6	>990	981	990	983	986	982	>990
7 to 9	>990	>990	>990	>990	>990	>990	>990

5.5. Discussion

5.5.1 Inter- and intra-specific variations in $\delta^{18}O_{CO3}$

Mean $\delta^{18}O_{CO3}$ values of the analysed species (Fig. 5.3) show no, or only minor, differences. This suggests that probably all taxa drank from isotopically similar water sources. The higher $\delta^{18}O_{CO3}$ in *R. norvegicus* compared to the other rodent species may be attributed to the juvenile status of the individuals and might reflect a remnant suckling signal.

Due to the lack of published small mammal $\delta^{18}O_{CO3}$ data, the intra-population variability of the analysed species can only be compared to published $\delta^{18}O_{PO4}$ values of rodents. The ranges from 2.0 to 3.9‰ (excluding one individual of *M. glareolus*, see results section) for the incisor teeth are much larger than the range in $\delta^{18}O_{PO4}$ of 0.7 to 0.8‰ for fat dormice (*Glis glis*). However, only three specimens were investigated by Lindars et al. (2001). Bones of *Pitymus* sp., *M. arvalis* and *A. terrestris* had $\delta^{18}O_{PO4}$ intra-population variations of 0.8 to 2.2‰, 0.4 ‰ and 1.3 to 2.3‰, respectively (Longinelli et al., 2003). These ranges are lower than or reach the lower limit of the rodent $\delta^{18}O_{CO3}$ variability in the present study. However, the lowest value of the aforementioned ranges is again based on three to four individuals only and derives mainly from mixed bone material.

Compared to large mammals, the observed variations of 2.0 to 3.9‰ are in the same range as previously reported $\delta^{18}O_{CO3}$ values for North American bison (*Bison bison*) with 2.4 to 3.0‰ (Hoppe, 2006), Baird's tapir (*Tapirus bairdii*) with 1.4 to 2.6‰ (DeSantis, 2011), feral and domestic horses (*Equus caballus*) with 2.0 to 6.5‰ (Hoppe et al., 2004;

2005; Wang et al., 2008), and bobcats (*Lynx rufus*) with 3.1‰ intra-population variability at a single locality (Clementz and Koch, 2001). Other published intra-population variabilities including three or more individuals for large terrestrial mammals are significantly larger than those observed in the present study, as is the case for mule deer (*Odocoileus hemionus*) with a range of 6.2‰, coyotes (*Canis latrans*) with 6.3‰ (Clementz and Koch, 2001), domestic yaks (*Bos grunniens*) with 3.7 to 8.5‰ and domestic goats (*Capra aegagrus hircus*) with 5.4 to 10.6‰ intra-population variability (Wang et al., 2008).

5.5.2 Inter- and intra-specific variations in $\delta^{13}C$

Mean $\delta^{13}C$ values of the analysed species are in part significantly distinct from each other, notably between arvicolids and murids, indicating dietary differences (Fig. 5.3). The intra-population variations in $\delta^{13}C$ have a wide range from 1.8 to 12.7‰, reflecting variations in the $\delta^{13}C$ values of their diet and in the nutritional behaviour (i.e., dietary specialists vs. dietary opportunists). Previously published data on intra-population variations from large mammals range from 0.7 to 8.5‰ (Clementz and Koch, 2001; Hoppe, 2006; Wang et al., 2008; DeSantis, 2011).

The average carbon isotope fractionation between diet and bioapatite in rodents (determined on bone material) is +9.9‰ (DeNiro and Epstein, 1978; Ambrose and Norr, 1003; Grimes et al., 2004a). This suggests average diet $\delta^{13}C$ values between –29.6 and –26.1‰ for the arvicolids. For the murids, the average diet $\delta^{13}C$ values are higher: –25.8‰ in *A*. *sylvaticus*, –22.0‰ in *M*. *musculus* and –19.5‰ in *R*. *norvegicus*.

The low intra-population variations of *A*. *terrestris*, *M. glareolus* and *M*. *agrestis* (<2.2‰) indicate little dietary variations, which is supported for *A*. *terrestris and M*. *agrestis* by the observation of nearly exclusively herbivorous diets (Krapp and Niethammer, 1982; Reichstein, 1982). An exclusively herbivorous diet is also known for *M. glareolus* in various regions (Viro and Niethammer, 1982). The diet of *M*. *arvalis* and *A*. *sylvaticus* consists of a considerable but varying amount of invertebrates (Niethammer, 1978; Niethammer and Krapp, 1982) explaining the higher variability of 4.0 and 5.3‰, respectively. Mean values of these species correspond to a typical C_3 diet. The highest variabilities in $\delta^{13}C$ within the individuals from a single population were observed in *R*. *norvegicus* and *M*. *musculus*, with 10.2 and 12.7‰, respectively. Both are synanthropic species with a very opportunistic diet that commonly includes human food supplies and

food waste (Freye and Freye, 1960; Becker, 1978; Reichstein, 1978). Thus, the high variability in $\delta^{13}C$ is likely caused by the presence or absence of C_4-sugars and/or products containing tissues from animals fed on a C_4 diet in the rodent diet.

5.5.3 Variations in $\delta^{18}O_{CO3}$ and $\delta^{13}C$ between incisor and bone material

The $\delta^{18}O_{CO3}$ values of the incisors differ by up to ~4‰ from that of bone material (Table S1), which can be explained by different time intervals in the mineralisation of both tissues. Rodent incisors (and also the molars of most arvicolids) are permanently growing and reflect a time span of a few weeks (Koenigswald and Golenishev, 1979; Klevezal et al., 1990), whereas no pronounced remodeling of bone tissue occurs in rodents. Thus, bones archive a nearly life-long record (Klevezal, 1996). This may also explain the phenomenon of why nearly 90% of the analysed individuals have higher $\delta^{18}O_{CO3}$ values in the incisors than in the bone material (Fig. 5.4). Taking into account the general population dynamics of small rodents in temperate regions with population maxima in late summer (see also materials and methods section), the incisor $\delta^{18}O_{CO3}$ of a large number of individuals are likely biased towards the ^{18}O-enriched precipitation of the warm summer months (Fig. 5.2). In contrast, bone material was formed over a longer time span, including the colder spring season or even the winter months in case of adult individuals that survived this period. This is further supported by the standard deviations of the bone-incisor offsets in each species (0.8 to 1.8‰), which reflects the different times of mineralisation of both tissues in relation to a variable age structure of the individual specimens. One exception is the juvenile *R*. *norvegicus* specimens that have a relatively uniform bone-incisor offset within the five analysed individuals (~3‰), with a small standard deviation of only 0.3‰. This likely reflects their more or less identical age and hence similar time intervals recorded in bone and incisor $\delta^{18}O_{CO3}$ values.

The $\delta^{13}C$ values of the bulk incisor teeth, with two exceptions (Table S1), deviate less than 2‰ from the $\delta^{13}C$ results of the respective bone material, and no general trend to a skewed variation, as is the case for $\delta^{18}O_{CO3}$, can be observed (Fig. 5.5). These variations can be explained by variations in the carbon isotope composition of the consumed food during the different mineralisation times of incisor and bone material.

5.5.4 Intra-jaw variations in $\delta^{18}O_{CO3}$ and $\delta^{13}C$ of *A*. *terrestris*

The $\delta^{18}O_{CO3}$ of the molars of *A*. *terrestris* deviates from the incisor oxygen isotope composition of the same individual between 0.3 and 1.9‰, indicating slight differences in

the time periods of mineralisation of both tooth types. For other arvicolids (*Microtus*) a complete renewal of incisors within four to seven weeks is reported (Klevezal et al., 1990), whereas first and second molars of *Microtus* underly a complete renewal in a time interval of eight to twelve weeks (Koenigswald and Golenishev, 1979). Considering this, as well as the fact that the molars mostly have lower $\delta^{18}O_{CO3}$ values than incisors (Table S1; analogous to the incisor-bone offset), a small bias by seasonally driven population dynamics is likely the cause for the inter-tooth offset.

The difference in $\delta^{13}C$ between molar teeth and incisors of all analysed individuals is less than 2‰, comparable to the bone-incisor variations and reflecting varying carbon isotope compositions of the ingested food (Table S1). Given that the owl pellets represent a seasonally biased taphocoenosis, the lower $\delta^{13}C$ values in nearly all incisors compared to the molars of the same individuals can result either from a seasonal change in availability of food plants or from seasonal changes in the carbon isotope composition of the same plant species, which can be in the range of several per mil within one plant species (e.g., Lowdon and Dyck, 1974; Heaton, 1999).

Variations among M1 to M3 of the same animal are generally lower, both in $\delta^{18}O_{CO3}$ (0.2 to 1‰) as well as in $\delta^{13}C$ (0.1 to 0.6‰), indicating a more or less contemporaneous growth and mineralisation of these molars.

5.5.5 The $\Delta^{18}O_{CO3\text{-}PO4}$ in *A. terrestris*

Comparing incisors, molars and bone, the differences between $\delta^{18}O_{CO3}$ and $\delta^{18}O_{PO4}$ of each element overlap within error (Table 3). The overall $\Delta^{18}O_{CO3\text{-}PO4}$ of 10.9 ± 0.8‰ is high and at the upper limit of previously reported values for large and medium-sized mammals (7.5 to 10.6‰; Bryant et al., 1996; Iacumin et al., 1996; Shahack-Gross et al., 1999; Zazzo et al., 2004; Martin et al., 2008; Pellegrini et al., 2011) that include perissodactyls, artiodactyls and carnivorans. The only reported data for rodents (laboratory rats, *Rattus norvegicus*) from two different settings show a highly variable $\Delta^{18}O_{CO3\text{-}PO4}$ of 8.5 and 11.4‰, respectively (Kirsanow and Tuross, 2011). Further studies are needed to evaluate a possible species or body temperature dependence as suggested by Martin et al. (2008) or a connection to seasonal variations in the $\delta^{18}O$ of drinking water and/or a food source of phosphate as supposed by Kirsanow and Tuross (2011).

5.5.6 Minimum sample size calculations

The bootstrapping results of our $\delta^{18}O_{CO3}$ data from rodents (more than 95% of the subsamples are within ± 1σ of the mean if n_{sub} ≥4, and even more than 99% if n_{sub} ≥7) agree to the minimum sample size recommendations for most large mammals given in previous studies (Clementz and Koch, 2001; Hoppe et al., 2005; Hoppe, 2006) as well as for the horses from the study of Wang et al. (2008). For goats and yaks, a considerably higher minimum sample size for reliable estimates of the population mean $\delta^{18}O$ within a 95% confidence level has been determined (Wang et al., 2008), presumably related to differences in physiology and/or a different nutritional or rather drinking behaviour. Our data for rodents indicate that the minimum sample size recommendations, determined for large mammals, potentially can be extended to small mammal species (i.e., rodents). Further taxon-specific studies, however, are needed to confirm if the present finding is valid for small mammals in general.

5.5.7 Suitability for the $\delta^{18}O$ reconstruction of local water

The $\delta^{18}O_{CO3}$ variability of different sympatric rodent taxa from the studied locality is low. This suggests the reliability of a $\delta^{18}O_{CO3/PO4}$-$\delta^{18}O_{LW}$ calibration equation based on a generic, family or even higher taxonomic level. However, factors that can affect the oxygen isotope composition of biogenic apatite (e.g., habitat, drinking behaviour, population dynamics, body size and thermophysiology) should be considered carefully before inferring drinking water $\delta^{18}O$ values from existing calibration equations or the development of new ones.

To assess if calibration equations developed on bone material can be unrestrictedly applied to tooth data and vice versa, incisor and bone mean values were compared to each of the three existing $\delta^{18}O_{PO4}$-$\delta^{18}O_{LW}$ calibration equations for different rodent taxa (Table 5.5).

Table 5.5: Existing calibration equations between $\delta^{18}O_{LW}$ and $\delta^{18}O_{PO4}$ for rodents

Study	developed calibration equation	skeletal tissue used	included genera
Luz and Kolodny (1985)	$\delta^{18}O_{LW} = (\delta^{18}O_{PO4}-17.88)/0.49$	bone	*Rattus*
Longinelli et al. (2003)	$\delta^{18}O_{LW} = (\delta^{18}O_{PO4}-23.07)/1.14$	bone (nearly solely)	*Apodemus*, *Pitymus*, *Arvicola*, *Microtus*
Navarro et al. (2004)	$\delta^{18}O_{LW} = (\delta^{18}O_{PO4}-20.98)/0.572$	molars, incisors	*Microtus*, *Myodes*, *Lemmus*

The $\delta^{18}O_{PO4}$ values were calculated from the measured $\delta^{18}O_{CO3}$ values, applying the $\Delta^{18}O_{CO3-PO4}$ of 10.9 ± 0.8‰ determined for *Arvicola terrestris*. Thus, combining the data of all seven analysed species, the calculated mean $\delta^{18}O_{PO4}$ values are 16.8 ± 0.8‰ (n=70) for

incisor teeth and 15.1 ± 1.1‰ (n=35) for bones.

These values were plotted versus the long-term local mean $\delta^{18}O_{LW}$ of –7.3‰ in relation to existing $\delta^{18}O_{PO4}$-$\delta^{18}O_{LW}$ regression lines for rodents (Luz and Kolodny, 1985; Longinelli et al., 2003; Navarro et al., 2004; Fig. 5.9). The regression line of Luz and Kolodny (1985) is based on bone material from laboratory rats, and that of Longinelli et al. (2003) is based nearly exclusively on bones of wild murids and arvicolids (including the genera *Apodemus*, *Arvicola*, *Microtus* and *Pitymus*). The regression of Navarro et al. (2004) was primarily derived using molar and incisor teeth from wild small arvicolids of the genera *Myodes* and *Microtus*.

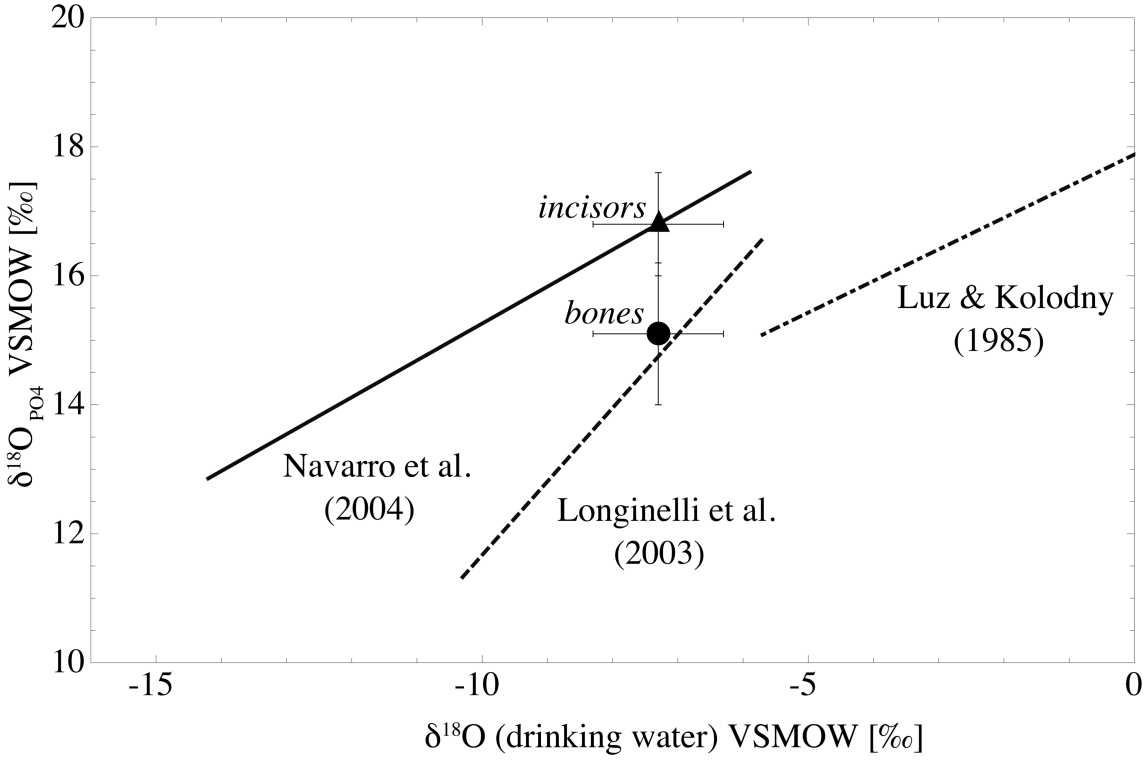

Fig. 5.9: Tooth (triangle) and bone (circle) mean values of all analysed samples converted from $\delta^{18}O_{CO3}$ to $\delta^{18}O_{PO4}$ and plotted versus the long term $\delta^{18}O$ average of local precipitation (–7.3‰). Dashed lines show the existing $\delta^{18}O_{PO4}$-$\delta^{18}O_{LW}$ regression lines for rodents developed mainly on bone material by Luz & Kolodny (1985) and Longinelli et al. (2003). The solid line shows the $\delta^{18}O_{PO4}$-$\delta^{18}O_{LW}$ calibration equation from Navarro et al. (2004), which is mainly based on tooth material.

As the calibration equation of Luz & Kolodny (2005) covers only a $\delta^{18}O_{LW}$ range outside the $\delta^{18}O$ of local precipitation in our sample area, a direct comparison to our data is precarious. However, extrapolation of the regression line reveals that the bone-derived $\delta^{18}O$ values from the present study are much closer to this line than the tooth values (Fig. 5.9).

A much better fit is obtained if the bone-based equation of Longinelli et al. (2003) is compared with our bone data, which directly plot on the respective calibration line. A similar concordance exists by comparing our tooth-data with the tooth-based equation of Navarro et al. (2004; Fig. 5.9).

This indicates that the choice of the skeletal element used for the calibration between the $\delta^{18}O$ of biogenic apatite and $\delta^{18}O_{LW}$ has an important influence, which can be assigned to different mineralisation periods and seasonally driven population dynamics in rodents as discussed above. In the case of the study by Luz and Kolodny (1985), an additional explanation for differences from our data could be the fact that the respective equation is based on laboratory animals that often differ in their physiology from field populations, which can have an impact on the oxygen isotope composition of their biogenic apatite (e.g., Grimes et al., 2008). Furthermore, as laboratory rats were raised under controlled conditions with a constant diet and water source, this precludes the effect of any seasonal bias.

Previous studies have shown that tooth enamel should be the material of choice for oxygen isotope studies in fossil mammals, because it is less prone to diagenetic alteration than dentine or bone material (Kohn and Cerling, 2002; Gehler et al., 2011). Therefore, future $\delta^{18}O_{PO4}$-$\delta^{18}O_{LW}$ calibration equations of modern taxa that aim to reconstruct palaeoenvironmental conditions should be based on tooth material instead of bone. Furthermore, the same tooth type available also from the fossil taxa should be used, in order to avoid seasonal bias due to different tooth formation patterns.

5.6 Conclusions

The observed inter-specific variations in $\delta^{18}O_{CO3}$ within arvicolid and murid incisors are low. Intra-specific variations in the $\delta^{18}O$ of the investigated rodent bioapatite samples are in the same range as most previously observed values from large mammals. Statistical evaluations show that minimum sample size recommendations from existing studies on large mammals agree well with the results from the present study, indicating at least 95% confidence that from a subsample size of ≥4 mean values range within 1σ of the mean of the sample population. The observed minor differences in the intra-specific $\delta^{18}O$ variability of rodents compared to large and medium-sized mammals corroborate the applicability of rodents in palaeoclimatic studies. Due to the differing time intervals

recorded in the different skeletal tissues (incisors, molars, bone), rodents can show considerable variations in $\delta^{18}O$ within a single individual, caused by seasonal biased $\delta^{18}O_{LW}$ ingested by individuals. This underscores the importance of using analogous tissue material when $\delta^{18}O$ data from fossil rodents are evaluated with $\delta^{18}O_{PO4}$-$\delta^{18}O_{LW}$ calibration equations based on modern taxa. Comparisons of the $\delta^{18}O$ data from the analysed arvicolids and murids with the existing calibration equations relative to the $\delta^{18}O$ data of local precipitation shows that a significant deviation from the expected value occurs when bone-based equations are applied to tooth-data and vice versa. The $\Delta^{18}O_{CO3\text{-}PO4}$ of 10.9 ± 0.8‰ determined for *A. terrestris* is at the upper limit of data from large mammals and ranges within the two previously reported values from another rodent species (*R. norvegicus*). Within the present study, no significant disadvantages in the interpretation of $\delta^{18}O$ data from rodent bioapatite compared to large- and medium-sized mammals were observed. Nevertheless, it has to be taken into account that fossil rodent taphocoenoses in temperate regions mostly underlie seasonal and spatial predator-prey population dynamics.

The $\delta^{13}C$ data mirror the different nutritional strategies of the analysed species (i.e., dietary specialisation vs. dietary opportunism). The range of variations within a single species can vary considerably but agrees well with field observations of the respective nutritional behaviour. Thus, multiple analyses from different individuals are an important prerequisite to get deeper insight into specific nutritional adaptions from fossil small mammals. Seasonally driven variations in the carbon isotope composition of the ingested food are reflected in different skeletal tissues, caused by differing time intervals of incisor, molar and bone mineralisation.

The present study underscores the high potential of stable isotope signatures of fossil small mammal skeletal remains to reconstruct past environmental and climatic conditions. However, further detailed systematic investigations of modern analogous communities of small mammals are necessary for a refined understanding of the incorporation of oxygen and carbon isotope compositions in the bioapatite of their teeth and bones and to explore the full potential of fossil rodents for palaeoenvironmental research.

Acknowledgements

The authors are grateful to B. von Bülow, Haltern am See, for providing the sample material. F. Mayer, Berlin is thanked for providing the elephant molar tooth to produce our internal bioapatite standard "AG-Lox". We thank W. von Koenigswald, Bonn, as well as L. Maul, Weimar, for references and advice regarding growth mechanisms in permanent growing rodent teeth. For assistance during the sample preparation and carbonate stable isotope analyses, we are grateful to I. Reuber and N. Albrecht. We thank S. Grimes, Plymouth and an anonymous reviewer for their comments and suggestions to improve the submitted manuscript as well as A. A. Farke, Claremont for the editorial handling. We acknowledge support by the German Research Foundation (DFG) and the Open Access Publication Funds of the Göttingen University.

References

Ambrose, S.H., Norr, L. (1993). Experimental evidence for the relationship of the carbon isotope ratios of whole diet and dietary protein to those of bone collagen and carbonate. In: Lambert, J., Grupe, G. (Eds.), *Prehistoric human bone, archaeology at the molecular level*. Springer (Berlin), pp. 1-37.

Bäumler, W. (1986). Populationsdynamik von Mäusen in verschiedenen Waldgebieten Bayerns. *Anzeiger für Schädlingskunde, Pflanzenschutz, Umweltschutz* **59**, 112-117.

Balasse, M., Ambrose, S.H., Smith, A.B., Price, T.D. (2002). The seasonal mobility model for prehistoric herders in the south-western cape of South Africa assessed by isotopic analysis of sheep tooth enamel. *Journal of Archaeological Science* **29**, 917-932.

Balasse, M., Smith, A.B., Ambrose, S.H., Leigh, S.R. (2003). Determining sheep birth seasonality by analysis of tooth enamel oxygen isotope ratios: the Late Stone Age site of Kasteelberg (South Africa). *Journal of Archaeological Science* **30**, 205-215.

Becker, K. (1978). *Rattus norvegicus* (Berkenhout, 1769) - Wanderratte. In: Niethammer, J., Krapp, F. (Eds.), *Handbuch der Säugetiere Europas*. Akademische Verlagsgesellschaft (Wiesbaden), pp. 401-420.

Bender, M.M. (1971). Variations in the $^{13}C/^{12}C$ ratios of plants in relation to the pathway of photosynthetic carbon dioxide fixation. *Phytochemistry* **10**, 1239-1244.

Bender, M.M., Rouhani, I., Vines, H.M., Black Jr., C.C. (1973). $^{13}C/^{12}C$ ratio changes in crassulacean acid metabolism plants. *Plant Physiology* **52**, 427-430.

Bocherens, H., Koch, P.L., Mariotti, A., Geraards, D., Jaeger, J.-J. (1996). Isotopic biogeochemistry (^{13}C, ^{18}O) of mammalian enamel from African Pleistocene Hominid Sites. *Palaios* **11**, 306-318.

Bowes, G. (1993). Facing the inevitable: plants and increasing atmospheric CO_2. *Annual Review of Plant Physiology and Plant Molecular Biology* **44**, 309-332.

Bryant, J.D., Froelich, P.N. (1995). A model of oxygen isotope fractionation in body water of large mammals. *Geochimica et Cosmochimica Acta* **59**, 4523-4537.

Bryant, J.D., Koch, P.L., Froelich, P.N., Showers, W.J., Genna, B.J. (1996). Oxygen isotope partitioning between phosphate and carbonate in mammalian apatite. *Geochimica et Cosmochimica Acta* **60**, 5145-5148.

Bülow, B.v. (1997). Kleinsäuger im NSG Rhader Wiesen in Dorsten. *Natur und Heimat* **57**, 37-40.

Cerling, T.E., Wang, Y., Quade, J. (1993). Expansion of C4 ecosystems as an indicator of global ecological change in the late Miocene. *Nature* **361**, 344-345.

Cerling, T.E., Harris, J.M., Ambrose, S.H., Leakey, M.G., Solounias, N. (1997). Dietary and environmental reconstruction with stable isotope analysis of herbivore tooth enamel from the Miocene locality of Fort Ternan, Kenya. *Journal of Human Evolution* **33**, 635-650.

Cerling, T.E., Harris, J.M., Leakey, M.G. (1999). Browsing and grazing in elephants: the isotope record of modern and fossil proboscideans. *Oecologica* **120**, 364-374.

Cerling, T.E., Hart, J.A., Hart, T.B. (2004). Stable isotope ecology in the Ituri Forest. *Oecologica* **138**, 5-12.

Clementz, M.T., Koch, P.L. (2001). Differentiating aquatic mammal habitat and foraging ecology with stable isotopes in tooth enamel. *Oecologica* **129**, 461-472.

Coplen, T.B. (1994). Reporting of stable hydrogen, carbon, and oxygen abundances. *Pure and Applied Chemistry* **66**, 273-276.

Dansgaard, W. (1964). Stable isotopes in precipitation. *Tellus* **16**, 436-468.

D'Angela, D., Longinelli, A. (1990). Oxygen isotopes in living mammal's bone phosphate: further results. *Chemical Geology* **86**, 75-82.

Deines, P. (1980). The isotopic composition of reduced organic carbon. In: Fritz, P., Fontes, C. (Eds.), *Handbook of environmental geochemistry, Vol 1*. Elsevier (New York), pp. 239-406.

DeNiro, M.J., Epstein S. (1978). Influence of diet on the distribution of carbon isotopes in animals. *Geochimica et Cosmochimica Acta* **42**, 495-506.

DeSantis, L.G. (2011). Stable isotope ecology of extant tapirs from the Americas. *Biotropica* **43**, 746-754.

Dettmann, D.L., Kohn, M.J., Quade, J., Ryerson, F.J., Ojha, T.P., Hamidullah, S. (2001). Seasonal stable isotope evidence for a stron Asian monsoon throughout the past 10.7 m.y. *Geology* **29**, 31-34.

Drucker, D., Bocherens, H., Bridault, A., Billiou, D. (2003). Carbon and nitrogen isotopic composition of red deer (*Cervus elaphus*) collagen as a tool for tracking palaeoenvironmental change during the Late-Glacial and Early Holocene in the northern Jura (France). *Palaeogeography, Palaeoclimatology, Palaeoecology* **195**, 375-388.

Drucker, D.G., Bridault, A., Hobson, K.A., Szuma, E., Bocherens, H. (2008). Can carbon-13 in large herbivores track canopy effect in temperate and boreal ecosystems? Evidence from modern and ancient ungulates. *Palaeogeography, Palaeoclimatology, Palaeoecology* **266**, 69-82.

Ehleringer, J.R., Cooper, T.A. (1988). Correlation between carbon isotope ratio and microhabitat in desert plants. *Oecologica* **76**, 562-566.

Farquhar, G.D., Ehleringer, J.R., Hubick, K.T. (1989). Carbon isotope discrimination and photosynthesis. *Annual Review of Plant Physiology and Plant Molecular Biology* **40**, 503-537.

Feranec, R.S., MacFadden, B.J. (2006). Isotopic discrimination of resource partitioning among ungulates in C_3-dominated communities from the Miocene of Florida and California. *Paleobiology* **32**, 191-205.

Feranec, R.S. (2007). Stable carbon isotope values reveal evidence of resource partitioning among ungulates from modern C_3-dominated ecosystems in North America. *Palaeogeography, Palaeoclimatology, Palaeoecology* **252**, 575-585.

Fox-Dobbs, K., Bump, J.K., Peterson, R.O., Fox, D.L., Koch, P.L. (2007). Carnivore-specific stable isotope variables and variation in the foraging ecology of modern and ancient wolf populations: case studies from Isle Royale, Minnesota, and La Brea. *Canadian Journal of Zoology* **85**, 458-471.

Freye, H.A., Freye, H. (1960). *Die Hausmaus*. A. Ziemsen (Wittenberg), 104 pp.

Fricke, H.C., O'Neil, J.R. (1996). Inter- and intra-tooth variation in the oxygen isotope composition of mammalian tooth enamel phosphate: implications for palaeoclimatological and palaeobiological research. *Palaeogeography, Palaeoclimatology, Palaeoecology* **126**, 91-99.

Fricke, H.C., O'Neil, J.R. (1999). The correlation between $^{18}O/^{16}O$ ratios of meteoric water and surface temperature: its use in investigating terrestrial climate change over geologic time. *Earth and Planetary Science Letters* **170**, 181-196.

Gehler, A., Tütken, T., Pack, A. (2011). Triple oxygen isotope analysis of bioapatite as tracer for diagenetic alteration of bones and teeth. *Palaeogeography, Palaeoclimatology, Palaeoecology* **310**, 84-91.

Grimes, S.T., Mattey, D.P., Hooker, J.J., Collinson, M.E. (2003). Eocene-Oligocene palaeoclimate reconstruction using oxygen isotopes: problems and solutions from the use of multiple palaeoproxies. *Geochimica et Cosmochimica Acta* **67**, 4033-4047.

Grimes, S.T., Collinson, M.E., Hooker, J.J., Mattey, D.P., Grassineau, N.V., Lowry, D. (2004a). Distinguishing the diets of coexisting fossil theridomyid and glirid rodents using carbon isotopes. *Palaeogeography, Palaeoclimatology, Palaeoecology* **208**, 103-119.

Grimes, S.T., Mattey, D.P., Collinson, M.E., Hooker, J.J. (2004b). Using mammal tooth phosphate with freshwater carbonate and phosphate palaeoproxies to obtain mean palaeotemperatures. *Quaternary Science Reviews* **23**, 967-976.

Grimes, S.T., Hooker, J.J., Collinson, M.E., Mattey, D.P. (2005). Summer temperatures of late Eocene to early Oligocene freshwaters. *Geology* **33**, 189-192.

Grimes, S.T., Collinson, M.E., Hooker, J.J., Mattey, D.P. (2008). Is small beautiful? A review of the advantages and limitations of using small mammal teeth and the direct laser fluorination analysis technique. *Palaeogeography, Palaeoclimatology, Palaeoecology* **266**, 39-50.

Harris, J.M., Cerling, T.E. (2002). Dietary adaptions of extant and Neogene African suids. *Journal of the Zoological Society of London* **256**, 45-54.

Heaton, T.H.E. (1999). Spatial, species and temporal Variations in the $^{13}C/^{12}C$ ratios of C_3 plants: implications for palaeodiet studies. *Journal of Archaeological Science* **26**, 637-649.

Héran, M.A., Lécuyer, C., Legendre, S. (2010). Cenozoic long-term terrestrial climatic evolution in Germany tracked by $\delta^{18}O$ of rodent tooth phosphate. *Palaeogeography, Palaeoclimatology, Palaeoecology* **285**, 331-342.

Hopley, P.J., Latham, A.G., Marshall, J.D. (2006). Palaeoenvironments and palaeodiets of mid-Pliocene micromammals from Makapansgat Limeworks, South Africa: A stable isotope and dental microwear approach. *Palaeogeography, Palaeoclimatology, Palaeoecology* **233**, 235-251.

Hoppe, K.A., Amundson, R., Vavra, M., McClaran, M.P., Anderson, D. (2004). Isotopic analysis of tooth enamel carbonate from modern North American feral horses: implications for palaeoenvironmental reconstructions. *Palaeogeography, Palaeoclimatology, Palaeoecology* **203**, 299-311.

Hoppe, K.A., Stuska, S., Amundson, R. (2005). Implications for palaeodietary and palaeoclimatic reconstructions of intrapopulation variability in the oxygen and carbon isotopes of teeth from modern feral horses. *Quaternary Research* **64**, 138-146.

Hoppe, K.A. (2006). Correlation between the oxygen isotope ratio of North American bison teeth and local waters: Implication for palaeoclimatic reconstructions. *Earth and Planetary Science Letters* **244**, 408-417.

Hynek, S.A., Passey, B.H., Prado, J.L., Brown, F.H., Cerling, T.E., Quade, J. (2012). Small mammal carbon isotope ecology across the Miocene-Pliocene boundary, northwestern Argentina. *Earth and Planetary Science Letters* **321-322**, 177-188.

Iacumin, P., Bocherens, H., Mariotti, A., Longinelli, A. (1996). Oxygen isotope analyses of co-existing carbonate and phosphate in biogenic apatite: a way to monitor diagenetic alteration of bone phosphate? *Earth and Planetary Science Letters* **142**, 1-6.

IAEA/WISER (2011). Water Isotope System for Data Analysis, Visualization and Electronic Retrieval, IAEA Water Resources Programme. Available at http://nds121.iaea.org/wiser/ accessed 21. May 2011.

Jones, A.M., Iacumin, P., Young, E.D. (1999). High-resolution $\delta^{18}O$ analysis of tooth enamel phosphate by isotope ratio monitoring gas chromatography mass spectrometry and ultraviolet laser fluorination. *Chemical Geology* **153**, 241-248.

Kemp, T.S. (2007). *The Origin and Evolution of Mammals*. Oxford University Press (New York), 331 pp.

Kirsanow, K., Tuross, N. (2011). Oxygen and hydrogen isotopes in rodent tissues: Impact of diet, water and ontogeny. *Palaeogeography, Palaeoclimatology, Palaeoecology* **310**, 9-16.

Klevezal, G.A., Pucek, M., Sukhovskaya, L.I. (1990). Incisor growth in voles. *Acta Theriologica* **35**, 331-344.

Klevezal, G.A. (1996). *Recording structures of mammals. Determination of age and reconstruction of life history*. Balkema (Rotterdam, Brookfield), 274 pp.

Koch, P.L., Tuross, N., Fogel, M.L. (1997). The effects of sample treatment and diagenesis on the isotopic integrity of carbonate in biogenic hydroxylapatite. *Journal of Archaeological Science* **24**, 417-429.

Koenigswald, W.v., Golenishev, F.N. (1979). A method for determining growth rates in continuously growing molars. *Journal of Mammalogy* **60**, 397-400.

Kohn, M.J., (1996). Predicting animal $\delta^{18}O$: Accounting for diet and physiological adaption. *Geochimica et Cosmochimica Acta* **60**, 4811-4829.

Kohn, M.J., Schoeninger, M.J., Valley, J.W. (1996). Herbivore tooth oxygen isotope compositions: Effects of diet and physiology. *Geochimica et Cosmochimica Acta* **60**, 3889-3896.

Kohn, M.J., Cerling, T.E. (2002). Stable isotope compositions of biological apatite. *Reviews in Mineralogy and Geochemistry* **48**, 455-488.

Krapp, F., Niethammer, J. (1982). *Microtus agrestis* (Linnaeus, 1761) - Erdmaus. In: Niethammer, J., Krapp, F. (Eds.), *Handbuch der Säugetiere Europas*. Akademische Verlagsgesellschaft (Wiesbaden), pp. 349-373.

Land, L.S., Lundelius, E.L., Valastro, S. (1980). Isotopic ecology of deer bones. *Palaeogeography, Palaeoclimatology, Palaeoecology* **32**, 143-151.

Levin, N.E., Cerling, T.E., Passey, B.H., Harris, J.M., Ehleringer, J.R. (2006). A stable isotope aridity index for terrestrial environments. *Proceedings of the National Academy of Sciences* **103**, 11201-11205.

Lindars, E.S., Grimes, S.T., Mattey, D.P., Collinson, M.E., Hooker, J.J., Jones, T.P. (2001). Phosphate $\delta^{18}O$ determination of modern rodent teeth by direct laser fluorination: An appraisal of methodology and potential application to palaeoclimate reconstruction. *Geochimica et Cosmochimica Acta* **65**, 2535-2548.

Longinelli, A. (1984). Oxygen isotopes in mammal bone phosphate: a new tool for paleohydrological and paleoclimatological research? *Geochimica et Cosmochimica Acta* **48**, 385-390.

Longinelli, A., Iacumin, P., Davanzo, S., Nikolaev, V. (2003). Modern reindeer and mice: revised phosphate-water isotope equations. *Earth and Planetary Science Letters* **214**, 491-498.

Lowdon, J.A., Dyck, W. (1974). Seasonal variations in the isotope ratios of carbon in maple leaves and other plants. *Canadian Journal of Earth Sciences* **11**, 79-88.

Luz, B., Kolodny, Y., Horowitz, M. (1984). Fractionation of oxygen isotopes between mammalian bone phosphate and environmental drinking water. *Geochimica et Cosmochimica Acta* **48**, 1689-1693.

Luz, B., Kolodny, Y. (1985). Oxygen isotope variations in phosphate of biogenic apatites, IV. Mammal teeth and bones. *Earth and Planetary Science Letters* **75**, 29-36.

MacFadden, B.J., Wang, Y., Cerling, T.E., Anaya, F. (1994). South American fossil mammals and carbon isotopes: a 25 million-year sequence from the Bolivian Andes. *Palaeogeography, Palaeoclimatology, Palaeoecology* **107**, 257-268.

MacFadden, B.J., Cerling, T.E. (1996). Mammalian herbivore communities, ancient feeding ecology and carbon isotopes: a 10-million-year sequence from the Neogene of Florida. *Journal of Vertebrate Paleontology* **16**, 103-115.

MacFadden, B.J., Solounias, N., Cerling, T.E. (1999). Ancient diets, ecology, and extinction of 5-million-year-old horses from Florida. *Science* **283**, 824-827.

MacFadden, B.J., Higgins, P. (2004). Ancient ecology of 15-million-year-old browsing mammals within C3 plant communities from Panama. *Oecologica* **140**, 169-182.

Mariotti, A. (1991). Le carbone 13 en abondance naturelle, traceur de la dynamique de la matière organique des sols et de l'évolution des paléoenvironnements continentaux. *Cahiers Orstom, série Pédologie* **26**, 299-313.

Martin, C., Bentaleb, I., Kaandorp, R., Iacumin, P., Chatri, K. (2008). Intra-tooth study of modern rhinoceros enamel $\delta^{18}O$: Is the difference between phosphate and carbonate $\delta^{18}O$ a sound diagenetic test? *Palaeogeography, Palaeoclimatology, Palaeoecology* **266**, 183-187.

Medina, E., Minchin, P. (1980). Stratification of $\delta^{13}C$ values of leaves in Amazonian rain forests. *Oecologica* **45**, 377-378.

Navarro, N., Lécuyer, C., Montuire, S., Langlois, C., Martineau, F. (2004). Oxygen isotope compositions of phosphate from arvicoline teeth and Quaternary climatic changes, Gigny, French Jura. *Quaternary Research* **62**, 172-182.

Nelson, S.V. (2007). Isotopic reconstructions of habitat change surrounding the extinction of *Sivapithecus*, a Miocene hominoid, in the Siwalik Group of Pakistan. *Palaeogeography, Palaeoclimatology, Palaeoecology* **243**, 204-222.

Niethammer, J. (1978). *Apodemus sylvaticus* (Linnaeus, 1758) - Waldmaus. In: Niethammer, J., Krapp, F. (Eds.), *Handbuch der Säugetiere Europas*. Akademische Verlagsgesellschaft (Wiesbaden), pp. 337-358.

Niethammer, J., Krapp, F. (1982). *Microtus arvalis* (Pallas, 1779) - Feldmaus. In: Niethammer, J., Krapp, F. (Eds.), *Handbuch der Säugetiere Europas*. Akademische Verlagsgesellschaft (Wiesbaden), pp. 284-318.

Norrdahl, K., Korpimäki, E. (2002). Seasonal changes in the numerical responses of predators to cyclic vole populations. *Ecography* **25**, 428-438.

O'Leary, M.H. (1988). Carbon isotopes in photosynthesis. *BioScience* **38**, 328-336.

Passey, B.H., Robinson, T.F., Ayliffe, L.K., Cerling, T.E., Sponheimer, M., Dearing, M.D., Roeder, B.L., Ehleringer, J.R. (2005). Carbon isotope fractionation between diet, breath CO_2, and bioapatite in different mammals. *Journal of Archaeological Science* **32**, 1459-1470.

Pellegrini, M., Lee-Thorp, J.A., Donahue, R.E. (2011). Exploring the variation of the $\delta^{18}O_p$ and $\delta^{18}O_c$ relationship in enamel increments. *Palaeogeography, Palaeoclimatology, Palaeoecology* **310**, 71-83.

Quade, J., Cerling, T.E., Barry, J.C., Morgan, M.E., Pilbeam, D.R., Chivas, A.R., Lee-Thorp, J., van der Merwe, N.J. (1992). A 16-Ma record of paleodiet using carbon and oxygen isotopes in fossil teeth from Pakistan. *Chemical Geology (Isotope Geoscience Section)* **94**, 183-192.

Quade, J., Cerling, T.E., Andrews, P., Alpagut, B. (1995). Paleodietary reconstruction of Miocene faunas from Pasalar, Turkey using stable carbon and oxygen isotopes of fossil tooth enamel. *Journal of Human Evolution* **28**, 373-384.

Reichstein, H. (1978). *Mus musculus* Linnaeus, 1758 - Hausmaus. In: Niethammer, J., Krapp, F. (Eds.), *Handbuch der Säugetiere Europas*. Akademische Verlagsgesellschaft (Wiesbaden), pp. 421-451.

Reichstein, H. (1982). *Arvicola terrestris* (Linnaeus, 1758) - Schermaus. In: Niethammer, J., Krapp, F. (Eds.), *Handbuch der Säugetiere Europas*. Akademische Verlagsgesellschaft (Wiesbaden), pp. 217-252.

Rogers, K.L., Wang, Y. (2002). Stable isotopes in pocket gopher teeth as evidence of a Late Matuyama climate shift in the southern Rocky Mountains. *Quaternary Research* **57**, 200-207.

Rozanski, K., Araguás-Araguás, L., Gonfiantini, R. (1993). Isotopic patterns in modern global precipitation. In: Swart, P.K., Lohmann, K.C., McKenzie, J., Savin, S. (Eds.), *Climate change in continental isotopic records* (= Geophysical Monograph **78**). Washington D. C. (American Geophysical Union), pp. 1-36.

Rozanski, K., Johnsen, S.J., Schotterer, U., Thompson, L.G. (1997). Reconstruction of past climates from stable isotope records of palaeo-precipitation preserved in continental archives. *Hydrological Sciences* **42**, 725-745.

Ruddy, M. (2008). Water vole incisors as records of palaeoclimate. *Quaternary Newsletter* **116**, 51-54.

Salamolard, M., Butet, A., Leroux, A., Bretagnolle, V. (2000). Responses of an avian predator to variations in prey density at a temperate latitude. *Ecology* **81**, 2428-2441.

Sayed, O.H. (2001). Crassulacean acid metabolism 1975-2000, a check list. *Photosynthetica* **39**, 339-352.

Schönfeld, M., Girbig, G. (1975). Beiträge zur Brutbiologie der Schleiereule, *Tyto alba*, unter besonderer Berücksichtigung der Abhängigkeit von der Feldmausdichte. *Hercynia N. F.* **12**, 257-319.

Schönfeld, M., Girbig, G., Sturm, H. (1977). Beiträge zur Populationsdynamik der Schleiereule, *Tyto alba*. *Hercynia N. F.* **14**, 303-351.

Shahack-Gross, R., Tchernov, E., Luz, B. (1999). Oxygen isotopic composition of mammalian skeletal phosphate from the Natufian Period, Hayonim Cave, Israel: Diagenesis and Paleoclimate. *Geoarchaeology* **14**, 1-13.

Still, C., Berry, J.A., Collatz, G.J., DeFries, R. (2003). Global distribution of C_3 and C_4 vegetation: Carbon cycle implications. *Global Biogeochemical Cycles* **17**, 6.1-6.14.

Stubbe, M. (1982). Dynamik der Kleinnagergesellschaft (Rodentia: Arvicolidae, Muridae) im Hakel. *Hercynia N. F.* **19**, 110-120.

Ting, I.P. (1985). Crassulacean acid metabolism. *Annual Review of Plant Physiology* **36**, 595-622.

Tóth, E., Görög, Á., Lécuyer, C., Moissette, P., Balter, V., Monostori, M. (2010). Palaeoenvironmental reconstruction of the Sarmatian (Middle Miocene) Central Paratethys based on palaeontological and geochemical analyses of foraminifera, ostracods, gastropods and rodents. *Geological Magazine* **147**, 299-314.

Tütken, T., Vennemann, T.W., Janz, H., Heizmann, E.P.J. (2006). Palaeoenvironment and palaeoclimate of the Middle Miocene lake in the Steinheim Basin, SW Germany: A reconstruction from C, O, and Sr isotopes of fossil remains. *Palaeogeography, Palaeoclimatology, Palaeoecology* **241**, 457-491.

Tütken, T., Vennemann, T. (2009). Stable isotope ecology of Miocene large mammals from Sandelzhausen, southern Germany. *Paläontologische Zeitschrift* **83**, 207-226.

van der Merwe N.J., Medina, E. (1989). Photosynthesis and $^{13}C/^{12}C$ ratios in Amazonian rain forests. *Geochimica et Cosmochimica Acta* **53**, 1091-1094.

van der Merwe N.J., Medina, E. (1991). The canopy effect, carbon isotope ratios and foodwebs in Amazonia. *Journal of Archaeological Science* **18**, 249-259.

Vennemann, T.W., Fricke, H.C., Blake, R.E., O'Neil, J.R., Colman, A. (2002). Oxygen isotope analyses of phosphates: a comparison of techniques for analysis of Ag_3PO_4. *Chemical Geology* **185**, 321-336.

Viro, P., Niethammer, J. (1982). *Clethrionomys glareolus* (Schreber, 1780) - Rötelmaus. In: Niethammer, J., Krapp, F. (Eds.), *Handbuch der Säugetiere Europas*. Akademische Verlagsgesellschaft (Wiesbaden), pp. 109-146.

Vogel, J.C. (1978). Recycling of carbon in a forest environment. *Oecologica Plantarum* **13**, 89-94.

Wang, Y., Kromhout, E., Zhang, C., Xu, Y., Parker, W., Deng, T., Qiu, Z. (2008). Stable isotopic variations in modern herbivore tooth enamel, plants and water on the Tibetan Plateau: Implications for paleoclimate and paleoelevation reconstructions. *Palaeogeography, Palaeoclimatology, Palaeoecology* **260**, 359-374.

Yeakel, J.D., Bennett, N.C., Koch, P.L., Dominy, N.J. (2007). The isotopic ecology of African mole rats informs hypotheses on the evolution of human diet. *Proceedings of the Royal Society (B)* **274**, 1723-1730.

Ylönen, H., Altner, H.J., Stubbe, M. (1991). Seasonal dynamics of small mammals in an isolated woodlot and its agricultural surroundings. *Annales Zoologici Fennici* **28**, 7-14.

Zanazzi, A., Kohn, M.J. (2008). Ecology and physiology of White River mammals based on stable isotope ratios of teeth. *Palaeogeography, Palaeoclimatology, Palaeoecology* **257**, 22-37.

Zazzo, A. (2001). *Validation méthodologique de l'utilisation des compositions isotopiques (13C, 18O) des bioapatites fossiles pour les reconstitutions des paléoenvironnements continentaux*. Paris: Université Pierre et Marie Curie, 504 pp.

Zazzo, A., Lécuyer, C., Sheppard, S.M.F., Grandjean, P., Mariotti, A. (2004). Diagenesis and the reconstruction of palaeoenvironments: A method to restore original $\delta^{18}O$ values of carbonate and phosphate from fossil tooth enamel. *Geochimica et Cosmochimica Acta* **68**, 2245-2258.

6. Conclusions and Outlook

Within the manuscripts of the thesis presented here, the triple oxygen isotope composition of mammalian bioapatite has been examined as well as its potential as a proxy for CO_2-levels throughout Earth's history (**chapters 3 and 4**) and diagenetically altered skeletal tissue (**chapter 2**). Furthermore, a basic contribution for the understanding of the oxygen and carbon isotope variations in rodents has been provided (**chapter 5**).

In **chapter 3**, it is confirmed that an anomalous triple oxygen signature (^{17}O-anomaly or ^{17}O-excess), transferred from ambient air O_2 via breathing into the mammalian body, can be analytically resolved. It is shown that the magnitude of the ^{17}O anomaly in mammalian bioapatite increases with decreasing body mass due to a higher portion of air oxygen intake relative to the other oxygen sources (such as drinking water and free water in food) towards a smaller body mass. A second parameter that can effect Δ^{17}O of mammalian bioapatite is the nutritional behaviour (i.e. a larger ^{17}O-excess in herbivores compared to carnivores of the same body mass). The analytical data from a large set of modern mammals with body masses between ~2g and ~5000 kg are supported by a detailed mass balance model.

Based on these results, tooth enamel of Middle Eocene to Upper Miocene herbivorous small mammals (i.e. rodents) are analysed for its triple oxygen isotope composition with the attempt to get insight into the respective Δ^{17}O of air oxygen that is a function of pCO_2 and bioproductivity.

It is shown that Δ^{17}O of fossil bioapatite has the potential to be used as a new alternative proxy for ancient CO_2 levels. The obtained data on Eocene, Oligocene and Miocene pCO_2 agree well with previous data of other pCO_2 proxies.

This approach is extended in **chapter 4** to the Late Palaeocene/Early Eocene with a larger set of samples of the single genus *Ectocion* (Mammalia: Condylarthra: Phenacodontidae). The Palaeocene-Eocene transition encompasses one of the most remarkable climatic changes within the Cenozoic, accompanied by large temperature fluctuations within a relatively short time interval (Palaeocene-Eocene Themal Maximum, PETM) and the addition of several Gt ^{13}C-depleted carbon to the exogenic carbon cycle (Carbon Isotope Excursion, CIE).

The $\Delta^{17}O$ data from *Ectocion* tooth enamel can simultaneously give evidence on both, temperature fluctuations and CO_2-levels during this critical interval in Earth's history. The reconstructed temperature change is in good agreement with previous results from $\delta^{18}O$ of mammalian tooth enamel and other temperature proxies within the same time slice. Contrasting to previous studies with other CO_2 proxies, pre-, peak- and post-PETM data on CO_2 could be obtained. The data suggest that CO_2-levels have not exceeded 1550 ppm and therefore support the theory that the release of marine methane clathrates has contributed as the major source for the contemporaneously observed CIE.

Both studies highlight the high application potential of $\Delta^{17}O$ studies on fossil mammalian bioapatite. The relatively large error estimates associated to the reconstructed pCO_2 are related to a large extent to uncertainties in physiology (i.e. total water flux and specific metabolic rate). Those have the potential to be reduced considerably by a more detailed survey of the triple oxygen isotope variability in modern mammal taxa and the use of close relatives from the fossil record to reconstruct pCO_2.

The different diagenetic susceptibility of mammalian tooth enamel, dentine and bone is evaluated in **chapter 2**. As suggested in the past from secondary proxies (e.g. apatite crystallinity, rare earth element contents) it could be proven by the detection of a distinct ^{17}O-anomaly that tooth enamel of fossil mammals can retain its original triple oxygen isotope composition. In contrast, dentine has largely lost the in vivo obtained oxygen isotope signal from air oxygen, presumably through exchange with diagenetic fluids.

In **chapter 5**, the interspecific, intraspecific and intraspecific variability of the oxygen and carbon isotope composition of seven different rodent species sampled from owl pellets of a single locality is evaluated. As stable isotope studies on bioapatite of small fossil mammals (i.e. rodents) have emerged in an increasing number within the last decade, the intent for this study was to contribute to an enhanced understanding of those variations in small mammals. Comparable studies in the past have been carried out only on large mammals. It is shown that the oxygen and carbon isotope variability of the investigated rodents in general is comparable to that of most previously studied large mammals. However, tissue-specific differences should be considered if findings obtained from modern taxa are applied to rodents in the fossil record.